THE REMOVAL OF PHORATE FROM WATER BY ADSORPTION ON
POWDERED ACTIVATED CARBON AND CHABAZITE

A THESIS SUBMITTED TO
THE GRADUATE SCHOOL OF NATURAL AND APPLIED SCIENCES
OF
MIDDLE EAST TECHNICAL UNIVERSITY

BY

CANSU POLAT

IN PARTIAL FULFILLMENT OF THE REQUIREMENTS
FOR
THE DEGREE OF MASTER OF SCIENCE
IN
ENVIRONMENTAL ENGINEERING

SEPTEMBER 2022

Approval of the thesis:

THE REMOVAL OF PHORATE FROM WATER BY ADSORPTION ON POWDERED ACTIVATED CARBON AND CHABAZITE

submitted by **CANSU POLAT** in partial fulfillment of the requirements for the degree of **Master of Science** in **Environmental Engineering, Middle East Technical University** by,

Prof. Dr. Halil Kalıpçılar
Dean, Graduate School of **Natural and Applied Sciences**

_____

Prof. Dr. Bülent İçgen
Head of the Department, **Environmental Engineering**

_____

Prof. Dr. Ülkü Yetiş
Supervisor, **Environmental Engineering, METU**

_____

Prof. Dr. Filiz Bengü Dilek
Co-Supervisor, **Environmental Engineering, METU**

_____

Examining Committee Members:

Prof. Dr. Bülent İçgen
Environmental Eng., METU

_____

Prof. Dr. Ülkü Yetiş
Environmental Eng., METU

_____

Prof. Dr. Niğmet Uzal
Civil Eng, Abdullah Gül Uni.

_____

Prof. Dr. Nuray Ateş
Environmental Eng., Erciyes Uni.

_____

Assist. Prof. Dr. Sema Sevinç Şengör
Environmental Eng., METU

_____

Date: 08.09.2022

I hereby declare that all information in this document has been obtained and presented in accordance with academic rules and ethical conduct. I also declare that, as required by these rules and conduct, I have fully cited and referenced all material and results that are not original to this work.

Name Last name : Cansu Polat

Signature :

ABSTRACT

THE REMOVAL OF PHORATE FROM WATER BY ADSORPTION ON POWDERED ACTIVATED CARBON AND CHABAZITE

Polat, Cansu
Master of Science, Environmental Engineering
Supervisor: Prof. Dr. Ülkü Yetiş
Co-Supervisor: Prof. Dr. Filiz Bengü Dilek

September 2022, 151 pages

The removal of phorate from aqueous solution by adsorption on two different adsorbents, powdered activated carbon (PAC) and natural zeolite chabazite (CHA), has been studied. Effects of operational conditions, such as initial phorate concentration (1, 0.75 and 0.5 mg/L), PAC and CHA doses (12.5, 25 and 37.5 mg/L), pH (3, 7 and 9), temperature (15, 25 and 35 ºC) and mixing intesities (120, 160 and 200 rpm) were investigated. Under acidic conditions (pH=3), PAC and CHA performes better. Especially when the adsorbent is CHA, the removal efficiency increased to appraximately 80% from 50% when pH is acidic. The initial concentration of phorate affects the adsorption on PAC and CHA differently. For PAC, the overall rate increases with decreasing initial concentration while it decreases for CHA. The effect of adsorbent amount for the removal of phorate is observed up to 25 mg/L for PAC and CHA which indicates that there is no enhancement in the removal of phorate after the aforementioned dose of adsorbent. The adsorption of phorate on CHA is especially affected by the shaking speed as the speed increases from 120 rpm to 200 rpm, the removal efficiency increases to 80% from 60%. The changes in temperature does not affect the equilibrium conditions significantly; however overall adsorption

rates for the two adsorbents react oppositely to the changes. The rate constant for PAC increases with increasing temperature while the rate constans for CHA decreases. Pseudo-first order (PFO) and pseudo-second-order (PSO) models were tested for adsorption kinetics of phorate on PAC and CHA under different operational conditions. For all operational conditions, PSO model is the best-fitted model for both PAC and CHA. In order to investigate the equilibrium behavior of phorate when adsorbed on PAC and CHA, adsorption isotherm experiments are conducted at neutral pH and room temperature with shaking speed of 160 rpm. Langmuir and Freundlich istoherm models are tested for this purpose. Adsorption onto PAC is well-defined by both Langmuir and Freundlich models while the equilibrium behavior is well-described by Freundlich model when adsorbent is CHA. Based on the Langmuir model, maximum adsorption capacity of PAC for phorate was calculated as 26 mg/g.

ÖZ

TOZ AKTİF KARBON VE ŞABAZİT ÜZERİNE ADSORPSİYON İLE FORATIN SUDAN GİDERİLMESİ

Polat, Cansu
Yüksek Lisans, Çevre Mühendisliği
Tez Yöneticisi: Prof. Dr. Ülkü Yetiş
Ortak Tez Yöneticisi: Prof. Dr. Filiz Bengü Dilek

Eylül 2022, 151 sayfa

Toz halinde aktif karbon (PAC) ve doğal zeolit şabazit (CHA) olmak üzere iki farklı adsorban üzerine adsorpsiyon ile sulu çözeltiden foratın uzaklaştırılması araştırılmıştır. Başlangıç forat konsantrasyonu (1, 0.75 ve 0.5 mg/L), PAC ve CHA dozları (12., 25 ve 37.5 mg/L), pH (3, 7 ve 9), sıcaklık (15, 25 ve 35 ºC) ve karıştırma hızları (120, 160 ve 200 rpm) incelenmiştir. Asidik koşullar altında (pH=3), PAC ve CHA daha iyi performans göstermiştir. Özellikle adsorban CHA olduğunda, pH düşükken uzaklaştırma verimi %50'den yaklaşık %80'e çıkmıştır. Başlangıçtaki forat konsantrasyonu, PAC ve CHA üzerindeki adsorpsiyonu farklı şekilde etkilemiştir. PAC için, genel hız, azalan başlangıç konsantrasyonu ile artarken, CHA için azalmıştır. PAC ve CHA için 25 mg/L'ye kadar adsorban miktarının, foratın uzaklaştırılması üzerine etkisi gözlenmiş, bu da yukarıda belirtilen adsorban dozundan sonra foratın uzaklaştırılmasında herhangi bir artış olmadığını göstermiştir. CHA üzerine phorat adsorpsiyonu özellikle çalkalama hızından etkilenmiş, hız 120 rpm'den 200 rpm'ye çıkarıldığında, uzaklaştırma verimi %60'tan %80'e yükselmiştir. Sıcaklıktaki değişiklikler denge koşullarını önemli ölçüde etkilememiştir; bununla birlikte, iki adsorban için de genel adsorpsiyon hızları , değişikliklere ters tepki vermiştir. PAC için hız sabiti artan sıcaklıkla artarken CHA için azalmıştır.Farklı

işletme koşulları altında PAC ve CHA üzerine foratın adsorpsiyon kinetiği için sözde-birinci-dereceden (PFO) ve sözde-ikinci-dereceden (PSO) modeller test edilmiştir. Tüm işletme koşulları için, PSO modeli hem PAC hem de CHA için en uygun model olmuştur. Foratın PAC ve CHA üzerine adsorpsiyonu sırasındaki denge davranışını araştırmak için, 160 rpm çalkalama hızı, nötr pH ve oda sıcaklığında adsorpsiyon izoterm deneyleri yapılmıştır. Bu amaçla, Langmuir ve Freundlich izoterm modelleri test edilmiştir. PAC ile adsorpsiyon, hem Langmuir hem de Freundlich modelleri tarafından tanımlanabilirken, CHA için denge davranışı sadece Freundlich modeli ile tanımlanabilmiştir.. Langmuir modelinden, PAC'ın forat için maksimum adsorpsiyon kapasitesi 26 mg/g olarak hesaplanmıştır.

Anahtar Kelimeler: Forat, adsorpsiyon, şabazit, kinetik, izoterm, toz aktif karbon

To the fragile sanity of mine

ACKNOWLEDGMENTS

TABLE OF CONTENTS

LIST OF TABLES

LIST OF FIGURES

FIGURES

LIST OF ABBREVIATIONS

ABBREVIATIONS

AC: Activated Carbon

ACN: Acetonitrile

AOP: Advanced Oxidation Process

AS: Activated Sludge

ASP: Activated Sludge Process

CHA: Chabazite

DO: Dissolved oxygen

DOM: Dissolved Organic Matter

DRIFT: Diffuse Refluctance Infrared Fourier Transform Spectroscopy

DT_{50} : Degradation time (time needed for the amount of pollutant decreased by half due to ligth or other radiant energy sources)

FAO: Food and Agriculture Organization of the United Nations

HPLC: High Performance Liquid Chromatography

LD_{50}: Lethal Dose 50

LOD: Limit of Detection

LOQ: Limit of Quantification

OP: Organophosphorous Pesticide

PAC: Powdered Activated Carbon

PFO: Pseudo-First Order

PSO: Pseudo-Second Order

TSI: Turkish Statistical Institution

UPW: Ultra Pure Water

WHO: World Health Organisation

WWTP: Wastewater Treatment Plant

CHAPTER 1

INTRODUCTION

1.1   General

Pesticides are chemical substances applied to the land in order to fight pests which are undesirable organisms including fungi, insects, mites etc. Pesticides can be categorized by their target organism (herbicides, fungicides, insecticides etc.) and their chemical nature (carbamates, organophosphorus, organochlorines, benzoic acids etc.) (Mojiri et al., 2020). Organophosphorous pesticides have been used widely since they are highly effective pesticides with lower persistency in the environment compared to organochlorines. They inhibit cholinesterase, which is a vital enzyme in the metabolism of one of the key neurotransmitters called acetylcholine (Hong et al., 2000; Mojiri et al., 2020). Thus, they may seriously harm public health and ecosystems. Regarding the target organism, herbicides, insecticides, and fungicides are the main groups of pesticides. Herbicide application is reported as almost half of the total pesticide application worldwide (Mojiri et al., 2020).

An increasing number of studies indicate that pesticides are present in surface water, groundwater, and drinking water (Syafrudin et al., 2021).These pollutants mainly originate from point sources that include discharge of urban and industrial wastewater treatment plants and from diffuse sources that mainly consist of agricultural and urban water runoff (Knowell, 2018; Syafrudin et al., 2021). The transfer of these chemicals to water courses occurs via surface runoff, wind/spray drift, deposition, leaching, and drainage lines. As a result of this transfer, a variety of pesticides are detected in the aquatic environment (Mojiri et al., 2020). The concentrations of some pesticides in ground, surface, and drinking water in different countries are presented in Table 1.1.

Table 1.1 The concentrations of some pesticides in different water sources worldwide (Mojiri et al., 2020)

Water source	Pesticide	Average Concentration (ng/L or ng/g)	Country	Reference
Surface water	Iprobenfos	10,400	Koise, Japan	Derbalah et al.,2018(Derbalah et al., 2018)
	Carbendazim	2.7	Ebro, Spain	Navarro-ortega et al., 2016
	Atrazine	410	Strymonas, Greece	Papadakis et al., 2018
	Diuron	150	Sjaelland, Denmark	Mcknight et al., 2015
	Chlorpyrifos	578	Nile, Egypt	Dahshan et al., 2016
	Phorate	190-310	India	Lari et al., 2014
	Phorate	20-940	India	Bhuvaneswari et al. ,2006
Drinking water	Malathion	11.948	Tap water, Ethiopia	Mekonen et al., 2016
	Atrazine	11.9	Community drinking water, Quebec/ Canada	Husk et al., 2019
	Parathion	19.2		
	Phosmet	9.2		
Groundwater	Pyraclostrobin	3.1	US	Reilly et al., 2012
	Atrazine	200	Italy	Piemonte & Toscana, 2010
	Alachlor	639.3	Catalonia, Spain	Köck-schulmeyer et al., 2014
	Bentazone	150	New Zealand	Close et al., 2010
Wastewater	Imidacloprid	36	WWTP effluent, Germany	Münze et al., 2017
	Atrazine	44.1	Domestic WWTP effluent, Quebec/Canada	Westlund & Yargeau, 2017

The concentrations presented in Table 1.1 show that pesticides have been detected all around the world in different water sources. That is why, to protect the environment and public health, pesticide removal from water and wastewater is a priority and it is crucial. Conventional wastewater treatment processes applied for wastewater treatment are not effective in the complete removal of the pesticides present in the raw

wastewater, which makes conventional wastewater treatment plants important sources of pesticides in the aquatic environment (Saleh et al., 2020).

Advanced treatment methods such as adsorption, advanced oxidation processes (AOPs), membrane filtration, phytoremediation, and bioremediation are effective in the removal of pesticides from water. Nevertheless, most methods are expensive, with poor flexibility, and most importantly, with a low treatment efficiency causing the formation of secondary pollutants. Among these treatment techniques, adsorption is regarded as an effective process that is commonly preferred to remove both organic and inorganic hazardous pollutants from wastewater discharges. Although its effectiveness varies with the properties of adsorbate and adsorbent due to being a surface phenomenon, adsorption is seen as a low-cost, rapid, and simple treatment alternative (Mojiri et al., 2020). The adsorption process has many other advantages, such as easy operation, flexible design, and not being affected by toxic pollutants. Numerous adsorbents; activated carbon (AC), graphene, zeolite, bentonite, biochar, chitosan, and nanoparticle adsorbents, have been commonly used for the removal of organic contaminants from aqueous solutions (Mojiri et al., 2020). Table 1.2 summarizes some of the studies on the adsorption of pesticides from water and wastewater.

Phorate is an insecticide under the sub-group of organophosphorus (OP) pesticides. It is commonly applied to corn, potato, coffee, and cotton fields to protect agricultural goods from being chewed and sucked by insects (Hodgson, 2012). Phorate is classified as extremely hazardous by World Health Organization (WHO) depending on the effect on humans and animals since it inhibits activating an enzyme called cholinesterase (Moyer, 2018; World Health Organization, 2020). Reported Lethal dose-50 (LD_{50}) varies between 1.1-2.3 mg/L depending on its entrance mode (Dar et al., 2022). Its usage has been banned in some countries such as Brazil and Canada. The reason for this decision was stated as the toxic effect of phorate on the agricultural workers during its application by Brazil and its observed adverse effects on all aquatic and terrestrial mammals by Canada. Additionally, phorate has been included in the Annex III chemical list of Rotterdam Convention which list the chemicals that are banned or

restricted for public health and environmental risk and subjected to prior informed consent procedure (UNEP/FAO, 2018). When phorate is used as an insecticide, it pollutes the environment via leaching to ground and surface waters and surface runoff, especially when it rains (Wu et al., 2010). Vryzas et al. (2009) examined the 147 substances in surface water bodies in the North of Greece near the Turkish and Bulgarian borders. Phorate sulfoxide, which is a known metabolite of phorate detected in the rivers in which samples were taken two months after the pesticide application (Vryzas et al., 2009). Furthermore, Lari et al. (2014) detected the phorate concentration varied between 0.19- 0.31 μg/L in surface waters of the three-region examined in India. Thus, the removal of phorate from water and wastewater is crucial for protecting the environment and public health.

Regarding the removal of phorate from water, an adsorption process could be considered as a promising method. As can be deduced from Table 1.2, there are no adsorption studies performed for phorate to the knowledge of the author. This gap in the literature is also addressed by Iwuozor et al. (2022). In their very recent review article in which they studied the adsorption of organophosphorus pesticides (OPPs), they stated that "Though lots of work has been done on the adsorption of various OPPs such as chlorpyrifos, diazinon, glyphosate, and malathion in the past eleven years, there still exists a paucity of published literature on the adsorption of some other types of OPPs such as acephate, azamethiophos, azinophos-methyl, ethion, isofenphos, paraoxon, phorate, tetrachlorovinphos, and terbufos" . So, the removal of phorate from water by adsorption process is worth to investigate. At this point, however, the selection of an effective, but cheaper, adsorbent to use is a challenging issue. Several different adsorbents were investigated for the removal of pesticides, as can be seen in Table 1.2. The maximum adsorption capacities depend on the pesticide and the adsorbent couple.

So, in this respect, natural zeolites, as a cheaper adsorbent, could be considered to test for the removal of phorate in comparison to the conventionally used adsorbent of activated carbon. There is no such a literature study; however, Ali (2022) recently used a natural zeolite of chabazite (CHA) as a heteregeneous catalyst in his study aiming the removal of two pesticides (carbendazim and malathion) from water by Fenton-like process. He observed that CHA yielded different adsorption capacities for carbendazim and malathion, attributing this difference to their different molecular sizes in comparison to the pore size of CHA. Carbendazim has molecular weight of 191.2 g/mol and kinetic diameter of 7.0 °A and, malathion has a molecular weight of 330.4 g/mol and 8.5 °A (Ali, 2022; Kowenje & Osewe, 2015). On the other hand, phorate has molecular weight of 260.4 g/mol and kinetic diameter of 7.9 (EPA, 2001; Kowenje & Osewe, 2015). Thus, phorate lies between carbendazim and malathion in terms of molecular weight and kinetic diameter. So, investigation of phorate removal by adsorption onto CHA would allow testing a cheap adsorbent as well as understanding the effect of molecular size of pesticides for their adsorption onto CHA.

Table 1.2 The studies on the adsorption of pesticides from aqueous solution onto different adsorbents

Pesticide	Adsorbent	q_{max} (mg/g)	Adsorption Isotherm/Kinetic Model	Notes	Reference
Deltamethrin	Oil shale ash	10.96	Langmuir	At 25 °C, pH 7.3	Al-qodah et al., 2007
4-chlorophenoxyacetic and 3-bromophenoxypropionic acids	Activated carbon	4.77 mmol/g	Langmuir	At 15, 25, 35, 55 °C, pH 2.2	Marczewski et al., 2016
2,4dichlorophenoxyacetic acid (2,4-D)	Peanut shells		Freundlich / PFO	25 °C	Demirhan & Culhaloglu, 2018
Bentazon, Clopyralid, Imidacloprid, isoproturon andmetalaxyl-m	Different zeolite types	-	Freundlich/PSO	22 °C	De Smedt et al., 2015
4-chloro-2-methyl phenoxy acetic acid (MCPA)	Coffee waste	34	Langmuir/PFO	25 °C	Al-Zaben & Mekhamer, 2017
Malathion	AC, Bentonite (B, Kaolinite (K)	37.7-72.6	Freundlich/PFO (K) -PSO (AC, B)	18 °C pH=6	Donia et al., 2012
Methylparathion	Vermicompost	0.17	Langmuir	pH=6.8	Mendes et al., 2012
Malathion	Waste jute fiber	71.68	Langmuir/PFO	At 28 °C, pH 6.57	Krishna, 2015

1.2 The Aim and Scope of the Study

This study mainly focuses on the removal of phorate from the water via adsorption onto powdered activated carbon (PAC) and chabazite (CHA), along with the determination of adsorption equilibrium and the kinetic behavior of PAC and CHA for phorate.

In order to achieve this goal, adsorption kinetics experiments under different operational parameters were performed for both of the adsorbents. The tested parameters were pH (3, 7, and 9), temperature (15, 25, and 35 ºC), shaking speed (120, 160, and 200 rpm), initial phorate concentration (1, 0.75, and 0.5 mg/L), and adsorbent doses (12.5, 25 and 37.5 mg/L). The effects of these parameters on the removal and adsorption kinetics were investigated. Additionally, in order to examine the equilibrium conditions of phorate adsorption onto PAC and CHA and to determine the maximum adsorption capacities of these adsorbents, adsorption equilibrium (isotherm) experiments were conducted by varying the initial phorate concentration (between 0.3 and 8 mg/L) at constant pH (pH 7), temperature (25±2 ºC) and mixing intensity (160 rpm).

CHAPTER 2

THEORETICAL BACKGROUND AND LITERATURE REVIEW

2.1 Pesticides

2.1.1 General Information

The pests, which include vectors, unwanted plants, and animals, can interfere with the production, harvesting, storage, processing, transportation, and even the marketing of food and agricultural goods. For the protection of these goods, pesticides which are artificial substances, are used to prevent, demolish or control pests. Pesticide, as a term, is known to describe a wide range of biologically active agents. Pesticides are categorized as fungicides, herbicides, bactericides, rodenticides, insecticides, nematicides, and molluscicides, depending on their biological target (Ahmad et al., 2010; Sud & Kaur, 2012).

Pesticides are composed of both 'active' and 'inert' ingredients. Active ingredients may function for the prevention, destruction, repellent, or mitigation of a pest or may function as a plant regulator, defoliant, desiccant, or nitrogen stabilizer, whereas all other ingredients are inert ingredients that are significant for usability and performance of the product. Active ingredients must be specified on the product's label by indicating the name and its percentage by weight. Several categories of active ingredients are present, which are conventional ones (all ingredients excluding biological pesticides and antimicrobial pesticides), antimicrobial ones (substances or mixtures of substances used for destruction or suppression of the growth of harmful microorganisms such as bacteria, viruses, or fungi on inanimate objects and surfaces) and biopesticides (types of ingredients obtained from certain natural materials). Inert ingredients, on the other hand, are added active ingredients to form a pesticide product.

They are chemicals and other substances such as food commodities and natural materials. The name 'inert' should not be confused with non-toxic. They serve as the promoter of the effectiveness and performance of the pesticide product (EPA, 2022a).

The application of pesticides increases as the demand for agricultural products increases. According to FAO, the average value of pesticide application rose from 2.06 kg/ha to 2.66 kg/ha between 2000 and 2018. Asia had higher pesticide use values in the years 2000 and 2018. The usage per hectare was 3.69 kg in 2000 and 3.54 kg in 2018 for this continent. For Europe, the average value in 2018 was given as 1.67 kg/ha (Sarkar et al., 2021). The pesticide use per hectare of cropland in developing countries can be seen in Figure 2.1.
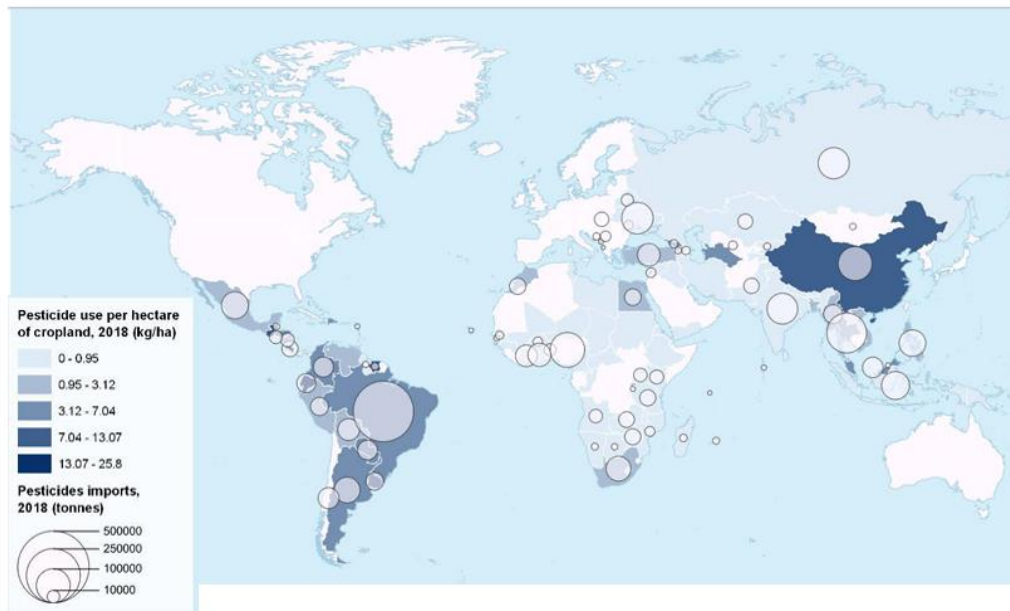
Figure 2.1 The pesticide use in developing countries (Sarkar et al., 2021)

The pesticide use per hectare of cropland in Turkey is shown in Figure 2.1. In Turkey, 0.95 – 3.12 kg of pesticide is used per hectare (TSI, 2021). According to data provided by the Turkish Standards Institute (TSI), 100.000 tonnes of pesticides were imported in 2018 and the total annual pesticide use in Turkey is nearly 60.000 tonnes in 2018, while it is around 55 000 tonnes in 2021 (Figure 2.2).
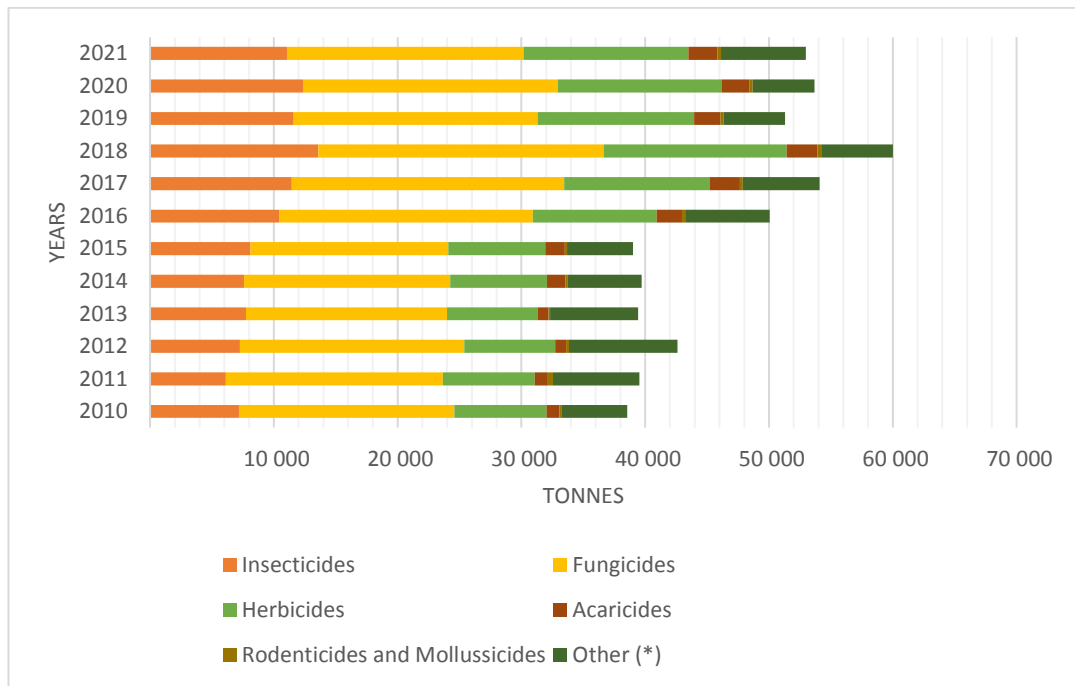
Figure 2.2 Pesticide usage in Turkey between 2010-2021 (TSI, 2021)

The intense use of pesticides for years has led to serious environment and public health-related problems. Pesticides being a pollutant, can disturb the characteristic of soil and harm biodiversity. It has been stated that less than 0.1% of the used pesticide reaches the target pest while the rest pollutes the environment (soil, water, and the air). This contamination can be caused by transportation, volatilization, erosion, leaching, surface runoff, and dispersion when the pesticides are sprayed (Sabzevari & Hofman, 2022). Some properties, such as being quite lipophilic, having a long half-life, being able to be transported in long distances and bioaccumulation, have positively affected their usage; hence, their potential to contaminate the environment (Jayaraj et al., 2016). Although pesticides are mostly applied to plants, their residues turn out to be present in food originating from animals. Due to the contamination of the environment and their inclusion in the food chain, the residual pesticides and their transformation products can reach humans and ecosystems where they can bioaccumulate (Jäger, 2019; Sabzevari & Hofman, 2022).

2.1.2 Classification of Pesticides

Pesticides are classified based on various measures such as hazard, target pest they kill and pesticide function, chemical composition, mode of entry, mode of action, how or when they work, formulations, and sources of origin are among these classification criteria (Akashe et al., 2018). World Health Organization (World Health Organization, 2020) has offered a classification of pesticides according to their hazard as tabulated in Table 2.1.

Table 2.1 Classification of pesticides regarding hazard level (World Health Organization, 2020)

Class		LD_{50} for the rat (mg/kg body weight)	
		Oral	**Dermal**
Ia	Extremely hazardous	< 5	< 50
Ib	Highly hazardous	5-50	50-200
II	Moderately hazardous	50-2000	200-2000
III	Slightly hazardous	Over 2000	Over 2000
U	Unlikely to present acute hazard	5000 or higher	

For this classification, the international conventions and their annexes were also taken into consideration. Phorate belongs to Class Ia (extremely hazardous) since LD_{50} value of it is 2, its exposure in the long term by low to moderate concentration results in death, and its trade on the international level is regulated by Rotterdam Convention (Montana et al., 2021; World Health Organization, 2020).

The classification of pesticides can be made with respect to their target organism as well (Akashe et al., 2018). Classification of pesticides according to their target organism to destroy is given in Table 2.2.

Table 2.2. Pesticide Type and Target Pest to Kill (Lade, 2017)

Nematicides	Nematodes (roundworms)
Molluscicides	Slugs and snails
Insecticides	Insects
Acaricides (or miticides)	Fleas, ticks, and mites
Piscicides	Fish
Avicides	Birds
Rodenticides	Rodents
Bactericides	Bacteria
Algicides	Algae
Fungicides	Fungi
Herbicides	Plants

Pesticides such as insecticides, fungicides, herbicides, and rodenticides are further divided into sub-branches according to their chemical composition (Akashe et al., 2018). The aforementioned sub-branches of pesticides based on their target organism with their possible chemical composition are presented in Table 2.3.

Pesticides can be classified as biopesticides or chemical pesticides according to the source of origin (Akashe et al., 2018). Bio-pesticides are then further divided into three categories. Biochemical pesticides are natural substances that are used in pest control in a non-toxic manner, microbial pesticides use microorganisms that control pests, and plant-incorporated protectants are formed upon addition of genetic material to the plants and production of pesticidal substances by this plant (EPA, 2022b). Biopesticides have some advantages over chemical pesticides. They are host-specific, eco-friendly, easily decomposable, required in low quantities, and less susceptible to genetic modification in plants (Yadav & Devi, 2017). On the other hand, chemical pesticides cause a decrease in insect population due to acting on non-target organisms in a more toxic way; hence biological balance and biodiversity of the treatment area may be affected. Also, they may leave chemical residues on the food sources either through direct application or biomagnification process. Their common use in

agricultural activity transport these chemicals into groundwater sources and consequently pollute the water bodies (Essiedu et al., 2020).

Table 2.3 Sub-branches of pesticides with respect to target organism and their possible chemical structure (IPCS, 2002)

Insecticides	Pyrethroids, organophosphorus, carbamates, organochlorine, manganese compounds
Herbicides	Bipyridyls, chlopehenoxy, glyphosate, acetanidiles, triazines
Fungicides	Thiocarbomates, dithiocarbamates, cupric salts, thiabendazole, triazoles, dicarboximides, dinitrophenol, organotin compounds, miscellaneous
Rodenticides	Warfarines, indanodiones
Fumigants	Aluminum and zinc phosphide, methyl bromide, ethylene dibromide
Insect Repellents	Diethyitoluamide

A representative figure covering some of the aforementioned classifications is given in Figure 2.3.

Classification of pesticides

Hazard level
- Extremely hazardous
- Highly hazardous
- Moderately hazardous
- Slightly hazardous
- Unlikely to present acute hazard

Type of the pest targeted
- Molluscicides
- Nematicides
- Acaricides
- Rodenticides
- Insecticides
- Acaricides
- Bactericides
- Algicides
- Fungicides
- Herbicides

Origin of the pesticide
- Bio-pesticides
- Chemical pesticides
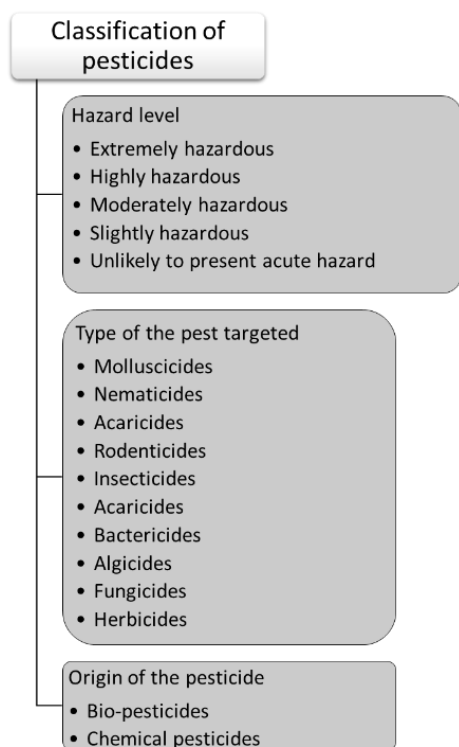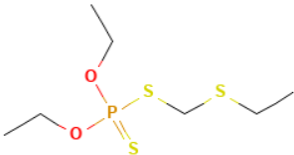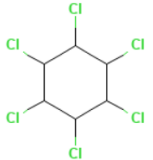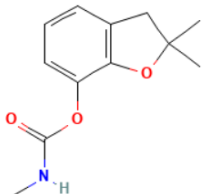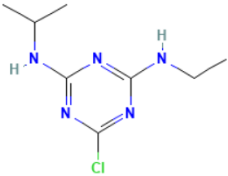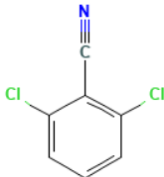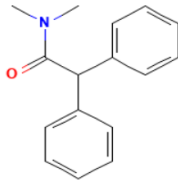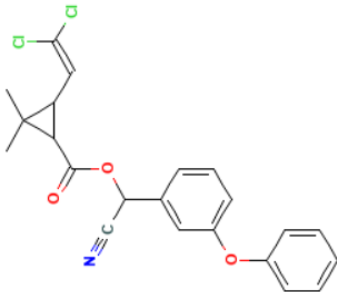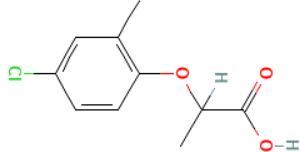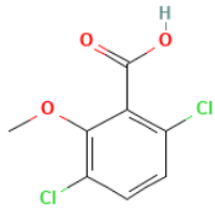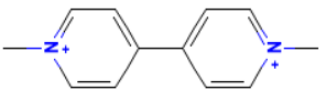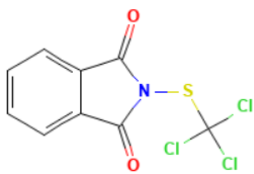
Figure 2.3 Classification of pesticides

When the chemical structure is considered, chemical pesticides are categorized as organochlorines, organophosphates, carbamates, triazines, benzonitriles, phenyl amides, pyrethroids, phenoxyalkonates, benzoic acid derivatives, dipyrids, phthalimide derivatives and miscellaneous etc. (Rani et al., 2021). These sub-groups of chemical pesticides, with an example, are given in Table 2.4.

Table 2.4 Chemical pesticides classified by their chemical structure and an example pesticide for each sub-group

Sub-Group	Example pesticide	Chemical structure*
Organophosphorus	Phorate	
Organochlorines	Lindane	
Carbamates	Carbofuran	
Triazines	Atrazine	

Sub-Group	Example pesticide	Chemical structure*
Benzonitriles	Dichlobenil	
Phenyl amides	Diphenamid	
Pyrethroids	Cypermethrin	
Phenoxyalkonates	Mecoprop	
Benzoic acid derivatives	Dicamba	
Dipyrids	Paraquat	

Sub-Group	Example pesticide	Chemical structure*
Phtalimide derivatives	Folpet	

*All chemical structures are taken from the corresponding PubChem webpage of pesticides

Organochlorine pesticides contain five or six Cl atoms in their structure. They are the first synthetic organic pesticides for agricultural and public use. In general, they are chemically stable, which results in persistent nature. Most organochlorines are insecticides that are used in insect control. These insecticides disrupt the nervous system of insects and paralyze them, which leads to the eventual death of these organisms. Most organochlorine insecticides are banned due to the severe effect on the endocrine system of mammals, birds, and fish (Jayaraj et al., 2016).

Another type of pesticide is organophosphorus (OP) compounds, which contains phosphate group and are considered highly toxic. The synthesized OP chemicals were used as warfare agents in World War II. Since then, they have been used as pesticides and in many other products, such as medicine and cosmetics. These pesticides inhibit the acetylcholinesterase enzyme in humans. The residues of these type of pesticides is one of the greatest threats to the environment, ecosystem and agricultural goods since their effects are irreversible and they are acutely toxic. Carbamates are pesticides that derivated from carbamic acid, and they inhibit the activation of acetylcholinesterase in a reversible way. These three mentioned pesticide groups (organochlorines, organophosphates, and carbamates) have severe toxic effects, and the later formulated pesticides such as pyrethroids and phenyl amides are less toxic (Özkara et al., 2016).

2.1.3 Occurrence of pesticides in the environment

The pesticides may end up in water courses due to point or non-point sources. Point sources may include storage areas where the pesticides are stored improperly, spills

from incidents, and disposal of pesticides without taking necessary precautions. Also, urban use of insecticides is viewed as a point source of contamination. On the other hand, large agricultural areas where it takes time for pesticides to reach water bodies are considered as non-point sources (Syafrudin et al., 2021).

Pesticides that are soluble in water can be transferred into the deeper layer of the soil and finally into the aquifers and surface waters, especially when there is precipitation. Detectable pesticide concentrations in surface and ground waters are observed near agricultural and urban land areas where pesticides are likely to be applied (Syafrudin et al., 2021; Torstensson, 2022).

The presence of pesticides in drinking water has been regulated by national institutions to protect the environment and public health. Table 2.5 presents the guideline levels determined by WHO for some of the pesticides (Hamilton et al., 2003).

Regarding the occurrence of pesticides in surface and groundwater, there are several studies published in the literature. In a recent study, Syafrudin et al. (2021) reported the presence of 11 pesticides in the Tengi River (Malaysia) at concentrations between approximately 3 ng/L to 5 µg/L. However, the outcome of the use of pesticides in a continuously increasing manner has polluted the drinking water source, the Tengi River, of a drinking water treatment plant. The effluent of the drinking water treatment plant contains 4 of 11 pesticides with a concentration range of 5.2 − 56.6 ng/L. Imidacloprid and tebuconazole, which are an insecticide and fungicide, respectively, have been detected frequently since they are applied to rice fields twice a month. The highest imidacloprid concentration is nearly 60 ng/L downstream, while tebuconazole has the highest concentration of about 510 ng/L in the middle of the river (Syafrudin et al., 2021).

Table 2.5 Guideline levels of some pesticides by WHO (Hamilton et al., 2003)

Pesticide	Guideline value (µg/L)
Alachlor	20
Carbofuran	7
Bentazone	300
Chlordane	0.2
DDT	2
Molinate	6
Trifluralin	20

A similar case study was reported for Japan. Due to pesticide application in paddy fields in the Shinano River Basin, the river that provides the majority of drinking water was polluted. In the river, 53 pesticides have been detected, including 22 herbicides, 15 insecticides, 11 fungicides and 5 transformation products. The pesticide concentration varied between 3 ng/L to 8.2 µg/L. It is highlighted that the transfer of these chemical substances to the sea through the river may affect marine ecosystems and animals (Syafrudin et al., 2021). In Costa Rica, a study was conducted between 2007-2012 to monitor the pesticide presence and concentration in a river basin which is located in a tropical agro-ecosystem. 135 water samples and 129 sediment samples were collected and analysed in total. In water samples, the pesticides determined at the highest concentrations were dimethoate, propanil, diuron, and terbutryn, with a concentration of 61.2, 30.6, 22.8, and 4.8 µg/L, respectively. On the other hand, triazophos, cypermethrin, permethrin, terbutryn, chlorpyrifos and diuron had the highest concentrations (491, 71.5, 47.8, 38.7, 18.2, and 11.75 µg/kg, respectively) in sediments. However, carbendazim and endosulfan were the most frequently detected in both water and sediment samples (Marta et al., 2018). Stehle et al. (2019) conducted a comprehensive meta-analysis of field studies and reported pesticide concentrations in surface waters of the U.S. The samples were collected from 34 different states, and 52 herbicides, 38 insecticides, 7 fungicides and 12 herbicides were detected. The most frequently detected ones were atrazine, diazinon and simazine (Stehle et al., 2019).

2.1.4   Fate and Transport of Pesticides

The fate, mobility, and persistence of pesticides are controlled by several factors, which are physicochemical properties of pesticide, characteristics of the site, climate, weather conditions, biodiversity, and the processes pesticide is handled (Gavrilescu, 2005). As the pesticides are released into the environment, they may be exposed to sunlight, water, other chemicals available, microbes, plants, and animals and therefore, they may be subject to photolysis, hydrolysis, oxidation/reduction, biodegradation or metabolization, and expectedly, broken down (NPIC, 2021).

There are three main fate processes of pesticides, which are adsorption, transfer, and degradation. Nonetheless, the degradation process is not a complete process. Most pesticides are broken down into their transformation products (Gassmann, 2021). Pesticides are bound to soil particles through an adsorption mechanism. They are transferred to different environmental compartments through volatilization, leaching, runoff, absorption/uptake, and removal of crops. They are also degraded in the environment by microbial, chemical, and photodegradation mechanisms (Fishel, 2003). The transportation of pesticides to air compartments by volatilization may increase the potential to be transported along long distances (Tiryaki & Temur Çinar, 2010).

In order to evaluate pesticide persistence in environmental compartments, scientists use a measure named 'half-life', which refers to the period that half of the chemical is broken down. The half-life of the pesticide is determined by the application of pesticide to soils, leaves, or other surfaces of concern and measuring the period that half of the pesticide is degraded (NPIC, 2021).

- **Sorption**

Sorption of the pesticide is driven by two phenomena, weak chemical bonds and diffusion of the compound into the soil structure. By sorption of pesticide to the soil, pesticide becomes mobile in the environment and the risk of contaminating the soil and water sources is born. Non-sorbing compounds behave as inert materials; they

travel along water flow without being sorbed, whereas sorbing ones retain on the sorption surface. Generally, irreversible sorption occurs upon chemical reactions between the pesticide and soil surface by covalent bonding. Hence, pesticides are retained by the humic acid available in soil (Børgesen et al., 2015).

- **Degradation**

The degradation process of pesticides results in transformation products which are also known as metabolites or daughter compounds. Generally, these compounds are more stable and mobile rather than their parent substances. Therefore, their occurrence in ground and surface waters is more frequent. In the environment, biological degradation, photodegradation, and hydrolysis may take place. Soil characteristics such as moisture, temperature, pH, and organic content are important for biodegradation since it occurs mostly in the soil. On the other hand, photolysis may occur in water under UV radiation or readily catalysed chemicals. Moreover, the pH of the liquid medium is a crucial factor in the hydrolysis of pesticides. Depending on the chemicals and the processes, the stable metabolite number differs. However, pesticides generally have 2-4 main stable transformation products and several less notable daughter compounds and these fractions end up as a specific metabolite (Gassmann, 2021).

- **Transfer**

Pesticides can be transferred to the air by evaporation or wind drift. This mass transfer may result in the detection of the pesticide in soil and water. When the pesticide is applied by spraying, the studies have shown that 1-5% of it lost due to wind. The wind speed is the most important factor since a slight increase in the speed may double the amount of pesticide lost. Moreover, pesticides can be detected in surface water bodies or drainage channels due to surface runoff. When it heavily rains, the soil is saturated with rain water, and the soluble material and particles are carried through with this runoff. The soil type and the time between the spraying and the rain are important for both leaching and runoff of the water. As the time between the spraying of the pesticide and the rain increases, the risk of contamination due to runoff decreases. For the soil types, silty and clayish soils intensify the risk of water pollution. In addition, surface

runoff is seen frequently when the snow on the ground is melted (Torstensson, 2022). The process mentioned above is depicted in Figure 2.4.
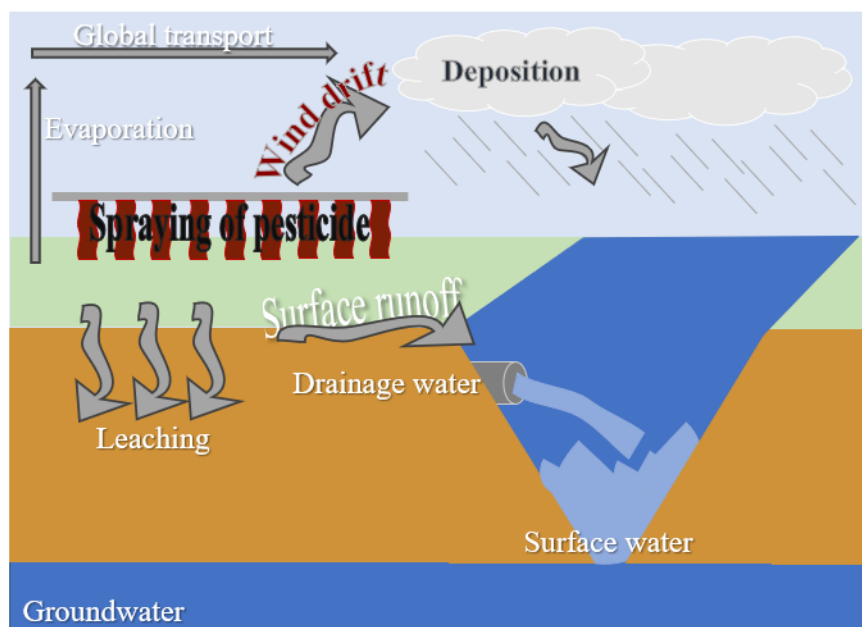
Figure 2.4 An example depiction of the transfer of pesticides (Torstensson, 2022)

When pesticides mix with streams via being transported by the surface runoff, their fate and behavior are controlled by chemical properties of pesticides such as water solubility, persistency, and Henry's law constant, and stream properties such as travel time, biological, physical, and chemical content of the stream, solid concentration and stream depth (Capel et al., 2001). When the pesticide is introduced to the aqueous environment, its effect is highly bounded to its water solubility. The ones that are capable of dissolving in water are more mobile, while fat-lover ones are prone to biomagnification in the food chain (Mojiri et al., 2020).

In surface water bodies, the contribution of photochemical degradation is undeniable for the fate of most pesticides. The photochemical degradation can take place directly or indirectly in water, and it can diminish the lifetime of pesticides. The measured photodegradation of a pollutant in a natural water system is the summation of direct and indirect mechanisms. Direct photodegradation occurs when a photon is absorbed

by the target pollutant and results in the chemical transformation to a more stable product. This mechanism matters in natural water streams only if the pollutant can absorb the sunlight which has a wavelength higher than 290 nm. In indirect photodegradation, an agent called photosensitizer absorbs the sunlight and generates reactive species, including radicals. Dissolved organic matters (DOMs) are a mixture of organic compounds that occur naturally in surface waters. They act as a photosensitizer and generate triplet DOM, hydrogen peroxide, hydrated electrons, singlet oxygen, and some radicals such as hydroxyl radical and peroxyl. These species may enhance the photodegradation of pesticides in water in some cases. However, it may also obscure direct photodegradation by acting as an anti-oxidant or as a sink for reactive molecules. Also, DOMs can decrease the direct photodegradation rate when they compete with pesticides for photon absorption (Remucal, 2014).

Another main mechanism for the transformation of pesticides in water is hydrolysis. This process can take place through either biotic or abiotic means. Abiotic hydrolysis may be the predominant process for the elimination of pesticides where biological activity is not observed. In hydrolysis, the pH of water is crucial since it occurs via H_2O, OH^- and H^+ species, and also pKa (acid-base dissociation constant) of the pollutant is another affecting factor. The rate of hydrolysis may be affected by other factors, such as temperature and solubility of pollutants. As solubility and temperature increase, the hydrolysis rate also increases. In addition, generally, the products of hydrolysis are more polar compared to the original compound and can be significantly more water soluble with less tendency to bioaccumulate. To exemplify, the hydrolysis of carbaryl, which is an insecticide, is the predominant first mechanism for degradation, and it takes place rapidly when pH is neutral or basic (Hamilton & Crossley, 2004).

2.1.5   Organophosphorus Pesticides

OP pesticides have been used for many different purposes, such as plasticizers, fire-retardants, fuel additives, agricultural chemicals, and even warfare agents. For most of these compounds, the toxicity is caused by the inhibition of acetylcholinesterase in the nervous systems. Among these several different usages, OPs are mostly used as pesticides to control insects. Organophosphate pesticides are the esters of phosphoric acid with a phosphor atom in the center. OP insecticides have become prominent in the 1970s due to the regulations on the application of organochlorine pesticides since OPs have higher efficiency with a less persistent nature (Dar et al., 2022; Pope, 2010).

OPs have been categorized into four subgroups regarding their molecular structures. These subgroups are phosphates, phosphorothioates, phosphorothioates, and phosphorothiolates (Figure 2.5) (Pehkonen & Zhang, 2010).
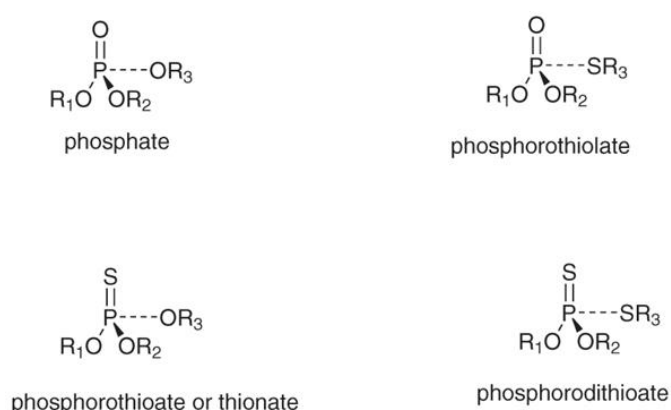
Figure 2.5 The chemical structure and nomenclature of the 4 subgroups of OPs (Pehkonen & Zhang, 2010)

Even though some of the OPs have been limited in terms of their application, several of them are allowed to be applied against pests. (Pehkonen & Zhang, 2010). In Table 2.6, the most commonly applied OPs are listed with some of their physicochemical properties.

24

Table 2.6 Some of the most commonly used OPs and their physicochemical properties (Pehkonen & Zhang, 2010)

Subgroup	OP name	Log Kow value	Vapor Pressure (mmHg)	Solubility in water at 20 ºC (mg/L)
Phosphorothiolate	Demeton-S	1.2	3.0×10^{-4}	3.3×10^{3}
	Oxydemeton-Me	-0.75	2.9×10^{-5}	10×10^{5}
Phosphate	Diazoxon	2.07	1.1×10^{-5}	2.5×10^{2}
	Mevinphos	0.13	1.3×10^{-4}	6.0×10^{5}
	Naled	1.38	2.0×10^{-3}	2.0×10^{3}
Phosphorothioate	Diazinon	3.81	1.1×10^{-2}	4.0×10^{1}
	Fenitrothion	3.30	5.4×10^{-5}	3.0×10^{1}
	Isazofos	3.82	8.7×10^{-5}	6.9×10^{2}
	Parathion	3.83	9.7×10^{-6}	6.5×10^{0}
Phosphorodithioate	Disulfoton	4.02	8.3×10^{-6}	2.4×10^{4}
	Malathion	2.36	7.9×10^{-6}	1.43×10^{2}
	Phorate	3.56	8.4×10^{-4}	5.0×10^{1}
	Phosmet	2.78	4.9×10^{-7}	2.4×10^{1}

When the physicochemical properties of OPs in Table 2.6 are evaluated, it can be said that they have relatively high-water solubility in the range of 6.5 (Parathion) – 1,000,000 (Oxydemeton-Me) mg/L. The compounds with vapor pressures lower than 1 Pa (10^{-5} atm = 7.6 x10^{-3} mmHg) can be stated as low volatile compounds (Interações et al., 2016). Hence, except naled (2.0×10^{-3} mmHg) and diazinon ($1.1 * 10^{-2}$ mmHg), all the pesticides given in Table 2.6 have low volatility. This indicates that they have strong intramolecular bonds and prefer the liquid phase of their pure solution instead of the gaseous phase. When the water solubility of these compounds is concerned, a wide range of solubility levels is encountered. Table 2.7 presents the water solubility ranges and the corresponding solubility levels.

Table 2.7 Water solubility concentrations and corresponding solubility level (Interações et al., 2016)

Aqueous solubility range (mg/L)	Solubility level
<1	Insoluble
1-10	Very low
11-50	Low
50-150	Intermediate
150-500	High
500-5000	Very high
5000>	Exteremely high

There is no insoluble pesticide among example pesticides; yet, parathion has very low water solubility (6.5 mg/L). Phosmet, diazinon, and fenitrothion have very low solubility (Table 2.6). Moreover, phorate has low to intermediate water solubility, while diazoxon and malathion have high water solubility. The rest have either very high or extremely high-water solubility. The solubility in water is increased when compounds have nitrogen, oxygen and sulphur containing functional groups and organic molecules such as alcohols, ketones, thiols, and amines by forming a hydrogen bond with water molecules. On the other hand, the presence of halogens or alkyl groups may decrease water solubility (Interações et al., 2016).

The degradation of OP pesticides in water may happen in several ways. The first way is oxidation which can be biological or abiotic means. In the bio-oxidation pathway, specific enzymes functions, whereas radicals, DO or dissolved chlorine perform in the abiotic oxidation of OPs. The second mechanism is the photolysis of OPs, which may take place directly or indirectly. Direct photodegradation of OPs is possible when OPs have an absorption spectrum coincidental with the solar spectrum. On the other hand, firstly, dissolved organic acids such as humic and fulvic acid may play the role of sensitizer, and secondly, particles may cause photodegradation assisted by semiconductors. Hydrolysis of OPs can take place in an SN2 mechanism in which water and hydroxide are the nucleophiles. Additionally, hydrolysis can be catalysed by dissolved metal ions. For example, divalent mercury ion is a catalyst for the

hydrolysis of malathion, fenthion, and fenitrothion. Another mechanism for the hydrolysis of OPs is surface-catalyzed hydrolysis, which is not clarified. Heterogeneous surfaces such as different clays and iron and aluminum oxides improve the hydrolysis rate through the surface sites where OPs and the nucleophiles can contact (Pehkonen & Zhang, 2010).

The degradation of OP pesticides in aqueous mediums can be achieved via adsorption, which also decreases the volatilization and leaching of these chemicals. The rate and degree of the adsorption, as well as the measure of complete degradation, are affected by the physicochemical characteristics of OPs. These characteristics may consist of volatility, solubility, overall charge polarity, molecular and chemical structure, and the diameter of the pest-controlling substances. The adsorption on soil particles can reinforce the abiotic degradation by which surface-catalyzed hydrolysis is meant while diminishing biodegradation by preventing contact between the OP and the enzyme. The adsorption of OP pesticides onto the soil particles can be physisorption which is established by Van der Waals forces. In addition, adsorption via ion exchange is also possible and effective for the sorption of cationic OPs on the soil particles, which have an overall negative charge. Furthermore, ion exchange-based adsorption may occur by the protonation of neutrally charged OP pesticides. Lastly, some ions like iron and aluminum ions can form a metal-ligand chelate with O, N, or S atoms of OPs (Pehkonen & Zhang, 2010). There are quite a number of articles studying the adsorption of OP compounds on different agents such as activated carbon, zeolites, mineral surfaces, and carbon-based material etc. This process is mainly dependent on the surface chemical structure and texture characteristics of the adsorbents (Skorodumova, 2018).

2.1.6   Phorate

Phorate is an OP insecticide (chemical name O,O-diethyl-S-ethylthiomethylphosphorodithioate, CAS No. 298-02-2) used for controlling several sucking and chewing insects, including Mexican bean beetle, corn rootworm, mites,

European corn borers, wireworms, white grubs, corn leaf aphids and seedcorn beetles (EPA, 2001; Hodgson, 2012; Pohanish, 2015). This insecticide is mostly implemented on crops such as corn, potato, cotton, fresh sweet potato, coffee, and peanut (Hodgson, 2012; EPA, 2001; Pohanish, 2015). By 2016, annual phorate production had been estimated at 3 million pounds, and annual acre treatment had been estimated at 2.5 million. Corn, potatoes, and cotton crops are the top highest usage of phorate in relation to pounds produced, having a share of 46%, 21% and 13% respectively, whereas potatoes, fresh sweet corns and peanuts crops have a proportion of 20%, 10% and 9% in terms of acres treated with phorate. It is also reported that phorate is not used for residential purposes (EPA, 2001). The 2D and 3D structures of phorate are given in Figure 2.6.
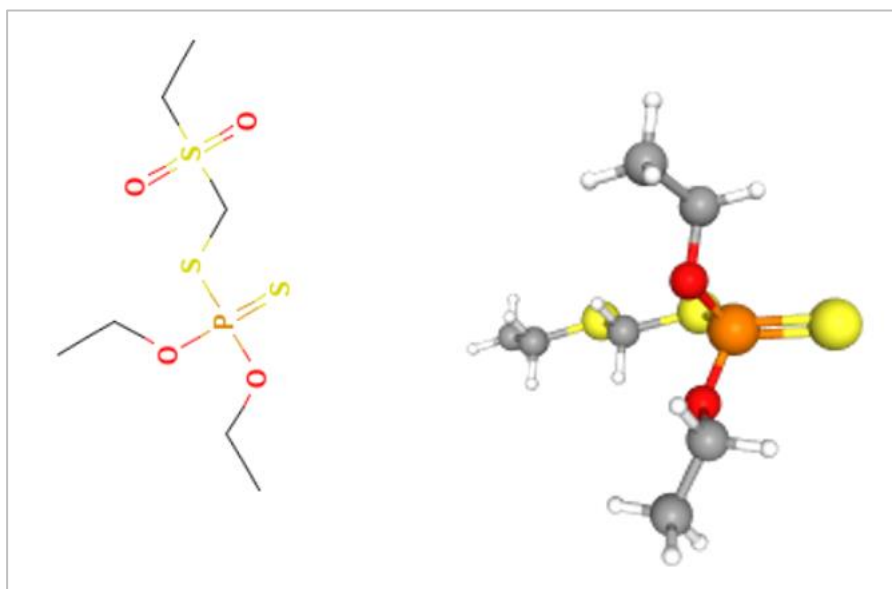
Figure 2.6 2D & 3D Chemical Structure of Phorate (National Center for Biotechnology Information, 2022)

Charge allocation among the atoms of a molecule gives information on the interaction mechanism between molecules. P atom in the phorate is suspected of nucleophilic attack since it has a charge density higher than zero, and O or S atom attached to the P atom may act as a nucleophile. This knowledge may be agible when designing decomposition mechanism processes both under acidic and basic conditions, which

leads to electrophilic or cationic attack, and nucleophilic attack, respectively. The P-S bond in phorate is the most suspected bond for both chemical and biological degradation (Kumar et al., 2018).

Phorate has a cholinesterase inhibition effect on humans, which causes the overstimulation of the nervous system resulting in nausea, dizziness, and confusion, and in case of high exposures due to accidents or major spills, it can lead to serious respiratory problems and death. Its primary toxicity mechanism of it is caused by its bioactivated oxon transformation product, also known as phoratoxon, which inhibits enzyme activation. It also poses a high risk for birds, fish, and mammals. Determined by the intake way, the average LD_{50} values of phorate vary between 1.1-2.3 mg/L (Dar et al., 2022; EPA, 2001; Moyer et al., 2018).

Classifications of phorate according to the classes described in Section 2.1.2 are tabulated in Table 2.8.

Table 2.8 Classification of Phorate Pesticide

Hazard	Extremely Hazardous	World Health Organization, 2020
Target Pest	Insecticide/nematicide	EPA, 2001
Chemical Class	Organophosphate insecticide	National Center for Biotechnology Information, 2022
Mode of Entry	Systemic, contact, and fumigant	T3DB, n.d.
Mode of Action	Systemic with contact and stomach action, acetylcholinesterase inhibitor	University of Hertfordshire, 2022
Formulation	Granular and emulsifiable concentrate formulations	E X T O X N E T, 1996
Source of origin	Chemical pesticide	EPA, 1985

The physico-chemical properties of compounds are important for their removal and degradation. Thus, some of the physicochemical properties of phorate, such as molecular weight, odor, vapor pressure, and more of phorate, are presented in

Table 2.9 Some physical and chemical properties of Phorate (Dar et al., 2022; National Center for Biotechnology Information, 2022; University of Hertfordshire, 2022)

Chemical Formula	$C_7H_{17}O_2PS_3$
Molecular weight (g/mol)	260,4
Density (kg/L)	1.156 (at 4-25 ºC)
Physical appearance	No color, light yellow
Odor	Skunk-like
Known metabolites	Phorate sulfoxide, Phorate sulfone
Stability	Stable for 2 years (technical grade, at room temperature) Optimum stability pH values between 5-7 for hydrolysis Degraded by light in aqueous solution ($DT_{50}= 1.1$ d)
Vapor Pressure (mmHg)	6.4×10^{-4} (at 25 ºC) (0.085 Pa and 8.4×10^{-7} atm)
Henry's law constant, K_H ($Pa*m^3/mol$)	5.9×10^{-1} (at 25 ºC)
LogKow	3.56
LogKaw (calculated by K_H/RT)	-3.62
Water solubility (mg/L)	50 (at 20 ºC)
Solubility in other solvents	Miscible in methanol, acetone, ethanol
Half-life (d)	2-15 (soil), 3 (hydrolysis)
Boiling point (ºC)	5-78 ºC (@ 0.1 mmHg), 118-120 ºC (@0.8 mmHg), 125-127 ºC (@ 2 mmHg)
Melting point (ºC)	-42.9 ºC
Topological polar surface area ($ºA^2$)	101
Calculated kinetic diameter (ºA)	7.9

Phorate has low volatility since it has vapor pressure lower than 1 atm, which approximately corresponds to 10^{-5} Pa. Thus, it can be stated that the phorate prefers its own liquid phase rather than the gaseous phase. Additionally, it has low-to-moderate solubility in water due to its solubility (50 mg/L) being the top limit for low water

solubility and the bottom limit for moderate water solubility. Also, it is extremely soluble in organic solvents such as methanol and acetonitrile. K_H values smaller than 0.1 Pa.m^3/mol at room temperature indicate a lower potential for volatilization from aqueous solution, while K_H higher than 100 Pa*m^3/mol indicates a higher potential for volatilization (Interações et al., 2016). Phorate has Henry's law constant value of 0.59 Pa.m^3/mol, which is higher than 0.1 Pa.m^3/mol and lower than 100 Pa.m^3/mol. Hence, it can be stated that it has a moderate potential for volatilization from water. This case can also be explained by K_{ow} (3.56) and K_{aw} (-3.62) values of phorate. As it can be seen from Figure 2.7, phorate does not have a strong affinity for any environmental compartment under environmental standard conditions. Hence, it can be asserted that the behavior of phorate in the environment is dependent of the specific environmental conditions. However, it can be noted that its tendency for aqueous and solid compartments is stronger than its tendency for the gaseous compartment.
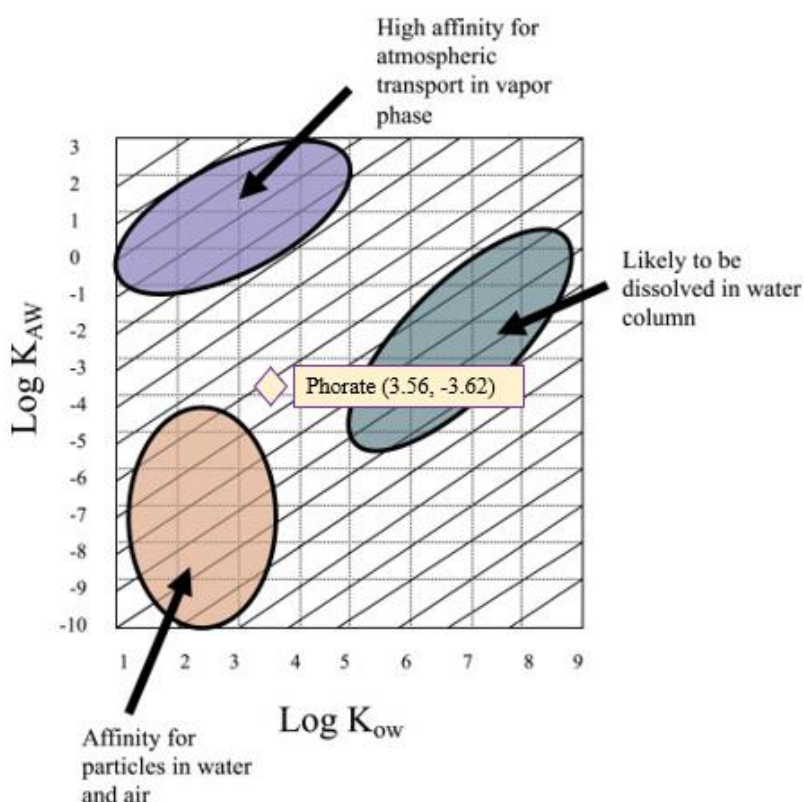
Figure 2.7 LogKow vs. LogKaw diagram and affinities of pollutants for environmental compartments under standard environmental conditions (Vallero, 2021)

Phorate is a dithioate OP pesticide similar to disulfoton which is a structural cousin of it. Phorate can be transformed into phorate oxon, phorate sulfoxide, and phorate sulfone by biotic or abiotic oxidation. Moreover, its hydrolysis is possible at the pH range of 5-9 in, which is observed in natural water bodies. The hydrolysis of phorate can occur via a nucleophilic attack on the central P atom or a C atom on a side chain at which the SN2 mechanism dominates with an OH^- or an H_2O molecule as nucleophiles (Hong et al., 2000). The hydrolysis rate constants for phorate for different pH and temperature values are given in Table 2.10.

Table 2.10 The homogenous hydrolysis rate constant of Phorate at different temperatures and pH values (Hong et al., 2000)

pH	Hydrolysis Rate Constant		
	11.4-14.0 ºC	24.5-27.2 ºC	35.5-36.5 ºC
5.7	$4.17*10^{-7} \pm 3.98*10^{-8}$	$3.71*10^{-6} \pm 3.69*10^{-7}$	$1.5*10^{-5} \pm 5.70*10^{-7}$
8.5	$3.75*10^{-7} \pm 1.96*10^{-8}$	$3.15*10^{-6} \pm 5.03*10^{-7}$	$1.47*10^{-5} \pm 2.67*10^{-6}$

From Table 2.10, it is apparent that with the increasing temperature, hydrolysis rates at both pH values increased (Hong et al., 2000).

OPPs show resistance toward biodegradation, especially in the land on which agricultural activities are held or factories of pesticide production, since they are detected in high concentrations which causes the toxic environment for microorganisms (Aislabie, 1995; Dar et al., 2022). Several bacterial strains which are capable of degrading phorate have been isolated and identified in various studies. The consortium isolated from soil samples from an agricultural field of India was proved to degrade phorate from 20 to 5.4 µg/mL in liquid samples in one week whereas in soil, 55% of biodegradation of phorate was attained (Dar et al., 2022). In another study, it has been stated that *Bacillus* and *Pseudomonas* spp. isolated from soils where agricultural activities are held were able to degrade phorate (40 mg/L) in 14 days.Similarly, two strains of *Sphingobium* sp. isolated from the agricultural soils of South Korea degraded phorate (24 mg/L) in seven days (Ahn et al., 2018). In another

article, it is revealed that the strains of *Bacillus, Pseudomonas, Staphylococcus* and *Brevibacterium* degraded phorate (50 mg/L) in a mineral salt medium within 21 days by 97% when phorate was the only carbon source (Dar et al., 2022).

The biodegradation of phorate occurs in two different ways. The first pathway consists of two steps of oxidation. Firstly, phorate is oxidized to phorate sulfoxide rapidly and in the second step, phorate sulfoxide is further oxidized to phorate sulfone slowly. These two transformation products of phorate are more toxic than phorate itself. The second pathway includes the enzyme called phosphotriesterase, which is crucial in the initial bacterial degradation of phorate. This enzyme attacks the bond between P and O which results in the formation of phosphodiesters. *Ralstonia eutropha* (AAJ1 strain) has been noted to biodegrade phorate to diethyldithiophosphate, a non-persistent daughter compound, by using phosphodiesterase with half-life of couple of hours. (Dar et al., 2022)

When phorate is used as an insecticide, it pollutes the environment via leaching to ground and surface waters and runoff when it rains (R. Wu et al., 2010). The study of Lari et al. (2014) aimed to detect some pesticide residue, including phorate, in water bodies where agricultural activities are intensely held. Among these regions, phorate concentration varies between 0.19- 0.31 µg/L in surface waters of the three regions examined in India (Lari et al., 2014). Capel et al. (2014) detected phorate in watersheds of the U.S. with areas higher than 10,000,000 ha. In the same study, it is stated that the two main removal mechanism for phorate was determined as transformation and volatilization.

Moreover, a lab-scale design was set and run for the evaluation and selection of optimum conditions for AOP of phorate, chlorpyrifos and dimethoate by Gandhi et al. in 2016. The results of this study demonstrated that UV degradation rates for these three pesticides were increased by the addition of H_2O_2/Fenton's reagent. Among the AOPs studied, UV/Fenton yielded the highest removal efficiency for chlorpyrifos (50.3 %), while UV/H_2O_2 was the most efficient method for dimethoate and phorate, with removal efficiencies of around 97 and 90 %, respectively (Gandhi et al., 2016).

Baser (2021) studied the removal of phorate by adsorption on modified biochars as a part of her thesis. The results of the thesis showed that the complete removal of phorate (100% of removal efficiency) from water is achieved via the adsorption of phorate on biochars which are hydrothermally treated and modified by urea and KOH (Baser, 2021).

2.2   Treatment Methods for Pesticides

The selection of the most proper treatment method to eliminate pesticides from water or wastewater can be made by considering the type of pesticide and the efficiency of the method. There are several treatment methods for the removal of pesticides from water; however, the current trend is the application of combined systems which include physical, chemical, and biological processes. Each treatment technique has leverages and limitations regarding flexibility of the design, both capital and operational cost, pre-treatment demand, ease of operation, reliability, efficiency, sludge and transformation product formation, and environmental impact (Saleh et al., 2020)

For the removal of pesticides from water, chemical methods such as chlorination, Fenton reaction, ozonation, and AOP can be applied. In general, these techniques are applied by combining with photocatalysis and membrane technologies (Saleh et al., 2020). Li et al. (2016) studied the impact of pre-chlorination of four OPs in a simulated water treatment process chain consisting of PAC, followed by coagulation/flocculation-sedimentation and filtration, and post-chlorination. In this study, it is stated that pre-chlorination of OPs results in more toxic products which can not be removed by the following treatment unit (Li et al., 2016). Another method used in order to remove pesticides from water is AOPs. In this technique, oxidizing agents such as hydroxyl radicals ($\cdot$OH) and sulfate radicals ($SO_4\cdot-$) are used for the oxidation of the contaminants. AOPs are environmentally safe and remove pollutants without transferring them from one medium to another and formation of high sludge amount. Nonetheless, these processes require skilled personnel due to chemical complexity and high operational costs (Saleh et al., 2020). In the study of Vela et al. (2019), the

degradation of seventeen pesticides in the EU Priority List by the oxidation of sodium persulfate was investigated. By using sunlight, sulfate radicals are obtained from sodium persulfate in order to degrade the pesticides into less harmful substances and then carbon dioxide and water. The results yield an 87% decrease in dissolved organic carbon (Vela et al., 2019). Ozonation is another chemical method used for pesticide removal. In this method, ozone itself and/or its radical performs oxidation on the contaminant (Saleh et al., 2020). Ormad et al. (2007), investigated the effect of ozonation on the removal of 44 pesticides detected in the Ebro River. They reported that by ozonation, 70% of the pesticide was removed. Also, it is stated that 90% of removal efficiency is obtained when AC adsorption is combined with ozonation (Ormad et al., 2008). Fenton technology is a further chemical process for the treatment of pesticides. It is one of the most efficient techniques for the oxidation of organic pollutants. In this process, there is a chain of reaction between hydrogen peroxide and ferrous iron, which results in the formation of hydroxyl, hydroperoxyl, and the targeted pollutant radicals. This technology has been reported to have quite high removal efficiencies (95-100%) for the removal of OP pesticides (Saleh et al., 2020). In the article of Elodie et al. (2003), the removal of three pesticides was studied by applying the Electro-Fenton process in an acidic solution. The HPLC analysis and COD measurements revealed that 80% of all pesticides were mineralized due to the rapid and non-selective nature of radicals (Elodie et al., 2003).

There are several biological systems to purify wastewater from pesticides. This system can be anaerobic or aerobic. The degradation of pesticides by biological means can be considered as difficult; however, once the system is established, it is easy to operate. For some pesticides, pre-treatments such as photodegradation or enzymatic processes may be needed (Saleh et al., 2020). Bouteh et al. (2021) investigated the biodegradation of two OP (malathion and chlorpyrifos) in a lab-scale moving bed biofilm reactor. They obtained relatively high removal efficiencies (70% for malathion and 55% for chlorpyrifos) when HRT equals 3 h. Also, it is reported that removal percentages increased with the increasing organic loading rate and HRTs (Bouteh et al., 2021). Another study on the biodegradation of pesticides was conducted by

Oliveira and his team in 2015. In the study, the biodegradation of four pesticides (atrazine, chlorfenvinphos, diuorun, and isoproturon) by filamentous fungi was studied. The results showed that other studied pesticides than chlorfenvinphos are resistant to biodegradation by fungi species. However, the concentration of chlorfenvinphos was decreased to under the detection level (Oliveira et al., 2015). Shawaqfeh (2010) tested the biodegradability of Vyadine, which is a pesticide, by operating two reactors, one under aerobic and the other in anaerobic conditions. He stated that HRT of 24 h for the aerobic reactor and 12 hours for the anaerobic reactor was optimum for decreasing the concentration of Vyadine under 0.1 mg/L (Shawaqfeh, 2010).

Another group of methods for removing pesticides is physical treatment processes such as adsorption, photodegradation, sedimentation, and filtration (Saleh et al., 2020). Photodegradation of pesticides can be achieved by direct photolysis. In this process, pesticide molecules absorb the energy that light carries and then transform when the energy absorbed is higher than the activation energy. On the other hand, in indirect photodegradation, pesticides are transformed by the other chemicals generated by photochemical means. The removal rates are low in direct photolysis but can be enhanced by using light sources with higher intensity, such as pulsed light. The pulsed light technology has been tested for several pesticides (atrazine, phosmet, simazine, azinphosethyl, chlorpyrifosmethyl, and pirimiphosmethyl and stated as a successful process (Marican & Durán-lara, 2018). Aslan (2005) conducted a lab-scale submerged biodenitrification system followed by a sand filter to remove nitrate and pesticides from drinking water. The effluent from the reactor was passed through the sand filter. Pesticides used in the experiment have a moderate tendency to adhere to sand. As a result, the removal rates of 20-55% for studied pesticides were reported for HRTs of 5.5 and 7 h (Aslan, 2005).

Ahmad et al. (2008) tested the use of four different NF membranes for the removal of atrazine and dimethoate. Among the four membranes, NF90 performed the best, with a rejection rate higher than 80% for both of the pesticides (A. L. Ahmad et al., 2008).

There are numerous adsorption studies of pesticides with different adsorbents in the literature. Adsorption is a prominent process in order to remove both inorganic and organic contaminants, including pesticides, from water. The most commonly used adsorbent, AC, has been proven to separate pesticides from water successfully due to its high specific surface area and porosity. However, the high cost of the production of AC restricts its application in the industry because of economic considerations. Hence, some low-cost adsorbents, such as fly ash, lignin, caron cloth etc., have been studied as an option for AC (Memon et al., 2008). Salman et al. (2011), prepared AC from banana stalk and tested its performance for the removal 2,4-dichlorophenoxyacetic acid (2,4-D) and bentazon. The adsorption system is well-represented by PSO kinetic model, and the Freundlich model shows a better correlation for equilibrium conditions (Salman et al., 2011). Mostafa et al. (2021) studied the adsorption of four pesticides on Chitosan/Zeolite A complex. It is reported that adsorption behavior followed PFO kinetic model and Langmuir isotherm model. The column tests yielded 60-80% removal of pesticides depending on the bed depth (Mostafa et al., 2021). Table 2.11 presents some of the studies on the removal of pesticides from waters by various treatment methods.

Table 2.11 Studies on the removal of pesticides from waters by various treatment methods

Treatment method	Advantages	Disadvantages	Reference
Biological treatment	AS: • Environmentally-friendlier than chlorination • Lower costs compared to AOP; • Smaller land requirement.	• High sludge production • Skilled personnel needs • High energy consumption • Pre-treatment may be required depending on the pesticide • Possibility of being resistance to certain microorganisms	Saleh et al., 2020 Oliveira et al., 2015 Cara & Jităreanu, 2022

(Table 2.11 continued)

Treatment method	Advantages	Disadvantages	Reference
		• Longer degradation times. • Additional unit need for the separation of microorganisms	
	MBR: • Efficient with a small footprint • Once established, easy to maintain	• Membrane fouling • May require exogenous species for better removal.	
AOP	• Low sludge production and retention time. • High reaction rates. • No transfer of pollutants from one phase to another. • Treatment of several pesticides at one step.	• High operational and maintenance costs. • Formation of by-products	Saleh et al., 2020 Cara & Jităreanu, 2022
Fenton	• Simple operation • High removal percentages with biodegradable and nonbiodegradable pesticides.	• High ferrous iron sludge. • Low pH requirement • Requirement for the use of a chemical agent in large amounts	Saleh et al., 2020 Cara & Jităreanu, 2022
Physical methods (coagulation-flocculation, sedimentation, filtration)	Membranes: • Low energy requirement. • No chemical conditioning or phase change.	• Concentrate formation requires further handling. • The short usage time of membrane.	Cara & Jităreanu, 2022
Other chemical methods (chlorinatio, ozonation)	• Chlorination is low-cost and easy to operate. • Ozonation: High removal results	• Pre-chlorination may lead to more toxic by-products. • Ozonation: In-site production of ozone due short half-life. Higher costs due to	Saleh et al., 2020

Treatment method	Advantages	Disadvantages	Reference
		in-site production of ozone.	
Adsorption	• Faster when compared to biological methods. • Easy operation and simple process. • Flexible design. • Insensitive towards toxicity. • Effective results for the removal of most of the contaminants.	• Regeneration of adsorbent is a requirement. • Not destructive process. The pollutant is transferred from one phase to another. • Relatively high cost when AC is the adsorbent.	Mojiri et al., 2020 Ormad et al., 2008 Saleh et al., 2020 Memon et al., 2008

When the advantages and disadvantages of the treatment methods are considered, it can be asserted that all kind of methods has their own limitations and advantages. Biological means are promising for the mineralization of pesticides, yet, they may require longer time and skilled personnel for the best performance. Also, selecting proper microorganism species matters since some pollutants may be toxic to certain species. On the other hand, physicochemical processes such as coagulation and flocculation may require a high amount of chemicals, and especially for the sedimentation, the sludge produced is a further concern as well. Chemical methods such as chlorination and ozonation have excellent removal efficiencies; however, chlorination may result in chlorinated toxic by-products, and ozone should be generated, which requires additional space and high energy consumption. AOP and Fenton reactions are advantageous since they involve radicals that are a highly efficient oxidizing agent. These processes are effective and simple; however, AOP has high operational costs due to energy consumption, and the Fenton process requires a high amount of chemicals which leads to a large amount of iron sludges. On the other hand, adsorption is a frequently preferred method with high removal rates. Also, the design of adsorption systems is more flexible and insensitive to toxic products. However, it may require high costs, and the process itself is not destructive, which means the

pollutants are transferred from one medium to another. Altogether, the adsorption process can be evaluated as the most promising method for the removal of pesticides from aqueous solutions.

2.3   Adsorption

Sorption is defined as the interaction of a substance with a solid phase. In the absorption phenomenon, the molecules are drawn into 3D structural space, while in adsorption, the particles are bonded to the surface, which is 2D space. Depending on the bonding strength, adsorption can be categorized as chemisorption or physisorption. Physisorption includes weak interactions such as London forces and Van der Waals forces, while chemisorption occurs via covalent or ionic bonds. The strength of the interactions in chemisorption is 100 times higher than those in physisorption. A monolayer formation of adsorbate molecules onto the surface of the adsorbent is seen in chemisorption; however, multi-layer formation is possible for physisorption. Unlike chemisorption, physisorption is reversible and has low enthalpy. In addition, chemisorption can take place at all temperatures, yet, physisorption can occur at the temperature under the boiling point of the adsorbate (Al-Ghouti & Da'ana, 2020).

The insights of the adsorption process have been known for decades. This process is known as a surface phenomenon, and mostly, the adsorbent, which has a porous structure, is in the center of the process along with the adsorbate in a liquid or gas solution is interacted with the surface of the adsorbent via physical or chemical means. The adsorbent should have sufficient capacity and good kinetics since the whole process depends on it. The suitable adsorbent for an effective adsorption process should pose small pore sizes with a large network between the pores and excess micropore volume in order not to interfere with the movement of adsorbate molecules to the interior parts of the adsorbent (Al-Ghouti & Da'ana, 2020).

2.3.1   Factors affecting the adsorption process

The performance of the adsorption process is affected by the type of pollutant with its physicochemical properties and chemical structure and the properties of the adsorbent. The characteristics of adsorbate, such as molecular weight, molecular structure and size, and polarity, should be known for evaluating the adsorption performance of the adsorbent. Besides, needless to state, the properties of an adsorbent, such as surface chemistry, particle size, and chemical nature, affect the adsorption process as well as ionic strength, pH and temperature of the solution, pressure, shaking speed, and contact time (Rapo & Tonk, 2021).

There are several factors that have an influence on the adsorption process. The adsorption process is sensitive to pH and temperature changes since chemical interactions are sensitive to these parameters. In general, there is an increase in adsorption when there is a decrease in pH and temperature. Moreover, the contact time of the adsorbate and the adsorbent is an important factor. As the length of contact and time increases, the amount of adsorbate adsorbed increases as well. If it is a continuous system, the contact can be improved by either lowering the flow rate or increasing the adsorbent amount (Cheremisinoff, 2002).

Martin and Al-Bahrani (1978) studied the effect of experimental conditions on the adsorption of pyridine on AC both in an agitated flask (batch mode) and in a packed bed (column study). The summary of the results of their study is as follows: i) The system is controlled by the intraparticle diffusion in the batch system, while film diffusion is the controlling step for most parts of the experiment in the column system. ii) The ionised forms of the adsorbates were also adsorbed onto AC and the adsorption of these species was more influenced by the change in pH of the solution due to the competition between H^+ or OH^- ions and the adsorbate molecules, and the effect of pH change on the structure of AC surface. iii) The adsorption rate enhanced as the initial concentration of pyridine was increased in the solution. However, after a certain concentration, the column system is slightly affected by the change in initial concentration. iv) It was observed that it is possible to predict the behavior of the

column system from the batch system outcomes when the solution contains a single solute (Martin, 1978).

The properties of the adsorbent should be known for a better understanding of the adsorption process. Thermal stability, hydrophilicity, surface chemistry adsorption properties, and physicochemical characteristics such as bulk density and hardness can be thought to be some of these properties. To ascertain these properties, several methods and techniques are available (Nguyen et al., 2017). These techniques and methods for each property are listed in Table 2.12.

Table 2.12 The adsorbent properties and common techniques for the determination of them (Modified from Nguyen et al., 2017)

Adsorbent property	Determination techniques
Morphology	SEM, TEM
Surface chemistry	DRIFT, XPS, FTIR, RS, Boehm titration, Potentiometric titration, Point of zero charge, Isoelectric point
Hydrophilicity	Water contact angle
Adsorption property	Iodine number, molasses number, and methylene blue index
Ultimate analysis	%C, %O, %H, %N and %S (element analysis)
Proximate analysis	Moisture, volatility, total ash, and fixed carbon
Physicochemical properties	$pH_{1:20}$, cationic exchanged capacity, hardness, and bulk density
Crystalline structure	XRD
Thermal stability	TGA
Textural property	N_2 adsorption/desorption isotherm

2.3.2   Adsorbents

2.3.2.1 Activated Carbon

Activated carbon is the most commonly used adsorbent since it is prominent for removing pesticides, other organic pollutants, and metal ions even at low concentrations (Al-qodah et al., 2007). Moreover, AC has a large porous surface area and modifiable pore structure. These properties are gained via its 3-step production. The first step is dehydration at which carbonaceous materials are heated to remove excess moisture. In the second step, the heating process continues with a higher temperature in the absence of air which results in the removal of impurities such as tar and methanol. This step is known as carbonization. Following carbonization, the activation is performed, which is the last step to producing activated carbon. In

activation step, pores are enlarged by removing amorphous residues with use of carbondioxide,air and steam mixture at high temperatures (750-950 °C) (Benefield et al., 1982). Also, it is not highly sensitive to acidic/basic conditions and is thermally stable. There are two main disadvantages of AC use in the industries, which are high cost and regeneration (Foo & Hameed, 2010)

Adsorption onto AC is a complex process and depends on several properties such as the properties of adsorbate, the structure of adsorbent and adsorbate, surface chemistry, and physicochemical properties (pH, temperature, ionic strength, etc.) of the solution. Despite GAC and PAC are the most known and used adsorbents, there are some other materials such as carbon cloth, carbon black, and carbon fibers. PAC can be effectively used to remove the pesticide from drinking water when temporal or emergent contamination by pesticides occurs. Also, PAC is more advantageous than GAC in terms of cost and flexibility (Marican & Durán-lara, 2018).

Ormad et al. (2008) investigated the adsorption of 44 pesticides onto PAC. The percentage removal by PAC for all pesticides is demonstrated in Figure 2.8.
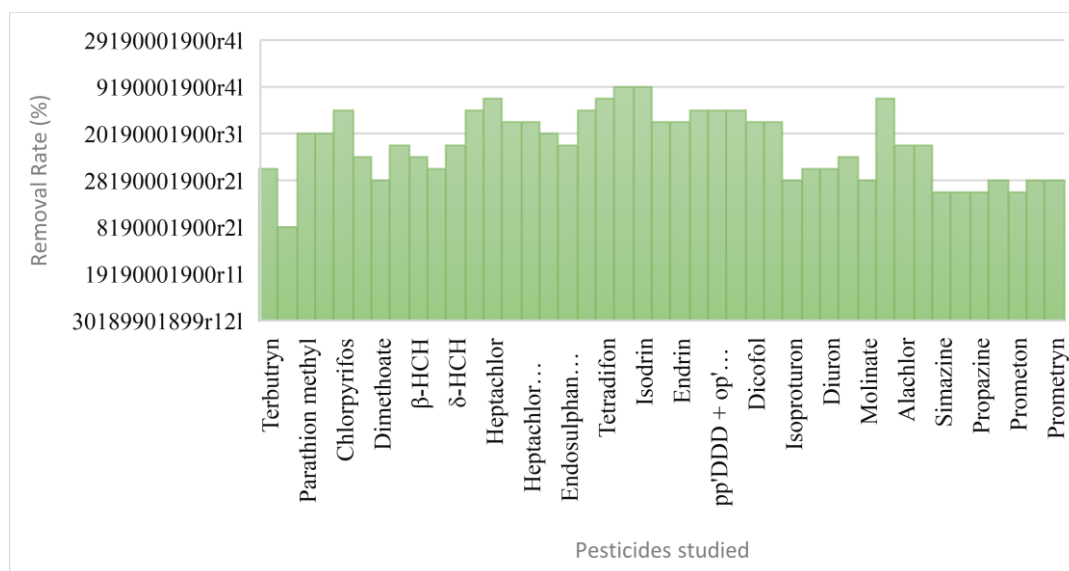
Figure 2.8 Pesticides studied and their removal percentages by PAC (Ormad et al., 2008)

From Figure 2.8, it is seen that the percent removals by PAC vary between 40-100 %, being around 75% on average. The lower removal rates (around 50%) are observed for the triazines having NH- groups. This is caused by the higher water solubility of these pesticides due to the amino groups. As a result, their adsorption onto PAC can be obstructed regarding this fact. On the other hand, higher than 90% of removals are reported for trifluralin, chlorpyrifos, hexachlorobenzene along with heptachlors, DDTS, and drins (Ormad et al., 2008).

2.3.2.2 Chabazite

Zeolites which are crystalline hydrated aluminosilicates with pores filled by water, alkali, and alkaline earth positively charged ions are natural adsorbents with high adsorption capacities. They are abundant in nature which makes them easily available. Additionally, they are low-cost adsorbents. Hence, they have been used as adsorbents for separation and purification purposes. A tectosilicate mineral of zeolites called chabazite is one of the most porous zeolite groups with a high surface area. It has stacked double six-membered ring prisms which are interconnected via four rings in a cubic and closed-packed array (Aysan et al., 2016). The structure of chabazite is presented in Figure 2.9.

6-ring at top of chabazite cage
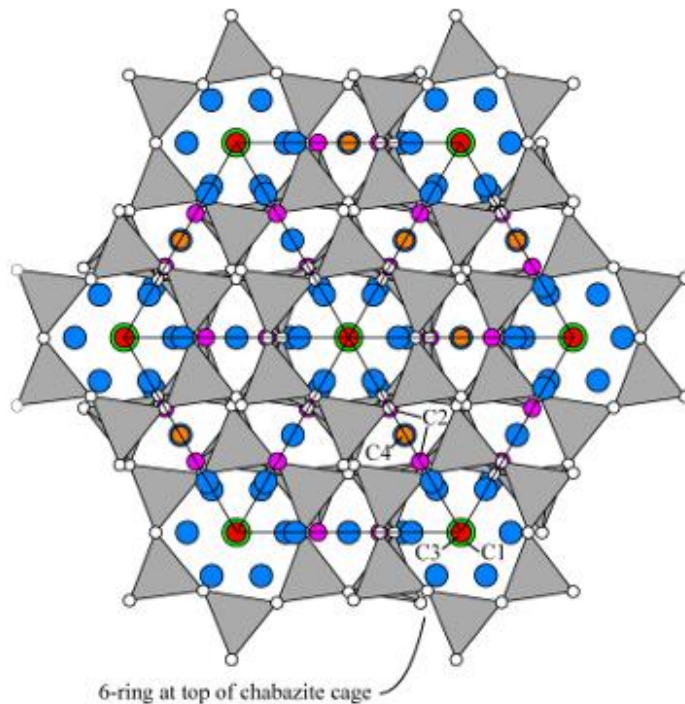
Figure 2.9 The chemical structure of chabazite (International Zeolite Association, 2022)

Chabazite is found in high quantities worldwide and has small pores, which allows for its use as an ion exchanger for the removal of contaminants (Aysan et al., 2016).

Zeolites have caught the attention of scientists due to their unique physicochemical characteristics, low cost, and availability. They are specially used for removing pesticides and heavy metals in pollution control, agriculture, and industry (Marican & Durán-lara, 2018).

Ogunah et al. (2013) investigated the adsorption of malathion onto zeolites X and Y types. They reported that when the concentration of malathion is low (5 and 10 mg/L), it is adsorbed by both types of zeolite. It is stated that adsorption capacity and the ratio of silica to aluminum should be known for the system design. Both adsorption onto zeolites and the catalytic effect of these adsorbents contributed immensely to the decrease in malathion concentration (Ogunah et al., 2013).

Another study on the adsorption of pesticides on natural zeolites were conducted by Salvestrini and his coworkers. Two different tuffs which are rich in zeolite were examined for the removal of atrazine from water. These adsorbents were Neapolitan yellow tuff containing 17% of chabazite and 37% phillipsite and clinoptilolitic tuff (79% clinoptilolitic) from Eskişehir/Turkey. The results illustrated that clinoptilolitic tuff had higher adsorption than neapolitan yellow tuff. Moreover, batch mode experiments were defined by PSO kinetic model. The pre-treatment of tuffs with increasing HCl concentrations yielded a significant boost in the adsorption capacity, followed by a gradual decrease for both of the tuffs studied. This reduction was explained by the acidic attack on Si and Al ions in the structure of the zeolites (Salvestrini et al., 2010).

Ali (2022) studied the pesticide (malathion and carbendazim) removal with the aim of developing a new heterogeneous catalyst from chabazite in order to apply for the Fenton-like process. Chabazite was subjected to pretreatment such as desilication, dealumination and ammonium exchange for the improvement of the physicochemical of chabazite. The pretreated and Fe-exchanged chabazite was applied for the oxidation of malathion and carbendazim and by using the Box-Behnken Design method, the effect of pH, catalyst dose, hydrogen peroxide and pH was examined. The results of experiments conducted indicated Fenton-like oxidation worked pH values between 3 and 7, which is a higher and wider range when compared to Fenton. For both of the pesticides, the highest removal efficiencies (81% for malathion and 88% for carbendazim) were observed under these conditions: 150 mg/L of hydrogen peroxide, 750 mg/L dose of Fe-exchange chabazite and at pH 5. The pretreated and Fe-exchanged chabazite was compared with two synthetic zeolites in terms of removal performance (Ali, 2022).

2.3.3   Adsorption Equilibrium

The adsorption of both organic and inorganic substances onto porous adsorbents such as AC, zeolite, and biochar can last for several days or weeks more to reach true

equilibrium conditions when compared to non-porous adsorbents (i.e., hydrochar and biosorbents). This time difference is mainly caused by the fact that pore diffusion is the generic adsorption mechanism among several mechanisms in porous adsorbents. Other mechanisms are hydrogen bonding, π-π interaction, electrostatic attraction, surface precipitation, cation exchange and η-π interactions (Nguyen et al., 2017). Thus, it is vital to know the relationships and mechanisms behind the adsorption process. In accordance with this fact, equilibrium relationships which are referred to as adsorption isotherms, define the interaction between the adsorbate and the adsorbent. Hence, obtaining the necessary information on the isotherm is crucial for an efficient adsorption system design, adsorption mechanism pathway optimization, and the statement of adsorbent capacity and properties of it (Foo & Hameed, 2010).

The isotherm models can be described as the functional relationship between the amount of adsorbate adsorbed by the adsorbent and the equilibrium concentration of the adsorbate in the liquid phase (or the pressure in the gas phase) at a constant temperature. These models are depended on the type of adsorbent and adsorbate and the physicochemical characteristics of the solution, which can be listed as pH, temperature, and ionic strength. The adsorption isotherms are determined if an adsorbate and adsorbent have sufficient contact time to establish a dynamic equilibrium between the concentration of the adsorbate in the interface and the bulk solution. Thus, the performance of the adsorbent can be depicted by the isotherm models when the equilibrium is reached and the temperature is constant. The obtained isotherms are commonly used for the characterization of adsorbents and the adsorption process for industrial purposes. Additionally, these models define the interaction mechanism between the adsorbate and the adsorbent considering the data belong to equilibrium state and adsorption characteristics. Six types of isotherm are classified by IUPAC regarding the shape of adsorbate-adsorbate pairs. The shape related to each type and hysteresis loops is illustrated in Figure 2.10 (Al-Ghouti & Da'ana, 2020).
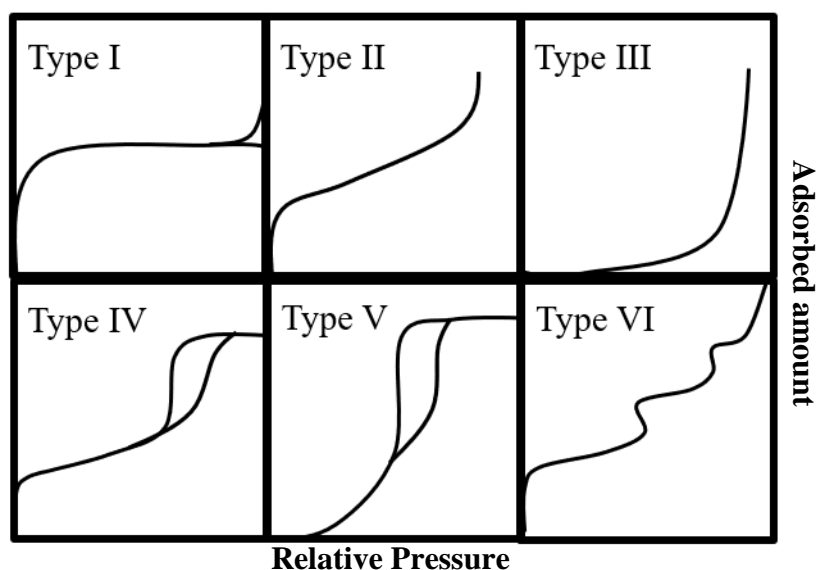
Figure 2.10 Classification of isotherms (Thommes et al., 2015)

For Type I isotherm, the curve is concave to the x-axis and the absorbed amount approaches a limiting value which is determined by the available micropore volume. This type is reversible and known by the solids such as some activated carbons and zeolites which have micropore-sized pores with small external surfaces. The sharp uptake at low relative pressure addresses the strong interaction between the adsorbate and the adsorbent in narrow micropores, which leads to the occupation of the micropores at low partial pressure. Type II is also reversible and formed by nonporous or macroporous adsorbents. The steep turning of the curve represents the completed monolayer formation, while a soft turning indicates the multilayer adsorption beginning. In Type III isotherm, there is no apparent monolayer forming. The adsorbate-adsorbent interactions are weaker, and the cluster of adsorbate molecules is seen on the favored sites of the nonporous or macroporous adsorbent. Many oxides gels and industrial adsorbents, which are mesoporous adsorbents, yield a Type IV isotherm curve. In mesopores, the adsorption behavior is governed by the adsorbate-adsorbent interactions and the molecular interactions in the condensed phase. In this type, before pore condensation, the primary mono-and multilayer formation takes place in the same way as the corresponding section of Type II. At low partial pressure, Type V isotherm behaves similarly to Type III, which can be deduced as weak

adsorbate-adsorbent interactions. On the other hand, at high relative pressure, molecular clustering and pore filling occur consecutively. To exemplify, the adsorption of water on hydrophobic microporous and mesoporous adsorbents gives this type of isotherm. The step-wise Type VI isotherm is reversible and is the model of layer-by-layer adsorption, including highly uniform nonporous adsorbent. The height of the steps corresponds to the layer adsorption capacity, whereas the sharpness of the steps relies on the temperature and the system. The adsorption of argon or krypton on graphitised carbon black can be considered the best example of yielding Type VI isotherm (Thommes et al., 2015).

Isotherm models are built by drawing a curve between the adsorbed amount by the adsorbate and the concentration of the adsorbate at equilibrium at constant temperature and pH. In general, isotherm data is modeled through a linear analysis to conjecture the adsorption behavior. In literature, there is a large spectrum of isotherm models such as Langmuir, Freundlich, BET, and Temkin etc. These models may approach to the adsorption phenomena through different concepts (i.e. dynamic equilibrium, thermodynamics etc.) as well as they may consist of the combination or the improved/extended version of other models (Al-Ghouti & Da'ana, 2020). However, in environmental adsorption studies, generally, Langmuir and Freundlich isotherm models agree well with the experimental data. Therefore, in this study, these models were tested. The examined isotherm models for the study are explained briefly in the following sub-sections.

In the adsorption field, the performance of adsorbent can be evaluated either calculating the amount of adsorptive adsorbed at equilibrium conditions or the percentage of adsorptive removed. The adsorbed amount when the equilibrium prevails (q_e) can be calculated by using the equation (Nguyen et al., 2017):

$$qe = \frac{Co - Ce}{m} V \ \dots\dots\dots \text{(Eq 21)},$$

where C_o is the initial adsorbate concentration (mg/L), C_e is the equilibrium concentration (mg/L) in solution, m (g or mg) is the dry mass of adsorbent used, V (L)

50

is the solution volume, and m/V (g/L or mg/L) is the solid/liquid ratio. Depending on the purpose, the unit of q_e can vary; for example, mg/g is the most commonly used unit for scientific, practical and engineering purposes (Nguyen et al., 2017).

2.3.3.1   Langmuir isotherm model

The theoretical equation for the Langmuir isotherm was proposed in 1932 by Irvig Langmuir. This model was originally applied for the adsorption of gaseous substances onto a solid material. The model developed by assuming that i) the number of active sites on the surface of solid material is fixed and they are homogeneous in terms of energy; ii) the adsorption onto the site is reversible; iii) when adsorbate molecule sorbed onto a site, there can not be further adsorption on that site (monolayer adsorption); and iv) adsorbate species do not interact with each other. The mathematical equations for this model are as follows (Nguyen et al., 2017):

$$\frac{dq}{dt} = k1 \, (qe - qt) \text{ (differential form) ....(Eq.1),}$$

$$qe = \frac{qmax*b*Ce}{1+bCe} \quad \text{(non-linear form) ……… (Eq.2),}$$

$$\frac{Ce}{qe} = \frac{Ce}{qmax} + \frac{1}{qmax*b} \text{ (linear form 1) ………. (Eq.3),}$$

$$\frac{1}{qe} = \frac{1}{qmax*b*Ce} + \frac{1}{qmax} \text{ (linear form 2) ………. (Eq.4),}$$

$$qe = qmax - \frac{qe}{b*Ce} \quad \text{(linear form 3) ……… (Eq.5),}$$

$$\frac{qe}{Ce} = qmax*b - b*qe \text{ (linear form 1) ………. (Eq.6),}$$

where q_e (mg/g) and C_e (mg/L) are equilibrium adsorption capacity and concentration, respectively. q_{max} (mg/g) is the maximum monolayer adsorption capacity, and b (L/mg) is affinity related constant.

Langmuir model is not valid for high pressures and it assumes a dynamic equilibrium where adsorption and desorption rates are equal to each other. When the pressure and

adsorbate concentration is low, the Langmuir model reduces to Henry's law. The nature of the adsorption can be defined by the separation constant, R. (Al-Ghouti & Da'ana, 2020)

$$R = \frac{1}{1+b*Co} \quad \text{(separation constant)} \ldots\ldots\ldots \text{(Eq.7)},$$

where C_o corresponds to initial adsorbate concentration (mg/L) and b is the Langmuir constant for adsorption capacity in mg/g. The separation factor is used as an indicator of the nature of adsorption. When R equals to zero, it indicates that the adsorption is irreversible, while values higher than 1 indicate that the adsorption is unfavorable. However, R has a value between zero and one, implying that the process is favorable (Al-Ghouti & Da'ana, 2020).

This isotherm model has a non-linear equation (Eq.1); however, in order to estimate its parameters, its linear forms are used since the linearization of Eq.1 allows a more simple, convenient, and easy way to calculate the parameters of Langmuir. The linear form 1 was reported to follow the least squares regression assumptions and yielded lower standard errors for the parameter estimation (Guo & Wang, 2019).

There are several articles exist in the literature reporting that the adsorption isotherm behavior of pesticides is defined by the Langmuir model. Table 2.13 summarizes some of these articles.

Table 2.13 Some examples from the article of which the adsorption isotherm behavior described by Langmuir model (Mojiri et al., 2020)

Pesticides	Adsorbent	Adsorption capacity (mg/g)	References
Bentazon	AC	169.4	Omri et al. (2016)
Carbofuran	AC	164.0	Salman and Hameed (2010)
Paraquat	AC	129.44	Zahoor (2013)
Methomyl	Natural clay	0.539	El-Geundi et al. (2012)

(Table 2.13 continued)

Pesticides	Adsorbent	Adsorption capacity (mg/g)	References
Diazinon	Modified magnetic nanotubes	112.36	Naeimi et al. (2018)
Paraquat	Magnetic biochar	34.23	Damdib et al. (2019)
Oxadiazon	Modified chitosan	5.02	Arvand et al. (2009)
Glyphosate	Chitosan	35.08	Rissouli et al. (2009)
Paraquat	Modified zeolite	166.71	Insuwan and Rangsriwatananon (2017)
Tebuconazole	Natural zeolite	0.5	Shikuku et al.
Aclonifen	PAC	110.74	Yılmaz,2019

Indeed, the results in Table 2.13 show that the adsorption of pesticides on zeolite and AC can be defined by the Langmuir isotherm model. These results may contribute to the fact that the adsorption behavior of porous adsorbents such as AC and zeolites is prone to follow the Langmuir isotherm model (Al-Ghouti & Da'ana, 2020). For the adsorption on AC, high adsorption capacities are observed, which indicates that AC is suitable for the removal of pesticides from the water via adsorption. For example, paraquat, which is a herbicide, has adsorption capacities of around 130 and 170 mg/g for AC and modified zeolite, respectively. However, its adsorption capacity on magnetic biochar (34.23 mg/g) is considerably less when compared to AC and zeolite.

2.3.3.2 Freundlich isotherm model

Herber Freundlich formulated the Freundlich isotherm, the first isotherm model, in 1939, using experimental data. The model is valid for heterogeneous adsorption; however, it can be converted to homogeneous adsorbents by equating n, which is the strength constant of 1. The equation of the model is given below (Thommes et al., 2015):

$$qe = Kf * Ce^{\frac{1}{n}} \quad \text{(non-linear form)} \dots\dots\dots \text{(Eq.8)},$$

$$logqe = logKf + \frac{1}{n}logCe \quad \text{(linear form)} \dots\dots\dots \text{(Eq.9)},$$

where q_e and C_e are equilibrium adsorption capacity (mg/g) and concentration, respectively (mg/L). K_f is the adsorption potential constant. n is the indicator for the type of adsorption, and 1/n shows the adsorption intensity. If the 1/n is lower than 1, it indicates that the adsorption is favorable, and better removal efficiencies are observed at low initial concentrations of adsorbate since the type of the adsorption is L-type and this type is defined by the increase at low initial concentrations. L-type isotherms are observed when adsorbate particles are sorbed in the form of monolayer and there is no competition between the water molecules and adsorbate molecules for the sites of the adsorbent, which explain increased affinity towards low concentrations. On the other hand, when 1/n equals to 1, the adsorption is irreversible, while values higher than 1 imply the process being unfavorable. (Al-Ghouti & Da'ana, 2020; Kushwaha et al., 2011; Thommes et al., 2015)

Freundlich isotherm defines the adsorption processes that are reversible and non-ideal. This model is not limited by the monolayer adsorption in contrast to the Langmuir isotherm model. The adsorption heat and affinity of sites can be distributed non-uniformly on the heterogeneous surface. This model shows that the ratio of the adsorbed amount on the adsorbent and the adsorbate amount in the solution is not constant. Hence, the total adsorbed amount is the summation of adsorption on each active site. Regarding the model, at first, stronger binding sites will be occupied and afterwards an exponential decrease will be observed in the adsorption energy while completing the adsorption. At low pressures, Freundlich isotherm behaves improperly with Henry's law, and at sufficiently high pressures, it does not approach a finite limit. Hence, the application range of this model is quite narrow (Al-Ghouti & Da'ana, 2020).

2.3.4 Adsorption Kinetics

Kinetic models address the information of adsorption rate, the performance of the adsorption, and the mass transfer. For the design of adsorption systems, adsorption kinetic information should be known. Mass transfer kinetic consists of three steps, namely, external diffusion, internal diffusion, and active adsorption sites (Figure 2.11) (Wang & Guo, 2020).
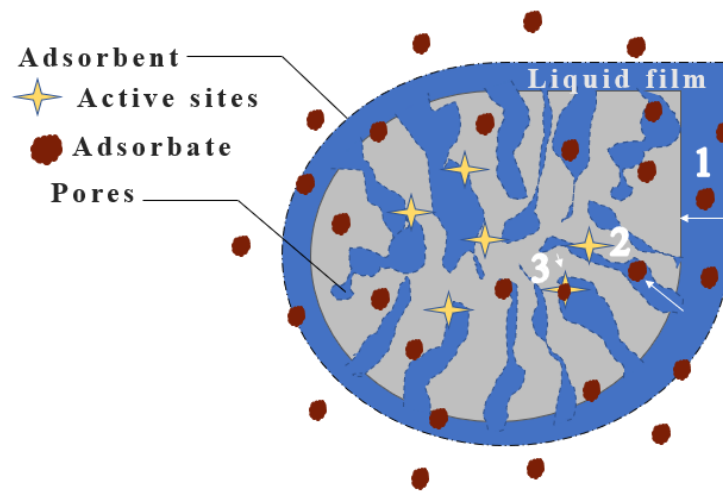
Figure 2.11 Mass transfer kinetics steps in adsorption (Wang & Guo, 2020)

The external diffusion is the first step, and the adsorbate moves through the liquid film layer which surrounds the adsorbents. The driving force in this step is the concentration gradient between the bulk liquid and the adsorbent surface. The second step is the internal diffusion which defines adsorbate diffusion through the pores. The last step is the adsorption of adsorbate onto the active sites of the adsorbent. These three steps are resistive to the adsorption process. The rate determined as a result of experiment is the overall adsorption rate which is the summation of resistances of three steps. Any reduction in the resistance in any step leads to an increase in adsorption. The resistance during the mass transfer can be affected by the properties of adsorbent and adsorbate and operational conditions. When compared to the first two steps, the last step, which is the attachment of the adsorbate molecule to the internal sites of the adsorbent, is the

fastest; thus, its resistance is ignorable. If one of the first two steps is the predominant one in the total resistance to the level that the resistance of the other reduced significantly, enhancing the adsorption, then that step is named as the rate-limiting step. The rate-controlling step may change throughout the adsorption process (Al-Ghouti & Da'ana, 2020; Wang & Guo, 2020). The basis of the kinetic study is tracking the adsorbed amount of adsorbate with respect to time. This study is used to establish a model to define the adsorption rate. Additionally, the ideal model should not be too complex, describes the rate-controlling mechanism, and be extrapolatable for the operational parameters considered (Al-Ghouti & Da'ana, 2020).

In order to define the kinetics of the adsorption process, numerous kinetic models such as Pseudo-first order (PFO), Pseudo-second-order (PSO), Elovich and mixed order kinetic models have been developed (Wang & Guo, 2020). PFO and PSO models have been applied in general for aqueous phase adsorption (Nguyen et al., 2017). The physical meanings of these two models are represented in Figure 2.12.

PFO model

$$\frac{dq_t}{dt} = k_1 (q_e - q_t)$$

$C_0 \gg \beta\theta$

1. C_0 is very high

2. At the initial stage of adsorption

3. A few active sites exist in the adsorbent

Langmuir kinetics model

$$\frac{d\theta}{dt} = k_a C_t (1-\theta) - k_d \theta$$

$$\frac{d\theta}{dt} = k_a (C_0 - \beta\theta)(1-\theta) - k_d \theta$$

PSO model

$$\frac{dq_t}{dt} = k_2 (q_e - q_t)^2$$

C_0 has the same orders of magnitude with $\beta\theta$

1. C_0 is low

2. At the final stage of adsorption

3. The adsorbent is abundant with active sites
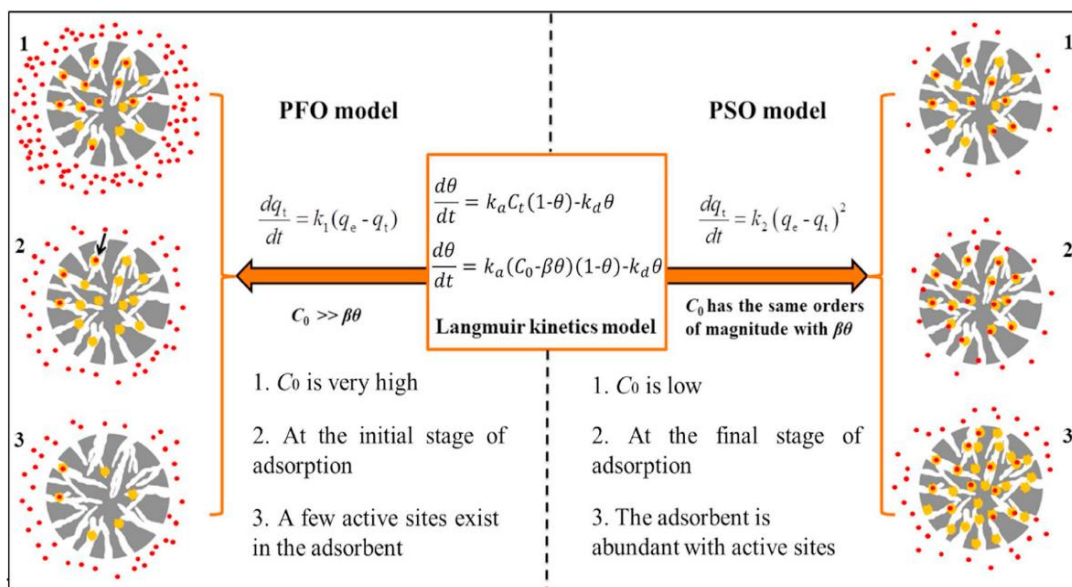
Figure 2.12 Physical meaning of the kinetics model- PFO and PSO (Wang & Guo, 2020)

56

When Figure 2.12 is examined, it is stated that if the initial adsorbate concentration is high with respect to adsorbed concentration and the adsorbent studied has a few active sites while including the data obtained from the beginning stage of adsorption, it is observed that PFO kinetic model defines such systems better. On the other hand, if the initial adsorbate concentration is low when compared to the adsorbed concentration of the adsorbate and the adsorbent has many active sites while considering the data from the experiments close to equilibrium conditions, PSO kinetic model is determined as the best-fittedd model for these systems (Wang & Guo, 2020). These aforementioned deductions were originally made by Azizian in 2004. In his article, he aimed to define the conditions at which PSO and PFO model must be used and deriving PFO and PSO models by a different method . For this aim, he studied the adsorption kinetics of four different adsorbate on four different adsorbent with different initial concentrations. The results of his experiments about the conditions at which kinetic model fits best was summarized in Figure 2.12.

Adsorption kinetics models demonstrate the mass transfer mechanism between the adsorbate and the adsorbent and how the adsorbent selected performs. Additionally, these models give information on the rate of adsorption. Therefore, while designing adsorption systems, it is vital to know the kinetics. There are three steps that are sequenced as external diffusion, internal diffusion, and sorption on the active sites when the mass transfer occurs between the adsorbent and the adsorbent. In the first step, the transfer takes place in the liquid film which surrounds the adsorbent. This transfer is induced by the adsorbate concentration gradient between the liquid film and the bulk liquid. The second step, namely internal diffusion, explains the diffusion in the pores of the adsorbent, whereas the last step describes the adsorption onto the active sites. Elovich, pseudo-first-order, pseudo-second-order, and mixed-order models are some examples of a large number of adsorption kinetics models (Wang & Guo, 2020). The kinetics of adsorption is affected by the type and characteristics of the adsorbate and adsorbent and the experimental conditions, e.g., pH, temperature, contact time etc. (Tan & Hameed, 2017). The studied models in the scope of this thesis are defined in short in the forthcoming sections.

2.3.4.1   PFO kinetic model

When reactants A and B interact with each other to form a single product, either A or B can be present in excess amount, and its concentration change over time can be negligible during the interaction. Thus, the concentration of the reactant with excess amount can be accepted as constant. This indicates that the reaction rate is only affected by the reactant, which is not in excess amount. If it is assumed that reactant A is the one with the excess amount than the reaction rate becomes the multiplication of the concentration of A and the rate constant. Hence, the reaction appears to follow first order kinetics; yet, it is second-order reaction in reality. These types of reactions are called pseudo-first-order reactions and their rate constants are referred to as pseudo-first-order rate constants (Benefield et al., 1982).

Lagergen presented the PFO model with his work on the adsorption of oxalic and malonic acid onto charcoal in 1898. The equations proposed are as follows (Nguyen et al., 2017):

$$qt = qe * (1 - e^{-k1t}) \quad \text{(integrated form for q(t=0) =0)} \ \text{.........} \ \text{(Eq. 10)},$$

$$In(qe - qt) = Inqe - k1t \quad \text{(linear form 1)} \ \text{.........} \ \text{(Eq.11)},$$

$$log(qe - qt) = logqe - \frac{k1t}{2.303} \quad \text{(linear form 2)} \ \text{.........} \ \text{(Eq.12)},$$

where, qe is the equilibrium amount estimated by the PFO model, t is time, qt is the adsorption amount at time t and k_1 is the rate constant. q_e and k_1 can be obtained from the graph of ln (qe-qt) vs. t (Nguyen et al., 2017). The rate constant, k_1 is related to the conditions of the process (especially pH and temperature) and is reported to increase with decreasing initial adsorbate concentration and smaller-sized particles. The rate-controlling step is dependent on the contact time and the experimental conditions (Tan & Hameed, 2017). When k_1 value is small and the difference between adsorption capacity at any time and at equilibrium is big, it indicates that the adsorption process is slow (Wang & Guo, 2020).

The problem with this model is that there are two unknowns, namely qe and k_1. Also, for most of the applications of the model, it is observed that it is suitable for the initial 30 min at most not for the whole contact time. Thus, both linear and non-linear equations yield linear trends. After nearly 30 min, the experimental data and theoretically obtained data are not coincidence well enough when they are represented by the PFO model. Another big problem is the decision of qe value since it can not be lower than the maximum adsorption in order to avoid mathematical errors due to linearization by taking the logarithm of a number lower than zero. Lastly, it is discussed that the difference between calculated and experimental qe values may be caused by the presence of a boundary layer that controls the beginning of the adsorption (Nguyen et al., 2017).

2.3.4.2   PSO kinetic model

Pseudo-second order model was originally proposed in 1984 by Gilles Blanchard for the removal of heavy metals from water by sorption onto natural zeolite (Nguyen et al., 2017). Since 1999, it has been used extensively for defining the adsorption process in the liquid phase (F. Wu et al., 2009). The differential and integrated equations of the model as follows (Nguyen et al., 2017):

$$\frac{dn}{dt} = K * (no - n)^2 \quad \text{(differential form)} \ldots\ldots\ldots \text{(Eq. 13)},$$

$$n = \frac{K*t*no + \alpha*no - 1}{K*t + \alpha} \quad \text{(integrated form)} \ldots\ldots\ldots \text{(Eq.14)},$$

where n is the amount of M^{+2} fixed or the amount of $NH4^+$ released at each instant, K is the constant of rate and n_o is the exchange capacity. When the boundary conditions of n=0 for time zero, it reveals that $\alpha=1/n$. Thus, Eq.14 becomes:

$$no = \frac{n^2 + Kt}{1 + Knt} \quad \text{(integrated form 2)} \ldots\ldots\ldots \text{(Eq.15)},$$

When qt is written instead of no, q_e for n, and K for k_2, Eq.15 can be expressed as:

$$qt = \frac{qe^2 + k2*t}{1 + k2*qe*t} \quad \text{(non-linear form)} \ldots\ldots \text{(Eq.16)},$$

where q_e (mg/g) is the adsorption capacity at equilibrium and q_t (mg/g) adsorption capacity at any time, t is the time, and k_2 (g/mg.min) is the rate constant.

There are four linear forms of the PSO model in the literature; these are as follows (Nguyen et al., 2017),

$$\frac{t}{qt} = \frac{1}{qe}t + \frac{1}{k2*qe^2} \quad \text{(linear form 1)} \ldots\ldots \text{(Eq.17)},$$

$$\frac{1}{qt} = \frac{1}{k2*qe^2*t} + \frac{1}{qe} \quad \text{(linear form 2)} \ldots\ldots \text{(Eq.18)},$$

$$qt = -\frac{1}{k2*qe}\frac{qt}{t} + qe \quad \text{(linear form 3)} \ldots\ldots \text{(Eq.19)},$$

$$\frac{qt}{t} = -(k2*qe)qt + k2*qe^2 \quad \text{(linear form 4)} \ldots\ldots \text{(Eq.20)}$$

CHAPTER 3

MATERIALS AND METHODS

3.1 Pesticide studied

In the scope of this thesis study, phorate (CAS: 298-02-2), which is an insecticide, was studied as a pollutant of concern. The general information and the physicochemical properties of phorate are given in Section 2.1.6. The brand of the pesticide was Sigma-Aldrich Co. (Analytical standard, with lot number BCBZ5640 and product number 33388). It has a purity of higher than 95% and color of colorless to very light yellow. The phorate was stored at +4 ºC at the refrigerator as recommended when it was not used.

The reason for selecting phorate to study is two-folds:

1. Phorate has not been studied for its removal from waters by adsorption
2. Phorate has a kinetic diameter between the kinetic diameters of previously studied two pesticides, namely, malathion and carbendazim by Ali (2022). Indeed, the main intention of this aforementioned previous study was not the removal of these pesticides by adsorption but by a Fenton-like process where CHA was used as a heterogeneous catalyst. However, adsorption onto CHA had been concerned as one of the removal mechanisms involved. Since the kinetic diameter of the pesticides, especially relative to the pore size of CHA, was found by Ali (2022), as an important parameter considering the pore diffusion step of adsorption, here in this study, the pesticide of phorate having a kinetic diameter between malathion and carbendazim was deemed worth to study. In a way, insight into the effect of the kinetic diameter of the pesticide on the adsorption onto CHA would be gained.

3.2   Adsorbents used

There are two adsorbents tested for the removal of phorate in this study, and they are namely PAC and CHA. The brand of the activated carbon was Norit N.V. (The Netherlands, with sample number SA 4). Chabazite is abundant in Central Anatolia and near Ankara. It is provided by Encon Co. as a big rock, and it is ground and sieved to 100-200 µm range before using as an adsorbent. The pictures of adsorbents, CHA and PAC, are presented in Figure 3.1.

Figure 3.1 Adsorbents used: CHA (on the left) and PAC (on the right)

3.3   Experiments

3.3.1   Experimental Procedure

All the experiments were done in batch mode and in duplicate reactors with a control beside them. The experimental procedure implemented throughout the study is summarized below. Also, a schematic representation of the procedure followed can be depicted in Figure 3.2.
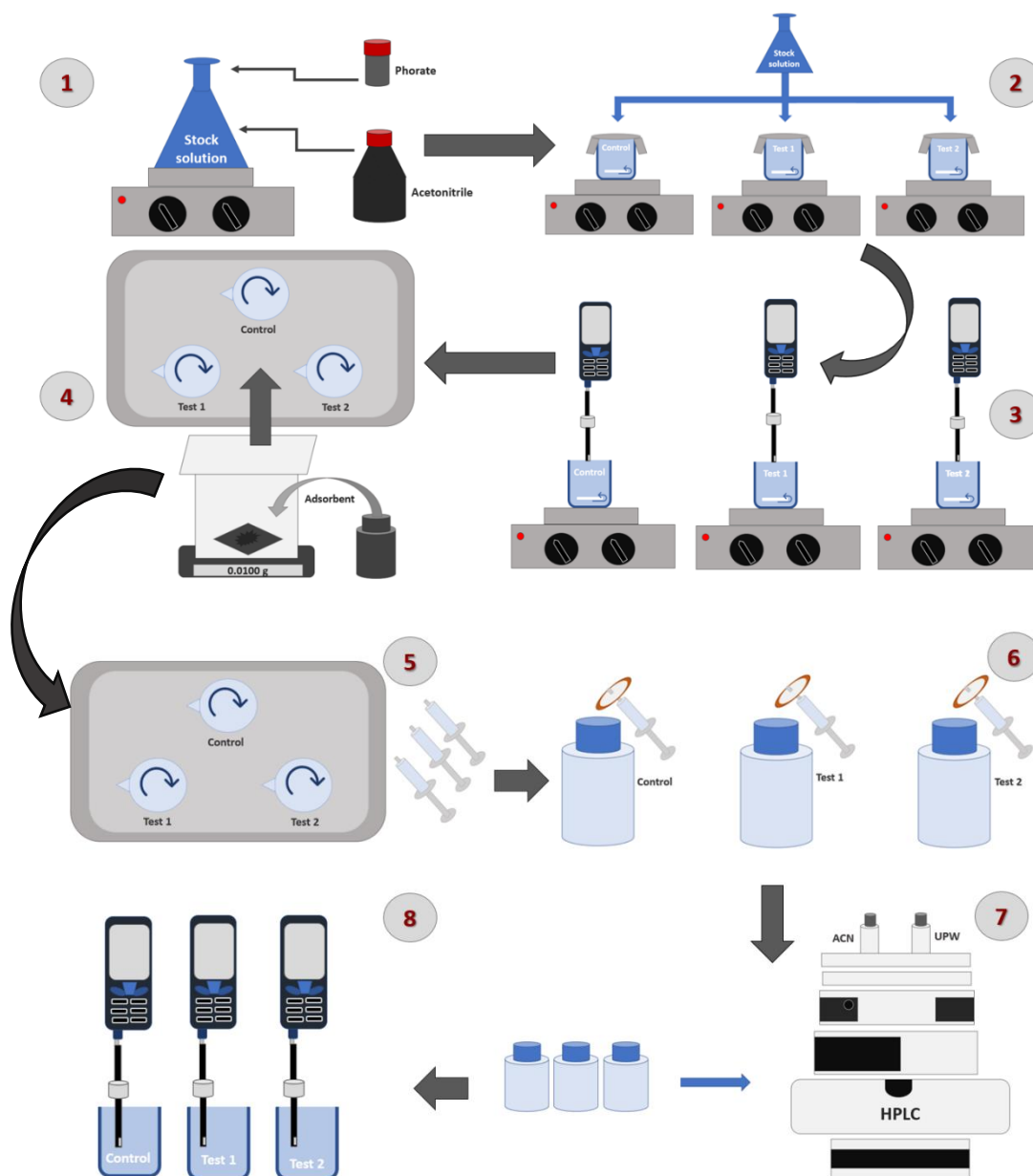
Figure 3.2 The flow diagram for the experimental procedure followed

As a first step, 0.5 L of stock solution of phorate is prepared with acetonitrile. The concentration of the stock solution was 100 mg/L. Afterward, the control and duplicate reactors were prepared by adding the necessary volume of the stock solution into the 0.4 mL of ultra-pure water. Control reactors were prepared to have the same concentration and pH as the duplicate reactors without adding any adsorbent under the

same operational conditions. The samples were put in a box to eliminate photodegradation and then placed on a magnetic stirrer (Chiltern Hotplate Magnetic Stirrer HS31) for homogeneous mixing. The pH was checked during mixing to arrange pH to the desired level by adding NaOH or H_2SO_4 solution. Additionally, pH was measured just before taking time zero samples from the reactors. The pre-determined adsorbent amounts were weighed by using precision scales and put into the reactors, excluding the control reactor. The samples with adsorbent in them and the control reactor were placed into the thermal shaker (ZHY200B Incubator Shaker), of which temperature and mixing intensity were pre-set and to block natural and artificial light, the glass part of the shaker and the top of the reactors were covered by aluminum folio (Figure 3.3). Samples (0.5 mL-1 mL) were taken from the reactors at certain time intervals for 210 min via syringes. The samples in the syringes were transferred to the HPLC vials after passing through a 0.45 µm sterile syringe filter (Step 6) to prevent the adsorbent from sticking to the vials. Thereupon, vials were placed in the autosampler chamber of the HPLC device, which was calibrated and ready to run the measurements. At the end of the shaking period, pH and temperature measurements of all reactors were carried out to control these parameters.

Figure 3.3 Thermal shaker used for the experiments

3.3.2　Experimental Design

The adsorption process is known to be affected primarily by the parameters of temperature, pH, adsorbate and adsorbent doses, and mixing intensity. Therefore, these five parameters, namely temperature, pH, mixing intensity, initial phorate concentration, and adsorbent (PAC and CHA) dose, were examined. The experiments were held by changing one parameter at a time in order to observe the effect of that parameter. The details of the experimental design are shown in Table 3.1. The basis for the selection of initial phorate concentration is to work with a concentration that is as close to detected values in waters as possible while obtaining detectable concentrations after the adsorption process. As it is previously mentioned in Section 1.1 and Section 2.1.6, phorate have been detected in the range of ng to µg per liter; however, to serve the latter purpose aforementioned above, the initial concentration was spiked to 1 mg/L.

Table 3.1 The Experimental Design Implemented

	pH	Temperature (°C)	Mixing intensity (rpm)	Initial phorate concentration (mg/L)	Adsorbent Dose (mg/L)
	3	15	120	0.50	12.5
PAC	7	25	160	0.75	25
	9	35	200	1.00	37.5
	3	15	120	0.50	12.5
CHA	7	25	160	0.75	25
	9	35	200	1.00	37.5

Based on the experimental findings of these studies, adsorption isotherm studies were conducted at pH 7, at the temperature of 25 °C, and mixing intensity of 160 rpm, while changing adsorbate concentrations and adsorbent dosages from 0.3 to 7.6 mg/L and from 12.5 to 37.5 mg/L, respectively.

Table 3.2 presents the experimental design for these tests. During these experiments, time course variation of phorate concentration was not followed; just initial and final concentrations (i.e. the equilibrium concentration corresponding to the equilibrium time identified during the kinetic tests) were measured.

Table 3.2 The PAC and CHA doses and the initial phorate concentrations (Co) applied for the isotherm study

PAC Dose (mg/ L)	12.5			25						37.5
Phorate (mg/L)	1.6	3.7	0.3	0.8	1.0	3.0	6.0	6.3	7.6	0.8
CHA Dose (mg/L)	12.5			25						37.5
Phorate (mg/L)	0.3	1.0	1.9	0.6	0.7	0.9	3.6	5.8	0.9	0.8

3.4 Data Analysis

Adsorption equilibrium:

For adsorption equilibrium experiments, a set of preliminary experiments at pH 3, 7 and 9 by keeping temperature at 25 ºC were performed to obtain equilibrium time and samples were taken intermittently for 24 h. The results of preliminary tests showed that the systems at different pH values reached the equilibrium around one hour. To be on the safe side, the duration of the experiments was set as 210 min.

The initial phorate concentrations and equilibrium concentrations presented in

Table 3.2 were used to calculate equilibrium adsorption capacity. Afterwards, in order to test the lineralized Langmuir isotherm model, C_e/q_e vs C_e graph was drawn with respect to Eq. 3 in . After plotting the curves, the slope of equation gives $1/q_{max}$; hence, 1/slope is equal to q_{max} value. After obtainig q_{max} value, Langmuir constant,b, can be calculated since y-intercept is equal to $1/q_{max} b$. Moreover, in order to test linearized Freundlich isotherm model, logarithm of q_e and C_e values were taken

and then $\log q_e$ ve $\log C_e$ (Eq.9 in <u>Section 2.3.3.2</u>) curve was plotted. The equation obtained from the curve was used to determine K_f and n since the value of y-intercept is equal to $\log K_f$ and the slope of the curve is equal to $1/n$.

Adsorption kinetics:

To obtain the necessary data for determining the adsorption kinetics model, several sets of experiments were performed. In these experiments, the influence of pH (3,7 and 9), temperature (15, 25 and 35 ºC), and the mixing intensity (120, 160 and 200 rpm) were examined for both PAC and CHA by keeping the amount of them as 10 mg. In addition, the effect of adsorbent dose were studied with 12.5, 25 and 37.5 mg/L with an initial phorate concentration of 1 mg/L at 25 ºC at neutral pH.The samples were taken at time 0, 0.5, 1, 2, 5, 10, 15, 20, 30, 40, 60, 80, and 100 min from the duplicate reactors.

The concentraion of phorate by time was obtained from kinetics experiments under different operational conditions and, equilibrium and instantaneous adsorpiton capacities were determined. The data was tested to determine the best-fitted model both for linearized PFO and PSO kinetic model. For testing the linearized PFO model (Eq.11 in <u>Section 2.3.4.1</u>), natural logarithm of $(q_e\text{-}q_t)$ values were taken and the grap of $\ln(q_e\text{-}q_t)$ vs time was plotted. The linear equation obtained from the plotted curve was used determine rate constant which equals to the slope of the curve and q_e which is equal to exponent of y-intercept. In order to test linearized PSO model (Eq.17 in <u>Section 2.3.4.2</u>), t/q_t vs t curve was plotted. The graph yielded a linear equation which was used to estimate q_e and rate constant. The slope of the equation equals to $1/q_e$ from which q_e was calculated. After calculating q_e , rate constant was calculated since it is equal to the value of y-intercept which is $1/kq_e^2$.

3.5 Analytical Instruments and Methods

3.5.1 Phorate analysis

For the HPLC analysis, acetonitrile and ultra-pure water were used as mobile phases. The Ultra Pure Water (UPW) was produced by using tap water. Tap water passes through the ion exchanger to reduce hardness and is distilled (MilliPore RiOs 16 Water Purification System, ionic rejection 94-99%) to obtain distilled water. Afterward, it passes through filters (MilliPore Milli-Q Gradient A10 Water Purification System) to produce ultra-pure water. On the other hand, the HPLC grade acetonitrile (CAS: 75-05-8) is purchased from Carlo Erba Reagents S.A.S (Batch number P1N541131N) in 2.5 L of brown bottles.

The measurement of phorate concentration was performed by using HPLC. For these experiments, Agilent Technologies branded 1200 Series Infinity II model HPLC device was used with the Zorbox C18 column (4,6 x 100 mm, 3,5 µm) Variable Wavelength Detector (Figure 3.4).

Figure 3.4 Agilent Technologies 1200 Series HPLC Device

The operating conditions for the phorate measurement are given in Table 3.3. Acetonitrile and ultra-pure water were used as mobile phases with a ratio of 75% and

25%, respectively. The calibration curves conducted throughout the measurements are provided in Appendix A.

Table 3.3 The operating conditions for the measurement of phorate concentration

Parameter	Value
Flow rate (mL/min)	0.5
Column furnace temperature (ºC)	40
Mobile phase ratio (ACN: UPW, %)	75:25
Retention time (min)	7
Wavelength (nm)	210
Injection volume (µL)	20

LOD and LOQ for phorate measurement were determined as 0.05 mg/L and 0.15 mg/L, respectively. These values were calculated based on the standard deviation of the response (signal areas corresponding to the concentrations) method and the slope of the calibration curve.

3.5.2   Other Analysis

pH and temperature were measured using a multimeter. The multimeter is calibrated regularly. The frequency of the calibration was 3-4 times a month. Additionally, it is calibrated when necessary; for instance, in the case of deviations between consecutive measurements and/or long response time to give a value. For the calibration, Hach branded single-use pH 4 and pH 7 solutions are used .

In order to weigh the adsorbent amount, Sartorius Brand (GC8035-0CE) digital precision scale was used for the experiments. For more accurate results, the water balance of the scale was checked before every measurement.

CHAPTER 4

RESULTS AND DISCUSSION

This section presents the results obtained from the adsorption studies performed on the adsorption of phorate onto the two adsorbents, namely, PAC and CHA, with relevant discussions. The performance of the two adsorbents was compared in terms of effectively removing the phorate from water. All these studies were mainly grouped into two as adsorption kinetic and adsorption equilibrium studies. The former aims to determine the rate of adsorption under different operational conditions and also to understand the rate-determining step as well as the removal mechanisms involved. The latter aims to depict the functional distribution between the phorate adsorbed onto the PAC and CHA and remaining in solution at equilibrium, which will ultimately enable determining the maximum adsorption capacities of PAC and CHA as well as their adsorption intensities.

4.1 Adsorption of Phorate onto PAC and CHA - Effects of operational parameters and kinetic analysis

In this section, the results obtained for the adsorption of phorate onto two different adsorbents, PAC and CHA, under different operational conditions are presented and discussed in an attempt to determine the rate of adsorption under different operational conditions and also to understand the rate-determining step as well as the removal mechanisms involved. The following sub-sections present the effect of pH, initial concentration of phorate, adsorbent dose, mixing intensity and temperature on the adsorption of phorate by PAC and CHA. The duration of the experiments was 100 min since the preliminary equilibrium tests revealed that the system reached an equilibrium between 60-80 min, depending on the operational conditions. For all sets of

71

experiments, a control reactor was operated. The removal of phorate due to volatilization was seen in every control in the range of 0.1-0.2 mg/L.

4.1.1 The effect of pH on Phorate adsorption and on its kinetics

4.1.1.1 When PAC used as adsorbent

The results of the experiments conducted for examining the pH effect on the adsorption rate of phorate onto the PAC are presented in Figure 4.1. The initial phorate concentration was 1 ± 0.1 mg/L for all pH values tested, namely, 3, 7 and 9. The temperature was kept at room temperature (25 °C ±2°C) while the shaking speed was set to 160 rpm, and the PAC dose was 25 ± 0.25 mg/ L.
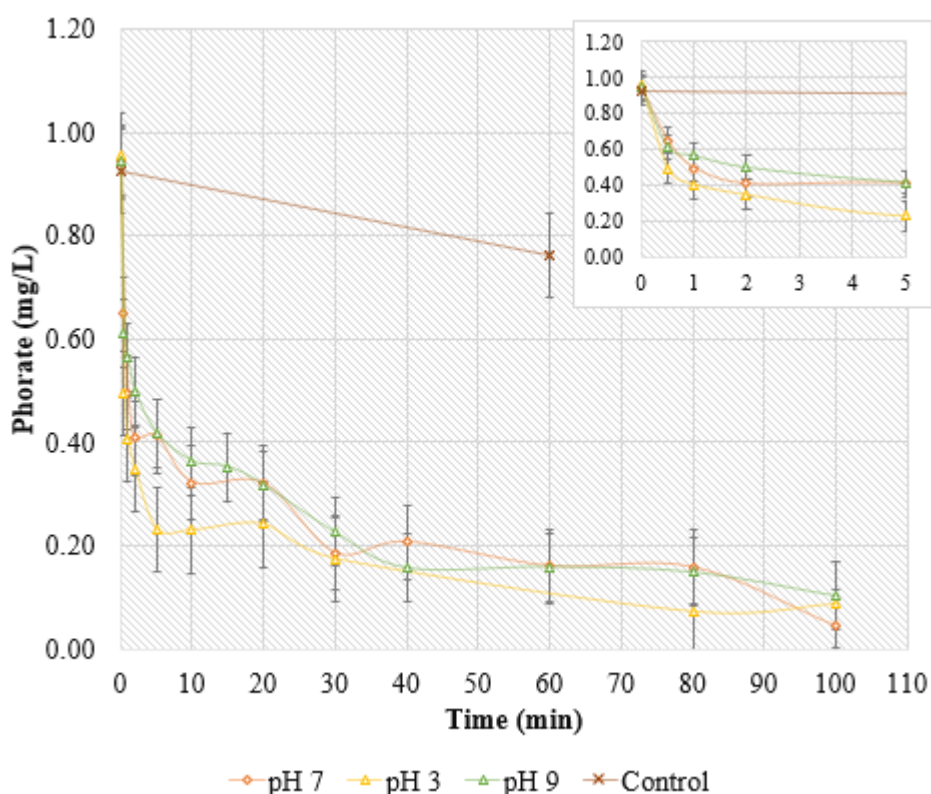
Figure 4.1 The effect of pH on the adsorption kinetic of phorate on PAC (C_o=1 mg/L at 160 rpm, 25 °C,25 mg PAC/L)

The adsorption of phorate onto PAC can be considered as a fast process by looking at the drastic drop in the first 2 minutes. Indeed, there are two phases of adsorption, a rapid phase and then a slow phase. During the rapid phase, the phorate concentration decreased from its initial value of around 1 mg/L to 0.5 mg/L in 30 sec at pH 3, in 60 sec at pH 7 and in 2 min at pH 9. Whereas during the slow phase, a further decrease in the phorate concentration to 0.1 mg/L, which was identified as the equilibrium concentration of phorate, was observed at 60 min for all pH values. So, it can be inferred that the overall removal efficiency for all pH values was around 90 %. The exact removal efficiencies for all pH values are 83%, 84,5% and 78% for pH 7,3 and 9, respectively. The slight decrease in removal efficiency for pH 9 could be explained by the competition between OH^- ions and adsorbate molecules for the adsorption on the active sites of PAC (Martin, 1978). Nevertheless, this effect of pH becomes observable in the second (slow) phase of adsorption, indicating the aforementioned competition between phorate and ions (H^+ or OH^-) occurs during the pore diffusion step of adsorption rather than the surface film diffusion step. This is understandable, probably because of easier diffusion of H^+ and OH^- into the pores than phorate since the size of phorate is larger than that of H^+ and OH^- ions. Here, one can infer that the rate-controlling step is surface film diffusion during the initial rapid phase of adsorption and pore diffusion during the second slow phase of adsorption. Further analysis of the kinetics of adsorption is provided below, which clarifies the mechanism of adsorption and rate controlling steps under different pH conditions better.

Kinetic Model:

In order to determine the kinetic model that describes the adsorption of phorate onto PAC and the relevant rate constants at three different pH, the experimental data provided in Figure 4.1 was subjected to the analysis for two different kinetic models, namely, PFO and PSO. The relevant analysis can be depicted in Figure 4.2.

Figure 4.2 Kinetic models for all pH values a) PFO, b) PSO

The results obtained through these analyses are presented comparatively in Table 4.1. Additionally, theoretical equilibrium adsorption capacities (q_e) calculated from the models are presented in Table 4.1.

Table 4.1 The results of the adsorption kinetics model analysis for PAC at pH 3, 7 and 9

pH	Kinetic model	R^2	Rate constant	q_e (mg/g)
3	PFO	0.747	0.030 min^{-1}	16.99
	PSO	0.999	0.035 g/mg.min	36.36
7	PFO	0.861	0.018 min^{-1}	19.93
	PSO	0.997	0.010 g/mg.min	37.18
9	PFO	0.791	0.020 min^{-1}	21.21
	PSO	0.998	0.013 g/mg.min	34.60

When the results are evaluated for all pH values, it is seen that the PSO model is followed perfectly for the phorate adsorption since it has very high R^2 values (0.997 for pH 7, 0.999 for pH 3, and 0.998 for pH 9). This outcome is not surprising since most adsorption kinetics data in the environmental applications agree well with the PSO model (Abdeen & Mohammad, 2022; Kushwaha et al., 2011; Tan & Hameed, 2017; Wanjeri et al., 2018; Yang et al., 2017). According to the study of Wang and

Guo (2020), there are several reasons for the better fit of PSO than other models. The first one could be the low initial concentration. In the literature, there are some evidences that the PSO model fits better when the initial adsorbate concentration is low (Sabarinathan et al., 2019). Another reason is that most of the kinetic studies include data up to the system reaching the equilibrium, which results in the inclusion of the final stage (i.e. slow second phase) of the adsorption process. The third reason is the high number of active sites on the adsorbent. The studies with modified adsorbents which are abundant in active sites yield the best fit for the PSO model (Wang & Guo, 2020).

The theoretical qe values of the PSO model are close to each other for all pH values being nearly 37 mg/mg for pH 7, 36 mg/mg for pH 3 and 35 mg/mg for pH 9. However, the rate constants differ considerably. The largest constant value was determined as 0.035 g/mg.min when pH is 3. Thus, one can state that the adsorption of phorate on PAC was the fastest under acidic conditions. Indeed, this result can not be explained by the chemical property of phorate since it is a non-ionic compound and quite stable at low pH values (Chen et al., 2004). However, organic matter adsorption onto activated carbon generally increases as pH decreases in column applications (Al-qodah et al., 2007). Also, it is stated that organic acids are easy to be adsorbed by AC at low pH values (Benefield et al., 1982), and phorate is an ester derivative of phosphoric acid (Dar et al., 2022). The reason for better adsorption at low pH may be the neutralization of negative charges at the surface of the adsorbent and thereby reducing hinderence to diffusion. On the other hand, since mixing was provided during our experiments, one should not expect surface film diffusion hinderence. However, since the negatively charged functional groups at the surface of the adsorbent are expected to be neutralized, and phorate is not supposed to get ionized, charge repelling will not be of concern. Therefore, faster adsorption at low pH is more probable.

4.1.1.2 When CHA used as adsorbent

The results of the experiments performed for examining the pH effect on the adsorption of phorate onto the CHA are presented in Figure 4.3. The initial concentration for all pH values tested was 1±0.1 mg/L. The temperature was kept at room temperature (25 ℃ ±2℃) while the shaking speed was set to 160 rpm and the CHA dose was 25±0.25 mg/0.4 L.
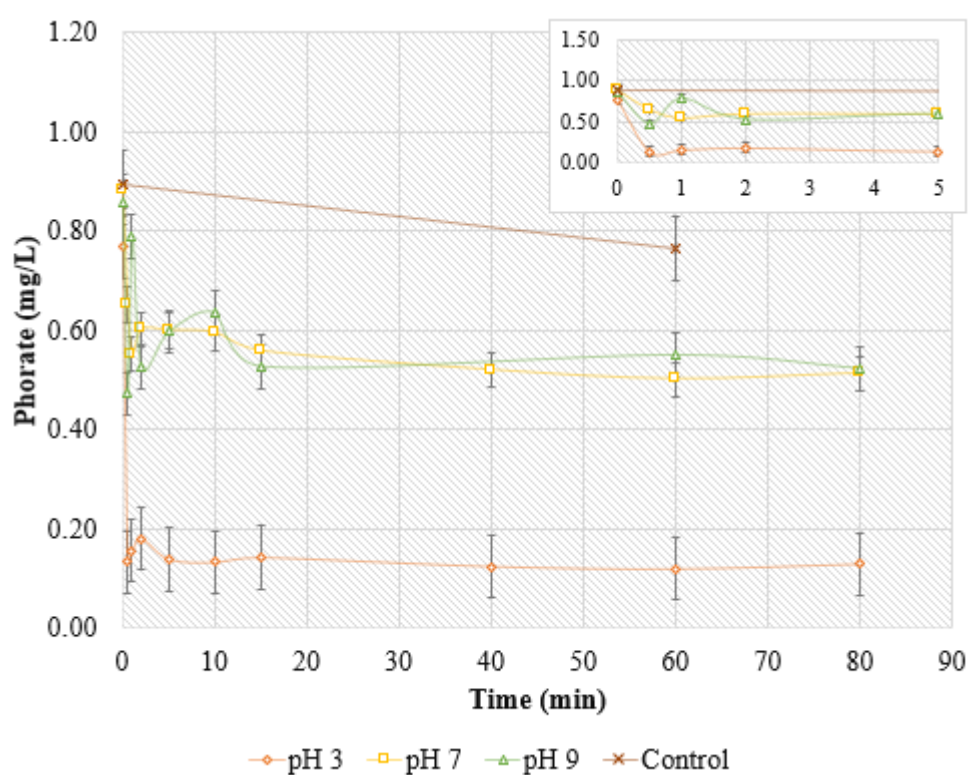
Figure 4.3 The effect of pH on the adsorption kinetic of phorate onto CHA (C_o=1 mg/L at 160 rpm, 25 ℃,25 mg CHA/L)

The graph presented in Figure 4.3 shows that the adsorption of phorate onto CHA is a quick process. For pH 7 and 9, the time course variations of phorate followed a similar trend and reached nearly half the initial concentration in 2 min. Additionally, the process seems even faster for pH 3. The phorate concentration declined to around 0.2 mg/L from 0.9 mg/L in 30 sec. The system reached the equilibrium concentration of

0.5 mg/L at 20 min for pH 7 and 9. However, a much lower equilibrium concentration (0.15 mg/L) obtained when pH is 3 may indicate that the affinity of vacant sites in pores of CHA is higher towards phorate rather than H^+ ions when pH is low during the slow phase of the adsorption, which is controlled by pore diffusion. For pH 3, the system reaches equilibrium at 10 min with a concentration of around 0.2 mg/L. Hence, the removal efficiencies for different pH values are nearly 45% for pH 7 and 9, and around 85% for pH 3. For higher pH values (7 and 9), the difference between equilibrium concentration and the concentration at the end of the fast adsorption phase (t=5 min) is very small (around 0.02 mg/L), which may indicate that after 5 min there was a strong competition between OH^- ions and phorate for adsorping on CHA surface since CHA has negatively charged on the surface between pH values of 2 and 11 (Metwally & Attallah, 2019). Additionally, the alteration in pH of the solution may upset the active sites on the adsorbent surface by dissociating the functional groups (Aysan et al., 2016). Hence, as the exposure time of high pH case increases, the functional groups may be influenced to have a lower affinity for phorate.

Kinetic Model:

In order to determine the kinetic model followed and the relevant rate constants at three different pH, the experimental data provided in Figure 4.3 are subjected to the analysis for two different kinetic models, namely, PFO and PSO models. The relevant analysis can be depicted from Figure 4.4.
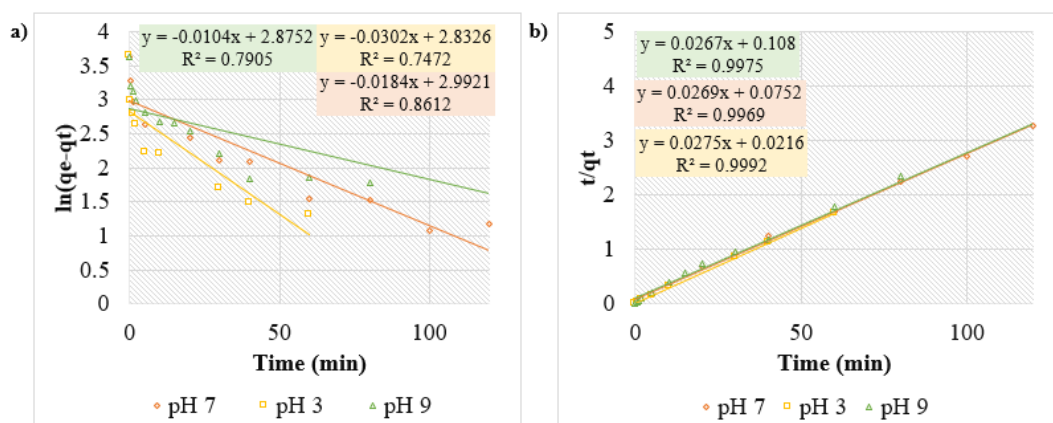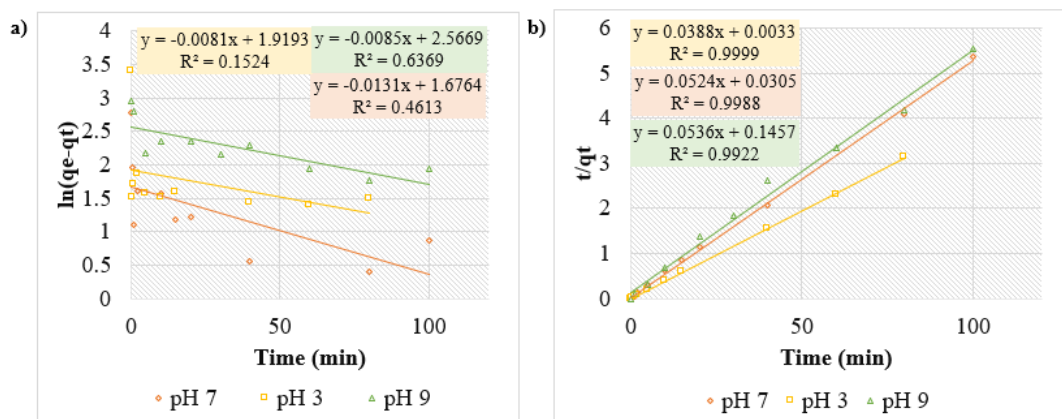
Figure 4.4 Kinetic models for different pH values a) PFO, b) PSO

The results obtained through these analyses are presented comparatively in Table 4.2. Additionally, theoretical equilibrium adsorption capacities (q_e) calculated from the models are presented in Table 4.2.

Table 4.2 The results of the adsorption kinetics model analysis for CHA at pH 3,7 and 9

pH	Kinetic model	R^2	Rate constant	q_e (mg/g)
3	PFO	0.152	0.002 min^{-1}	6.15
	PSO	0.999	0.243 g/mg.min	25.97
7	PFO	0.461	0.013 min^{-1}	5.35
	PSO	0.998	0.043 g/mg.min	19.72
9	PFO	0.637	0.009 min^{-1}	13.03
	PSO	0.992	0.020 g/mg.min	18.66

When the results of the relevant regression analysis are considered, it can be mentioned that for all three pH values, the system is well-defined by the PSO model since it has R^2 value of 0.99. The calculated equilibrium capacities (26 mg/g for pH 3, 20 mg/g for pH 7 and 19 mg/g for pH 9) and the estimated rate constants (0.24 g/mg.min for pH 3, 0.04 g/mg.min for pH 7 and 0.02 g/mg.min for pH 9) by PSO model have an increasing trend with decreasing pH. This shows that the adsorption performance of CHA is better

78

in terms of removal efficiency and rate under acidic conditions due to the neutralization of the negatively charged surface of CHA (Metwally & Attallah, 2019) which leads to more opening for the diffusion of phorate.

4.1.2 The effect of initial concentration of Phorate on adsorption and on its kinetics

4.1.2.1 When PAC used as adsorbent

The results of the experiments conducted to observe the effect of the initial concentration of adsorbate on adsorption kinetics are presented in Figure 4.5. The initial concentration tested are 1 ± 0.05 mg/L, 0.75 ± 0.1 mg/L and 0.5 ± 0.2 mg/L at neutral pH. The temperature was kept at room temperature (25 ºC ±2ºC). While the shaking speed was set to 160 rpm and the PAC dose was 25 ± 0.25 mg/L.
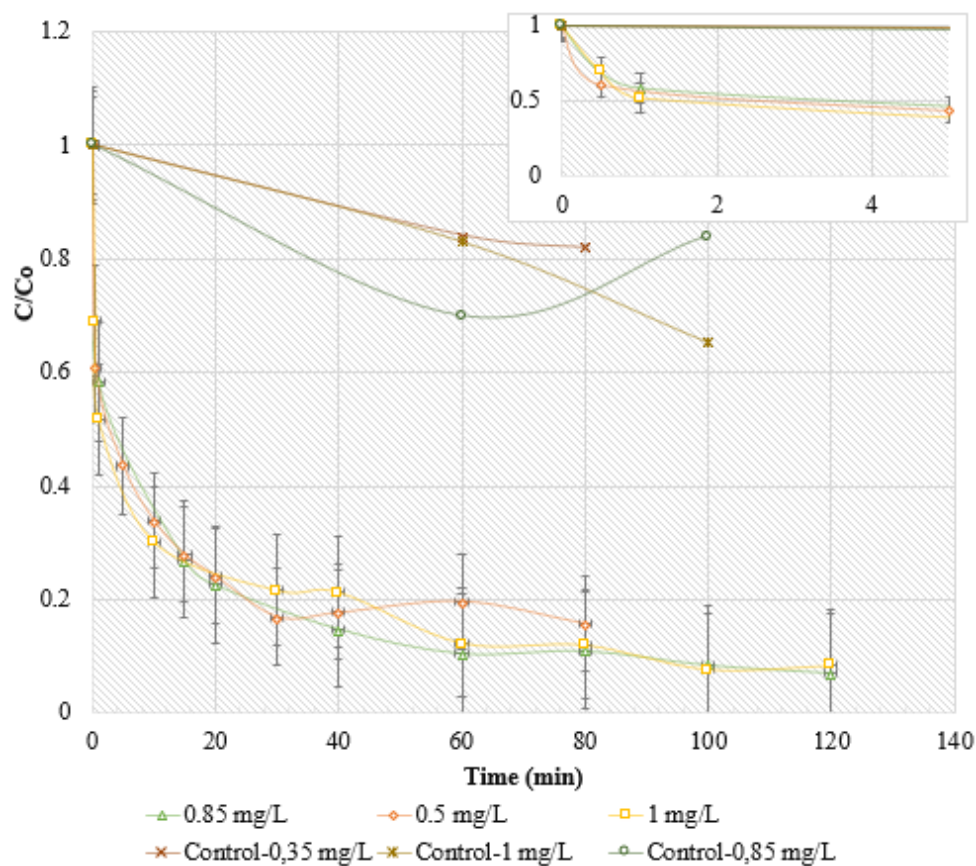
Figure 4.5 The effect of initial phorate concentration on the adsorption kinetic of phorate on PAC (PAC dose:25 mg/ L at 25 ºC, 160 rpm, pH 7)

The initial concentrations decreased by half in 2 min for Co=1 mg/L, in approximately 3 min for Co=0.85 mg/L, and in 4 min for Co=0.35 mg/L in the first fast phase of adsorption. On the other hand, in the slow adsorption phase, all reactors reached the equilibrium at 60 min with a concentration of around 0.1 mg/L (0.12 mg/L for Co=1 mg/L, 0.09 mg/L for Co=0.85 mg/L and 0.07 mg/L for Co=0.35 mg/L which correspond to removal efficiencies of 87%, 89% and 80%, respectively). Hence, it can be said that the initial concentration has a slight impact on the removal efficiency of phorate via adsorption onto PAC. However, in the study of Krishna (2015), they observed the considerable effect of the initial concentration of malathion on the adsorption of it onto the examined adsorbent with respect to equilibrium time. They conducted the experiments with higher concentrations and higher concentration difference (10 mg/L of difference) which results in higher equilibrium time for higher concentrations (180, 220, 240 and 260 min for Co, malathion = 10, 20, 30 and 40 mg/L, respectively).

Kinetic Model:

In order to determine the kinetic model followed and the relevant rate constants at three different initial concentrations, the experimental data provided in Figure 4.5 are subjected to the analysis for two different kinetic models, namely, PFO and PSO models. The relevant analysis can be depicted in Figure 4.6.

Figure 4.6 Kinetic models for different initial concentrations a) PFO, b) PSO

The results obtained through regression analysis are presented comparatively in Table 4.3. Additionally, theoretical equilibrium adsorption capacities for the models are provided.

Table 4.3 The results of the adsorption kinetics model analysis for PAC with different initial concentrations

C_o (mg/L)	Kinetic model	R^2	Rate constant	q_e (mg/g)
1	PFO	0.861	0.018 min^{-1}	19.93
	PSO	0.997	0.010 g/mg.min	37.18
0.85	PFO	0.770	0.016 min^{-1}	16.59
	PSO	0.999	0.012 g/mg.min	31.85
0.35	PFO	0.663	0.024 min^{-1}	5.35
	PSO	0.999	0.057 g/mg.min	13.91

When the results are evaluated for all initial phorate concentrations, the PSO model seems the best fitting one since it has the highest R^2 value (0.997 for Co=1 mg/L, 0.999 for Co=0.85 mg/L and 0.35 mg/L). As the initial phorate concentration decreases (from 1 mg/L to 0.35 mg/L), the adsorption capacity is decreasing (from 37.18 to 13.91 mg/g). When the rate constants of the PSO model are examined, one can state that the initial concentration is the lowest while the rate constant is the highest;yet, the rate

constant should be the same for all initial concentration values since the rate is dependent of initial concentration unlike rate constant due to mathematical nature of kinetic models. In other words, the rate constant is indepedent of the initial adsorbate concentration (Benefield et al., 1982). However, adsorption is a complex process which includes two more steps (film and pore diffusion steps) other than adsorption (Wang & Guo, 2020). Thus, the difference in the rate constants is due to other factors other than concentration . Nevertheless, the change in rate constant with different initial concentration have reported in the literature. For example, Ardejani et al. (2007), performed dye adsortpion on a almond shell based adsorbents and obtained different PFO (5.30×10^{-3} , 7.83×10^{-3}, and 1.08×10^{-2} min^{-1} for initial concentrations of 0, 100 and 150 mg/L, respectively) and PSO (1.88×10^{-3}, 1.42×10^{-2}, and 6.69×10^{-2} min^{-1} for initial concentrations of 0, 100 and 150 mg/L, respectively) rate constant for different initial concentration of the dye concerned.

4.1.2.2   When CHA Used as Adsorbent

The results of the experiments performed for examining the effect of initial concentration on the adsorption of phorate onto the CHA are presented in Figure 4.7. The initial concentration tested was 1±0.1, 0.75±0.01 and 0.5±0.1 mg/L. The temperature was kept at room temperature (25 ºC ±2ºC) during the experiment, which has a duration of 100 min. The shaking speed was set to 160 rpm and the PAC dose was 25 ±0.25 mg/ L. The pH of the solution was adjusted to 7.
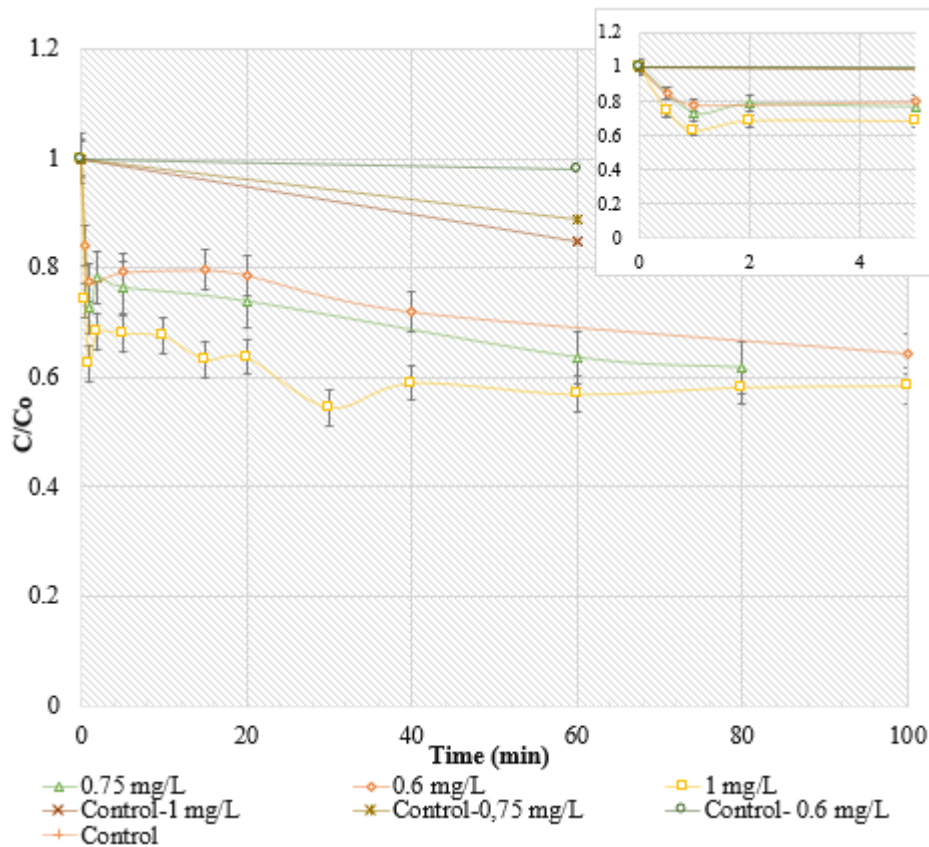
Figure 4.7 The effect of initial concentration on the adsorption kinetic of phorate on CHA (CHA dose:25 mg/ L at 25 ºC, 160 rpm, pH 7)

When the behaviours for the three initial concentrations were examined from the graph presented in Figure 4.7, one can infer that regardless of the initial concentration, the system reaches the equilibrium in 60 min for all three concentrations. The reactor with 1 mg/L reaches equilibrium around at 0.5 mg/L, while the system with 0.75 mg/L establishes equilibrium also with an equilibrium concentration close to 0.5 mg/L. For the initial concentration 0.6 mg/L, the system attained equilibrium at around 0.40 mg/L. The removal efficiency in the systems appears to be independent of the initial concentration for the removal of phorate by CHA since the removal efficiencies are similar which are approximately 45%, 40%, and 42% for Co=1 mg/L, 0.75 mg/L, and 0.6 mg/L, respectively. The decrease in removal efficiency with decreasing initial concentration is observed in the studies of Al-qodah et al. (2007) and Salman et al.

(2011). The smaller removal efficiencies with lower concentration can be explained by the lower driving force in mass transfer due to the lower number of adsorbate molecules contributed to the driving force (Salman et al., 2011).

Kinetic Model:

In order to determine the kinetic model followed and the relevant rate constants for three different initial concentrations, the experimental data provided in Figure 4.7, are subjected to the analysis for two different kinetic models, namely, PFO and PSO models. The relevant analysis can be depicted in Figure 4.8.

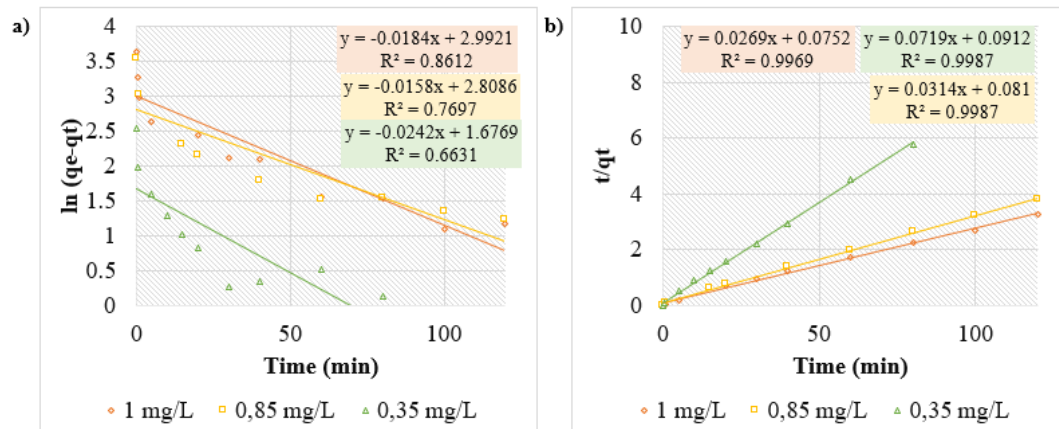Figure 4.8 Kinetic models for different initial concentrations a) PFO, b) PSO

The results obtained through these analyses are presented comparatively in Table 4.4. Additionally, theoretical equilibrium adsorption capacities for the models are introduced.

Table 4.4 The results of the adsorption kinetics model analysis for CHA with different initial concentrations

Co (mg/L)	Kinetic model	R^2	Rate constant	q_e (mg/g)
1	PFO	0.501	0.018 min^{-1}	5.44
	PSO	0.998	0.074 g/mg.min	19.72
0.75	PFO	0.761	0.013 min^{-1}	9.0
	PSO	0.997	0.036 g/mg.min	21.93
0.60	PFO	0.715	0.007 min^{-1}	10.26
	PSO	0.996	0.010 g/mg.min	27.32

When the outcomes of the analysis are evaluated, it can be stated that for all initial concentration cases, R^2 values are close to unity.This hints that the PSO model can be suggested for describing the adsorption kinetics for these concentrations. The adsorption capacities (20 mg/g for Co=1 mg/L, 22 mg/g for Co=0.75 mg/L and 27 mg/L for Co=0.60 mg/g) slightly increase with decreasing initial concentration. On the other hand, when the rate constants are considered, it is observed that the rate drops from 0.074 g/mg.min to 0.036 g/mg.min and then 0.010 g/mg.min with decreasing initial concentration tested from 1 to 0.75 and then to 0.6 mg/L, respectively.However, as it is mentioned in Section 4.1.2.2, the rate constant should be the same for all initial concentration values since the rate is dependent of initial concentration unlike rate constant due to mathematical nature of kinetic models. In other words, the rate constant does not change with varying initial adsorbate concentration (Benefield et al., 1982). However, adsorption is a complex process which includes two more steps (film and pore diffusion steps) other than adsorption (Wang & Guo, 2020). Thus, the difference in the rate constants is due to other factors other than concentration . Nevertheless, the change in rate constant with different initial concentration have reported in the literature. To examplify, Cu(II) adsorption on pre-treated rubber wood sawdust yields PFO and PSO rate constants vary 0.0181 and 0.0336 min^{-1} for initial concentrations 10 (0.0336 min^{-1}, 0.7324 g/mg.min),20 (0.0182 min^{-1}, 0.1306 g/mg.min),30 (0.0181

min^{-1}, 0.7871 g/mg.min), and 40 (0.0262 min^{-1}, 0.8656 g/mg.min), mg/L (Kalavathy et al., 2005).

4.1.3   The effect of adsorbent dose

4.1.3.1   When PAC used as adsorbent

The results of the experiments conducted for examining the adsorbent dose effect on the adsorption of phorate onto the PAC are presented in Figure 4.9. The initial concentration for all adsorbent amounts tested was 1±0.1 mg/L. The temperature was kept at room temperature (25 ºC ± 2ºC). The shaking speed was set to 160 rpm and pH value was 7. The adsorbent dosages tested were 12.5, 25, 37.5 mg PAC/L.
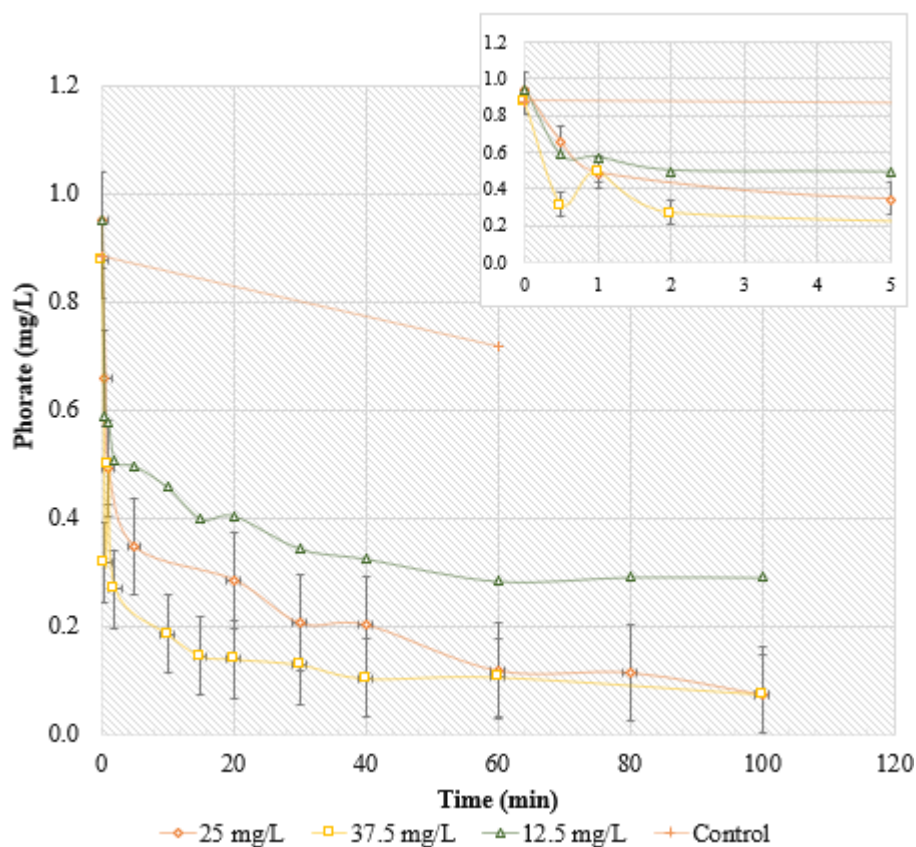
Figure 4.9 The effect of PAC dose on the adsorption kinetic of phorate on PAC ($C_o=1$ mg/L at 25 ºC, 160 rpm, pH 7)

When the graph provided in Figure 4.9 is evaluated, it is observed that the adsorbent doses 25 and 37.5 mg/L PAC behave similarly. For both PAC doses, the equilibrium concentration is 0.1 mg/L and this concentration is attained at 60 min. On the other hand, the equilibrium concentration is observed as approximately 0.3 mg/L when PAC dose is 12.5 mg/L, although the equilibrium time is the same. Indeed, this is expected to observe since the total available sites of PAC decrease with decreasing added amount; thus, an increase in the adsorbent amount may result in a boost in the adsorbed percent (Mojiri et al., 2020). Consequently, the system with a lower adsorbent amount reaches equilibrium at a higher concentration. However, the equilibrium time is not affected and stays the same as 60 min. Here, it is worth stating that the amount alone is not a parameter to affect the extent of adsorption directly, but the ratio of the adsorbate to adsorbent amounts. So, these results should be evaluated together with those presented in Section 4.1.4.1, which refers to the effect of the adsorbate to adsorbent ratio, which is a more realistic parameter to consider.

Kinetic Model:

In order to determine the kinetic model followed and the relevant rate constants at three different adsorbent amounts, the experimental data provided in Figure 4.9 are subjected to the analysis for two different kinetic models, namely, PFO and PSO models. The relevant analysis can be depicted in Figure 4.10.
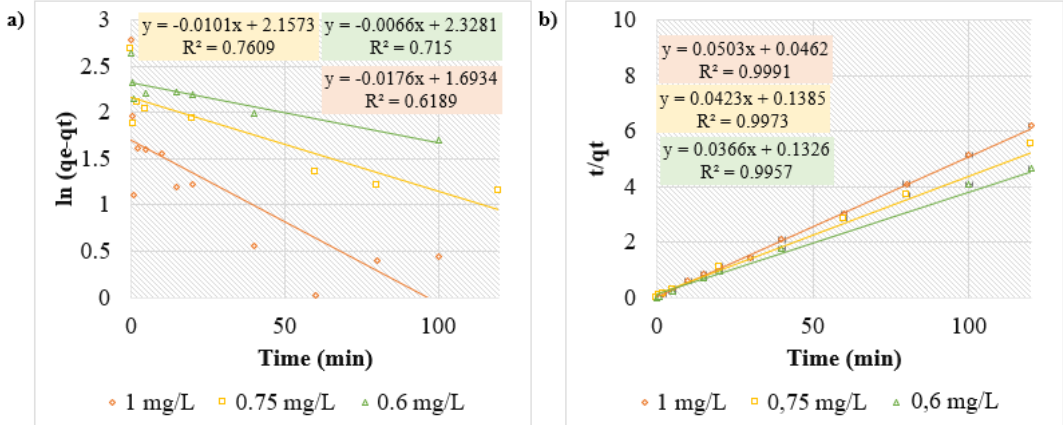
Figure 4.10 Kinetic models for different PAC doses a) PFO, b) PSO

The results from the regression analysis, rate constant and equilibrium adsorption capacities with respect to kinetic models are presented in Table 4.5.

Table 4.5 The results of the adsorption kinetics model analysis for different amounts of PAC

PAC (mg/ L)	Kinetic model	R^2	Rate constant	q_e (mg/g)
12.5	PFO	0.720	0.011 min^{-1}	16.18
	PSO	0.998	0.010 g/mg.min	30.96
25	PFO	0.861	0.018 min^{-1}	19.93
	PSO	0.997	0.010 g/mg.min	37.18
37.5	PFO	0.605	0.015 min^{-1}	11.56
	PSO	0.999	0.029 g/mg.min	37.18

For all PAC doses, it can be stated that the best-fitted kinetic model is PSO, as it has the highest R^2 values. When the adsorption capacities at equilibrium conditions are compared, the PAC dose of 25 and 37.5 mg/L have the same value (37 mg/g) and this value is larger than the equilibrium adsorption capacity of PAC dose of 12.5 mg/L (31 mg/g). Thus, it can be said that the optimum PAC dose for the adsorption of phorate on PAC is 25 mg/L. Obtaining lower adsorption capacity with a lower adsorbent amount can be explained by the positive correlation between adsorbed percentage and

adsorbent amount, which is caused by the rise in the free surface area of sorbent for the adsorption (Kushwaha et al., 2011). So, one can state that higher adsorbent amounts, 25 and 37.5 mg/L for this case, lead to higher equilibrium adsorption capacities. When the rate constants of the PSO model for each adsorbent amount are examined, it is observed that 12.5 and 25 mg/L have the same value which is 0.010 g/mg.min while the rate constant for 37.5 mg/L is 0.029 g/mg.min. One can infer that the rate stays constant up to a certain PAC dose (i.e. 25 mg/L) and then with increasing adsorbent dose the rate of adsorption is inclined as well. However, one should note that rate constants are not affected by the adsorbent dose only here since the adsorbate to adsorbent ratio will also change when the adsorbent dose is changed.

4.1.3.2   When CHA used as adsorbent

The results of the experiments performed for examining the effect of adsorbent dose on the adsorption of phorate onto the CHA are presented in Figure 4.11. The adsorbent dose tested were 12.5, 25 and 37.5 mg/L. The initial concentration for all adsorbent amounts tested was 1±0.1 mg/L. The temperature was kept at room temperature (25 ºC ±2ºC) during the experiment, which has a duration of 100 min. The shaking speed was set to 160 rpm during the experiment period.
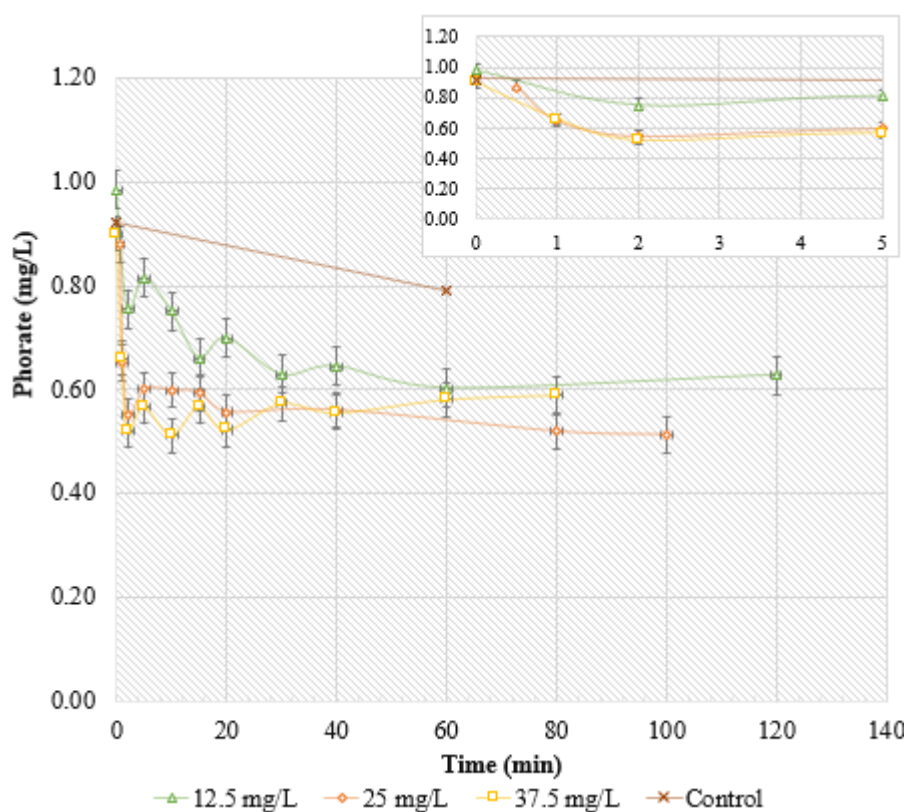
Figure 4.11 The effect of CHA dosage on the kinetics of adsorption of phorate onto CHA (C_o=1 mg/L at 25 ºC, 160 rpm, pH 7)

As it can be seen from Figure 4.11, the reactor with 12.5 mg/L of CHA reaches the equilibrium at 0.6 mg/L at 60 min, while the reactor with 25 mg/L of CHA reaches the equilibrium concentration of 0.5 mg/L at 60 min. Moreover, the reactor with 37.5 mg/L establishes equilibrium at 0.6 mg/L at the end of 60 min. Thus, it can be stated that the equilibrium time is not affected by the adsorbent dose. However, the equilibrium concentration decreases to 0.5 mg/L from 0.6 mg/L when the adsorbent dose is doubled from 12.5 to 25 mg/L. The corresponding removal efficiencies for different CHA amounts are 40% for 12.5 and 37.5 mg/ L and 50% for 25 mg/L. Therefore, it can be stated that after a certain dose of adsorbent, the system is not affected by the adsorbent dose significantly, which is also stated in the article of Mojiri et al. (2020) and explained by the increase in total surface area available for adsorption.

As stated in the case of PAC (Sec 4.3.1.1), here, it is worth stating that the amount alone is not a parameter to affect the extent of adsorption directly, but the ratio of the adsorbate to adsorbent amounts. So, these results should be evaluated together with those presented in Section 4.1.4.2, which refers to the effect of the adsorbate to the adsorbent ratio, which is a more realistic parameter to consider.

Kinetic Model:

In order to determine the kinetic model followed and the relevant rate constants with three different adsorbent dosages, the experimental data provided in Figure 4.11 are subjected to the analysis for two different kinetic models, namely, PFO and PSO models. The relevant analysis can be depicted in Figure 4.12.

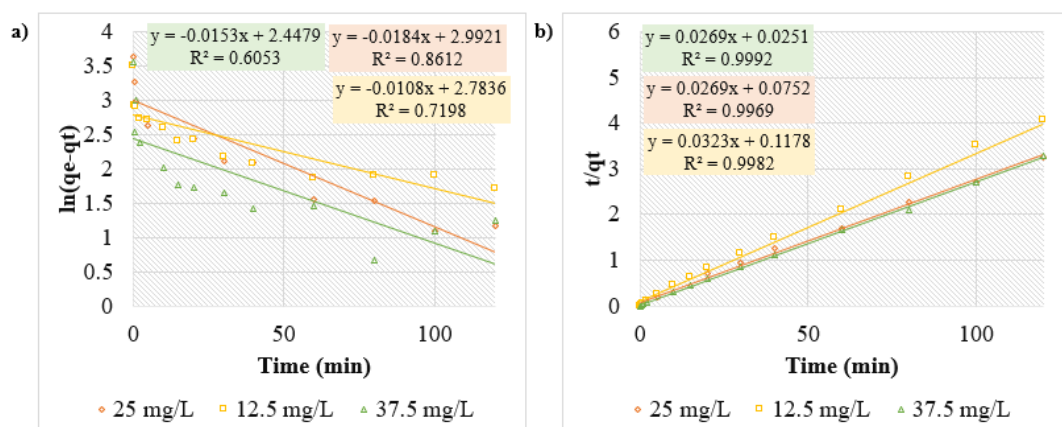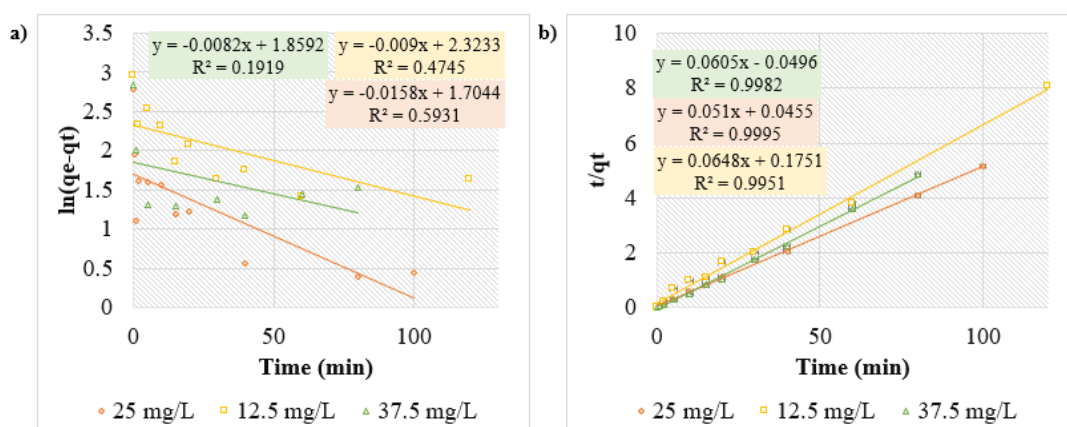

Figure 4.12 Kinetic models for different CHA dosages a) PFO, b) PSO

The results obtained through these analyses are presented comparatively in Table 4.6. Additionally, theoretical equilibrium adsorption capacities for the models are introduced.

Table 4.6 The results of the adsorption kinetics model analysis for different amounts of CHA

CHA (mg/ L)	Kinetic model	R^2	Rate constant	q_e (mg/g)
12.5	PFO	0.475	0.009 min^{-1}	10.21
	PSO	0.995	0.024 g/mg.min	15.43
25	PFO	0.593	0.016 min^{-1}	5.50
	PSO	0.999	0.042 g/mg.min	19.90
37.5	PFO	0.192	0.008 min^{-1}	6.42
	PSO	0.998	0.310 g/mg.min	18.73

From the regression results, one can state that the PSO model is the best-fitted one for all CHA doses due to high R^2. The highest adsorption capacity (20 mg/g) when equilibrium is established belongs to the CHA dose of 25 mg/L, which aligns with the highest removal efficiency (50%). The adsorption capacity of CHA increased with increasing CHA dose. However, after 25 mg/L, a small decrease in adsorption capacity from 20 to 19 mg/g is observed. Thus, one can assert that the optimum dose for the adsorption of phorate on CHA is 25 mg/L. The highest rate constant (0.310 g/mg.min) is obtained when the CHA amount is 37.5 mg/ L and the equilibrium time (30 min) is the lowest when the CHA dose is the highest.

4.1.4 The effect of adsorbate to adsorbent ratio

4.1.4.1 When PAC used as adsorbent

The effect of adsorbate to adsorbent ratio on adsorption kinetics at 25 ºC under neutral pH is presented in Figure 4.13. The shaking speed was set to 160 rpm for all ratios. The ratios were 0.080 (1/12.5), 0.040 (1/25), 0.034 (0.85/25), 0.027 (1/37.5) and 0.014 (0.35/25).
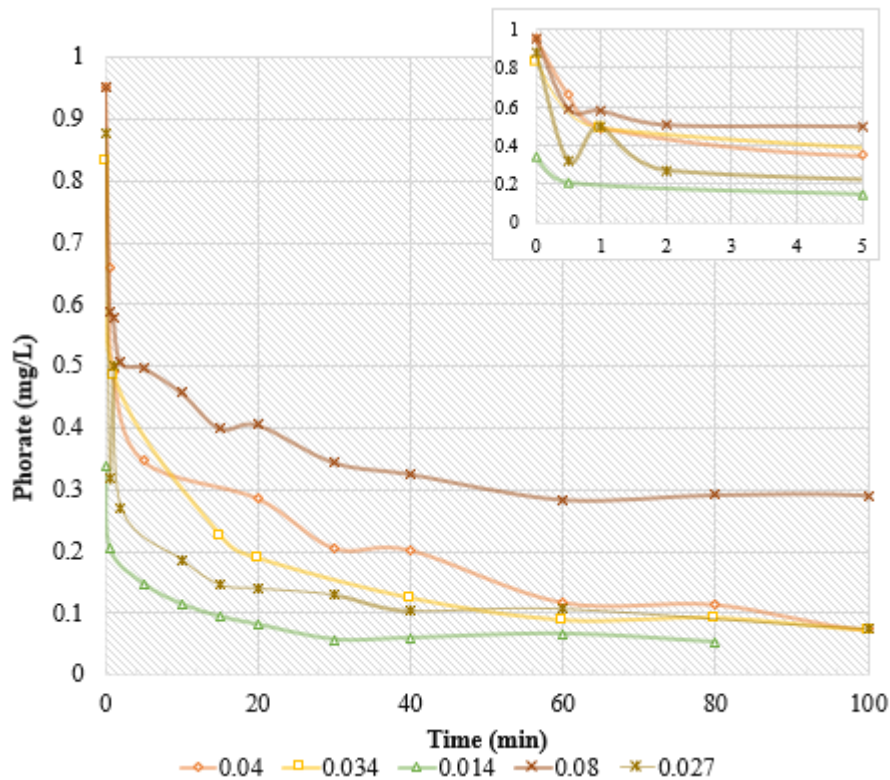
Figure 4.13 The effect of adsorbate to adsorbent ratio on the adsorption kinetic of phorate on PAC (160 rpm, pH 7, 25 ºC)

When the graph provided in Figure 4.13 is evaluated, it is observed that the adsorbate to adsorbent ratios of 0.04, 0.027 0.034 and 0.014 behave similarly. For all ratios, the equilibrium concentration is around 0.1 mg/L and this concentration is attained at 60 min. On the other hand, the equilibrium concentration is observed as approximately 0.3 mg/L when the ratio is 0.08, although the equilibrium time is the same. Indeed, this is expected to observe since as the ratio increases it indicates that per one unit of adsorbent, the amount of adsorbate to be sorbed is higher.Consequently, the system with a higher ratio reaches equilibrium at a higher concentration. However, the equilibrium time is not affected and stays the same as 60 min. Yılmaz (2019) studied aclonifen removal via adsorption on PAC and carbon nanotubes with different adsorbate to adsorbent ratios (0.010, 0.015, 0.02,0.040 and 0.100). The results with PAC showed that the highest ratio (0.100) has a slightly lower removal efficieny (85%) when compared to other ratio which yields removal efficiencies bigger than 90 %.

93

Kinetic Model:

In order to determine the kinetic model followed and the relevant rate constants for five different adsorbate to adsorbent ratio, the experimental data provided in Figure 4.13, are subjected to the analysis for two kinetic models, namely, PFO and PSO models. The relevant analysis can be depicted from Figure 4.14.

Figure 4.14 Kinetic models for different adsorbate to adsorbent ratios a) PFO, b) PSO

The results from the regression analysis, rate constant and equilibrium adsorption capacities with respect to kinetic models are presented in Table 4.9 The results of the adsorption kinetics model analysis for PAC at different shaking speedsC at different adsorbate to adsorbent ratio.

Table 4.7 The results of the adsorption kinetics model analysis for different adsorbate to adsorbent ratio

Ratio	Kinetic model	R^2	Rate constant	q_e (mg/g)
0.014	PFO	0.663	0.024 min^{-1}	5.35
	PSO	0.999	0.057 g/mg.min	13.91
0.027	PFO	0.605	0.015 min^{-1}	11.56
	PSO	0.999	0.029 g/mg.min	37.18
0.034	PFO	0.770	0.016 min^{-1}	16.59
	PSO	0.999	0.012 g/mg.min	31.85
0.040	PFO	0.861	0.018 min^{-1}	19.93
	PSO	0.997	0.010 g/mg.min	37.18
0.080	PFO	0.720	0.011 min^{-1}	16.18
	PSO	0.998	0.010 g/mg.min	30.96

For all different adsorbate to adsorbent ratios, it can be stated that the best-fitted kinetic model is PSO, as it has the highest R^2 values. When the adsorption capacities at equilibrium conditions are compared, the capacities increase up to the ratio of 0.027 from 14 to 37 mg/g.Then, when the ratio is further increased to 0.034, a small decrease in capacity is observed from 37 to 32 mg/g. However, as the ratio increased to 0.040, the capacity is increased to 37 mg/g and decreases again to 31 mg/g when the ratio is increased to 0.080. Hence, it is hard to establish a solid relationship between the ratio and adsorption capacity;yet, by disregarding the small deviations (from 37 to 32 mg/g), one can state that the capacity increases, as the ratio increases up to a certain point (0.040). When the rate constants are evaluated, it can be observed that the constants decreases (from 0.057 to 0.010 g/mg.min) by increasing ratio (0.014 to 0.040). Beyond the ratio of 0.040, there is no change in the rate constant.This relationship is also stated by Yılmaz (2019) for the adsorption of aclonifen onto PAC. In her study, the PSO rate constant decreases from 0.512 to 0.004 g/mg.min as the ratio increases from 0.015 to 0.1.

4.1.4.2   When CHA used as adsorbent

The effect of adsorbate to adsorbent ratio on adsorption kinetics at 25 ºC under neutral pH is presented in Figure 4.13. The shaking speed was set to 160 rpm for all ratios. The ratios were 0.080 (1/12.5), 0.040 (1/25), 0.030 (0.75/25), 0.027 (1/37.5) and 0.024 (0.60/25).
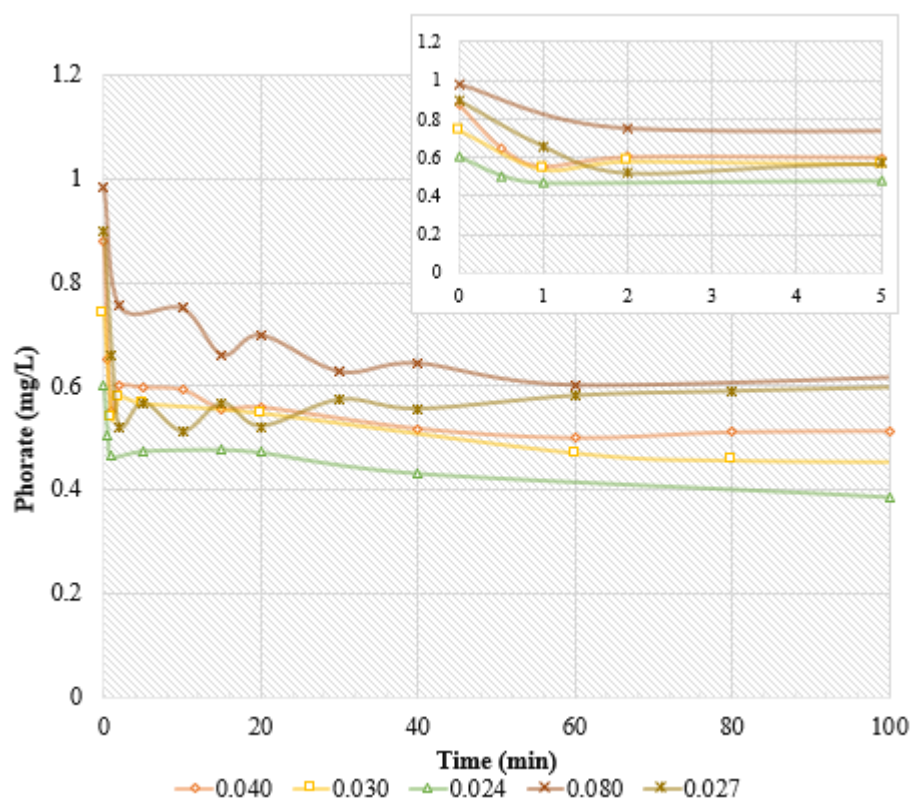
Figure 4.15 The effect of adsorbate to adsorbent ratio on the adsorption kinetic of phorate on CHA (160 rpm, pH 7, 25 ºC)

When the graph provided in Figure 4.15 is evaluated, it is observed that all adsorbate to adsorbent ratios reaches equilibrium at 60 min. The ratios of 0.080 and 0.027 have an equilibrium concentration of 0.6 mg/L while the ratios 0.040 and 0.03 have 0.5 mg/L at equilibrium. Additionally, the lowest ratio (0.024) has the lowest equilibrium concentration (0.4 mg/L). Lower ratio means that per unit mass of adsorbent, there is less amount of adsorbate; thus, obtaining lower equilibrium concentration (i.e. higher

removal efficiency) is observed due to the increased number of active sites of adsorbent per unit mass of adsorbate (Kushwaha et al., 2011). Yılmaz (2019) studied aclonifen removal via adsorption on PAC and carbon nanotubes with different adsorbate to adsorbent ratios (0.010, 0.015, 0.02,0.040 and 0.100). The results with multi-walled carbon nanotubes also showed that the lowest ratio (0.01) has a quite high removal efficieny (above 95%) among other ratios.

Kinetic Model:

In order to determine the kinetic model followed and the relevant rate constants for five different adsorbate to adsorbent ratio, the experimental data provided in Figure 4.15 are subjected to the analysis for two kinetic models, namely, PFO and PSO models. The relevant analysis can be depicted from Figure 4.16.
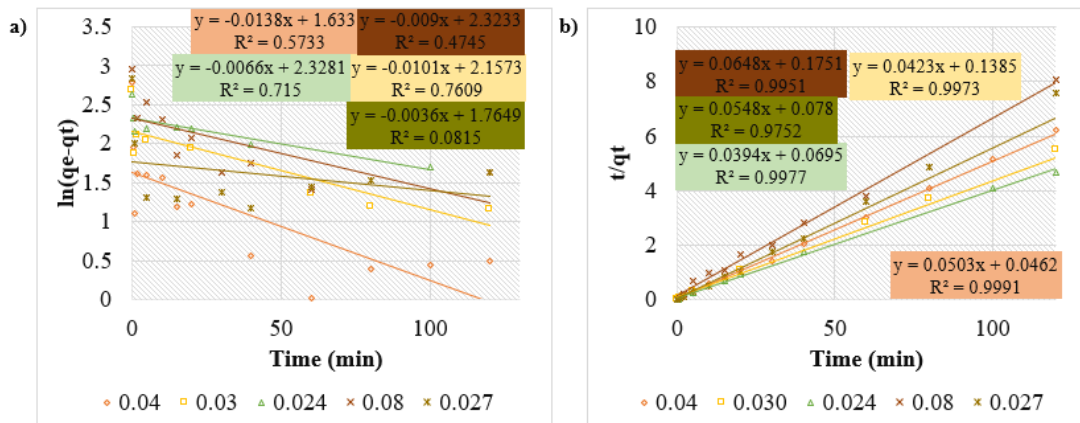
Figure 4.16 Kinetic models for different adsorbate to adsorbent ratios a) PFO, b) PSO

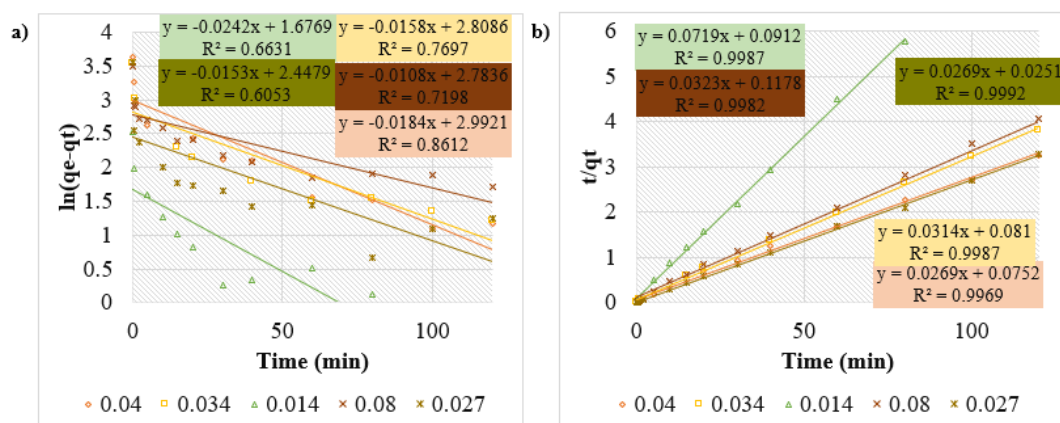The results from the regression analysis, rate constant and equilibrium adsorption capacities with respect to kinetic models are presented in Table 4.8. The results of adsorption kinetics model analysis for different adsorbate to adsorbent ratio.

Table 4.8 The results of the adsorption kinetics model analysis for different adsorbate to adsorbent ratio

Ratio	Kinetic model	R^2	Rate constant	q_e (mg/g)
0.024	PFO	0.715	0.007 min^{-1}	10.26
	PSO	0.996	0.010 g/mg.min	27.32
0.027	PFO	0.192	0.008 min^{-1}	6.42
	PSO	0.998	0.310 g/mg.min	18.73
0.030	PFO	0.761	0.013 min^{-1}	9.0
	PSO	0.997	0.036 g/mg.min	21.93
0.040	PFO	0.501	0.018 min^{-1}	5.44
	PSO	0.998	0.074 g/mg.min	19.72
0.080	PFO	0.475	0.009 min^{-1}	10.21
	PSO	0.995	0.024 g/mg.min	15.43

For all different adsorbate to adsorbent ratios, it can be stated that the best-fitted kinetic model is PSO, as it has the highest R^2 values. When the adsorption capacities at equilibrium conditions are compared, the capacities have a tendecy to decrease with increasing ratio. The lowest ratio (0.024) has the highest adsorption capacity (27 mg/g) at equilbrium while the highest ratio (0.080) has the lowest capacity (15 mg/g). The ratios in between (0.027, 0.030, 0.040) have close equilibrium adsorption capacities (19, 22 an 20 mg/g for 0.027, 0.030, 0.040, respectively). When the rate constants are evaluated, it can be observed that there is no proportional relationship between the adsorbate to adsorbent ratio and the rate constant when the adsorbent is CHA. However, Yılmaz (2019) studied the adsorption of aclonifen which is a pesticide onto multi-walled carbon nanotubes and it is reported that the PSO rate constant decreases from 0.1868 to 0.004 g/mg.min as the ratio increases from 0.01 to 0.1.

**4.1.5	The effect of mixing intensity**

**4.1.5.1	When PAC used as adsorbent**

The results of the experiments performed to observe the effect of mixing intensity (shaking speed) of adsorbate on adsorption kinetics is presented in Figure 4.17. Three experiments were conducted with different shaking speeds. The shaking speed was set to 120, 160 and 200 rpm for this purpose. The initial concentration of the reactors was 1±0.05 mg/L at neutral pH. The temperature was kept at room temperature (25 ºC ±2ºC) and the PAC dose was 25 mg/L.

Figure 4.17 The effect of mixing speed on the adsorption kinetic of phorate on PAC (C$_o$=1 mg/L at 25 ºC, 25 mg PAC/L, pH 7)

The initial concentrations decreased by half in 1 min for all shaking speeds in the fast phase of adsorption. On the other hand, in the slow adsorption phase, reactors were

shaken at 200, 160 and 120 rpm and reached the equilibrium at 60 min with different concentrations, 0.1 mg/L (for 160 and 200 rpm) and 0.2 mg/L for 120 rpm. The lower speeds of shaking may decrease the possibility of effective contact between adsorbent and adsorbate since turbulence decreases as well. Additionally, the higher shaking speeds decrease the resistance in the film diffusion step by thinning or breaking the boundary film layer (Al-qodah et al., 2007). Hence, the adsorption might be enhanced. Evidently, the reactor shaken at 120 rpm resulted in a higher equilibrium concentration than that at 160 and 200 rpm.

Kinetic Model:

In order to determine the kinetic model followed and the relevant rate constants at three different shaking speeds, the experimental data provided in Figure 4.17, are subjected to the analysis for two kinetic models, namely, PFO and PSO models. The relevant analysis can be depicted from Figure 4.18.
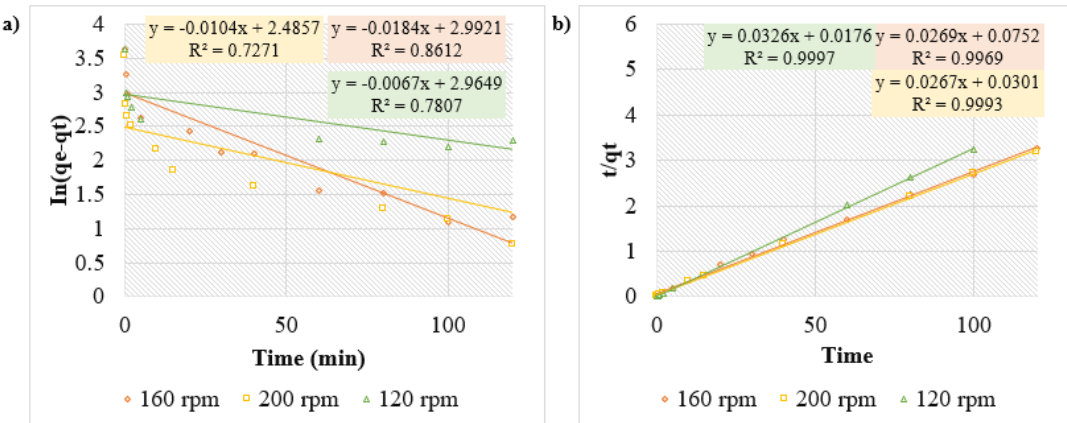
Figure 4.18 Kinetic models for different shaking speeds a) PFO, b) PSO

The results obtained from the implementation of the kinetic models, including rate constants and equilibrium adsorption capacities for different shaking speeds, are presented in Table 4.9.

Table 4.9 The results of the adsorption kinetics model analysis for PAC at different shaking speeds

| Shaking speed (rpm)	Kinetic model	R^2	Rate constant	q_e (mg/g)
120	PFO	0.781	0.009 min^{-1}	20.00
	PSO	0,999	0.060 g/mg.min	30.68
160	PFO	0.861	0.006 min^{-1}	19.93
	PSO	0.997	0.010 g/mg.min	37.18
200	PFO	0.727	0.017 min^{-1}	14.19
	PSO	0.999	0.031 g/mg.min	36.90

For all tested shaking speeds, it can be articulated that the best-fitted kinetic model is PSO as it has the highest R^2 values. When the adsorption capacities at equilibrium conditions are compared, shaking speeds of 160 and 200 rpm have very close values, which is 37 mg/g and this value is larger than the equilibrium adsorption capacity of shaking speed of 120 rpm is 31 mg/g. One can expect this outcome since higher speeds enable the contact of adsorbate to the adsorbent better due to a decline in the thickness of the boundary layer which surrounds the adsorbent particles (Al-qodah et al., 2007). However, Ahsan et al. (2014), in their study, observed that after a certain speed, the extent of adsorption decreases significantly. Thus, an optimum shaking speed should be defined for adsorption systems to work effectively. Despite the positive effect of higher shaking speeds on the adsorption capacities, the same was not observed in terms of the rate constants. When the rate constants for shaking speed are evaluated, it is observed that the rate decreased from 0.060 to 0.010 g/mg.min when shaking speed increased from 120 to 160 rpm. Afterward, it increased to 0.031 g/mg.min again when the speed of the shaker increased to 200 rpm. The reason for this unexpected outcome remained unexplained.

4.1.5.2   When CHA used as adsorbent

The results of the experiments performed to observe the effect of mixing intensity on adsorption kinetics are presented in Figure 4.19. Three experiments were conducted with different shaking speeds. A control reactor was built for all different shaking speeds, but the average of these three control results is represented on the graph for the sake of a plain demonstration since there were no significant differences between these three reactors. The shaking speed was set to 120, 160 and 200 rpm in order to examine the effect of the shaking speed. The initial concentration of the reactors was 1 ± 0.05 mg/L at neutral pH. The temperature was kept at room temperature (25 ºC ±2ºC) and the CHA dose was 25 mg/L.
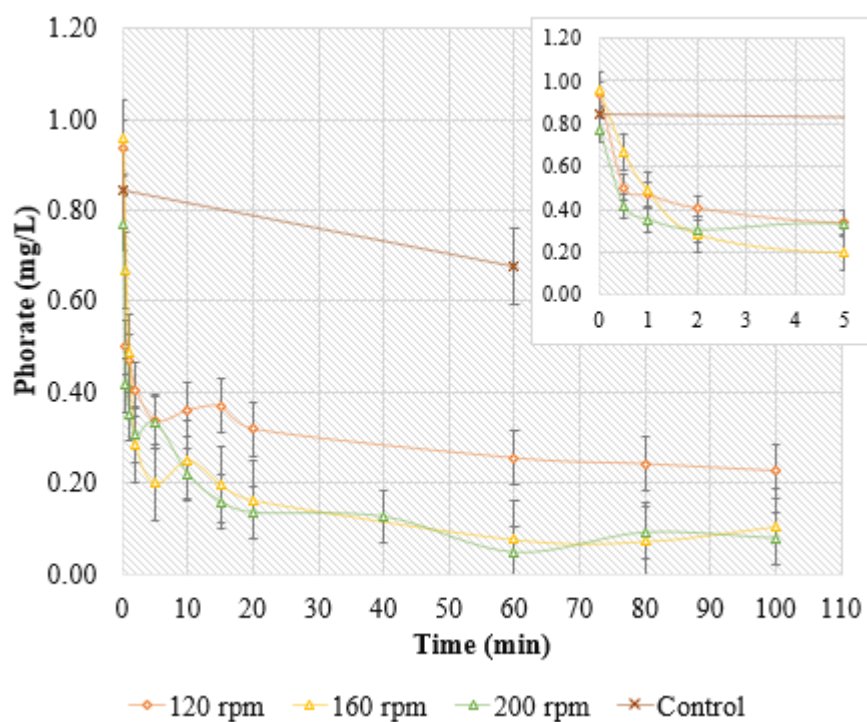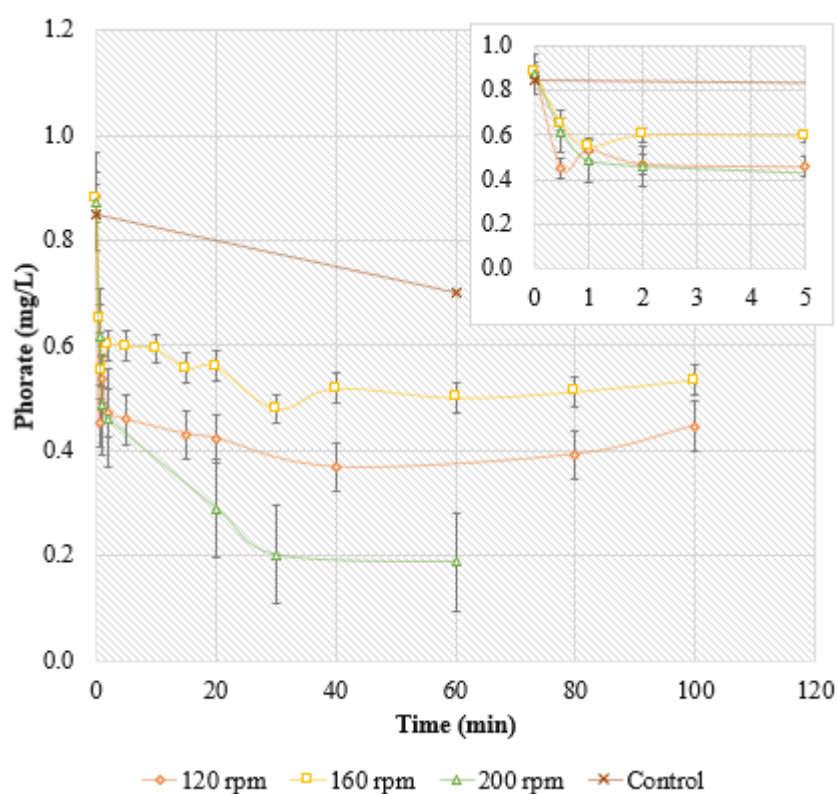

Figure 4.19 The effect of mixing speed on the adsorption kinetic of phorate on CHA (C_o=1 mg/L at 25 ºC, 25 mg CHA/L, pH 7)

102

As seen in Figure 4.19, the trend for the adsorption of phorate onto CHA illustrates a rapid process, especially for the mixing intensities of 120 and 160 rpm. At the end of the 5 min, these two reactors are very close to the equilibrium conditions. The equilibrium conditions (concentration and time) are 0.4 mg/L and 20 min for 120 rpm (removal efficiency= ~60%), 0.5 mg/L and 60 min for 160 rpm (removal efficiency=~50%), and 0.2 mg/L and 30 min for 200 rpm (removal efficiency=~80%). It is hard to establish a meaningful relationship between equilibrium concentration and time with the mixing intensity since there is no inverse or direct proportion between these variables. However, one can state that when the shaking speed is highest (200 rpm), the removal of phorate is highest (removal efficiency= ~80%) and it is fast (equilibrium time of 30 min). This could be attributed to the better contact between adsorbate and adsorbent at higher shaking speeds. Also, breaking the surface film due to the creation of more intense agitation conditions could remove the mass transfer resistance likely offered by the surface film. Thus, the optimum speed can be asserted as 200 rpm for the adsorption of phorate on CHA.

Kinetic Model:

In order to determine the kinetic model followed and the relevant rate constants at three different shaking speeds, the experimental data provided in Figure 4.19 are subjected to the analysis for three different kinetic models, namely, PFO and PSO models. The relevant analysis can be depicted in Figure 4.20.
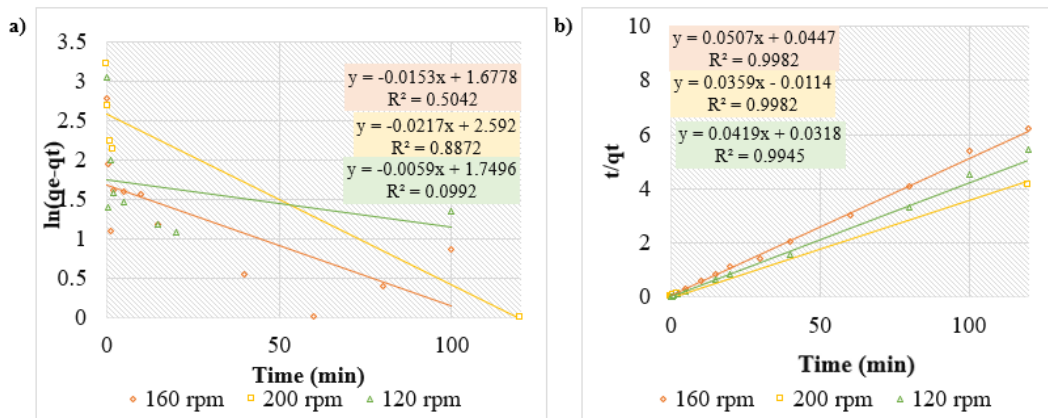
Figure 4.20 Kinetic models for different shaking speeds a) PFO, b) PSO

The results from the regression analysis, rate constant and equilibrium adsorption capacities with respect to kinetic models are presented in Table 4.10.

Table 4.10 The results of the adsorption kinetics model analysis for CHA at different shaking speeds

Shaking speed (rpm)	Kinetic model	R^2	Rate constant	q_e (mg/g)
120	PFO	0.099	0.006 min^{-1}	5.75
	PSO	0.996	0.149 g/mg.min	22.99
160	PFO	0.501	0.012 min^{-1}	5.10
	PSO	0.998	0.157 g/mg.min	19.23
200	PFO	0.887	0.011 min^{-1}	11.56
	PSO	0.998	0.035 g/mg.min	28.90

When the results of the regression analysis are analysed, it can be declared that PSO model can be recommended as the best-fitted kinetic model for all shaking speeds. This is because it has a correlation coefficient close to unity. The adsorption capacity (~29 mg/g) obtained at equilibrium is highest when the shaking speed was 200 rpm. This is foreseen since the lowest equilibrium concentration (0.2 mg/L) is also obtained

at 200 rpm. Al-qodah et al. (2007) reported that as the agitation speed increases, the adsorption capacity also increases. However, after a certain speed, the change in adsorption capacity was stated as insignificant. When the rate constants in Table 4.10 are evaluated, it can be observed that the rate constant increases from 0.149 g/mg.min to 0.157 g/mg.min when the speed increased from 120 to 160 rpm. This increase can be explained by the decrease in the thickness of the liquid film due to turbulence (Al-qodah et al., 2007). However, the rate decreased drastically (0.035 g/mg.min) when the speed increased to 200 rpm.

4.1.5.3 When PAC used as adsorbent

The results of the experiments conducted for examining the effect of temperature on the adsorption of phorate onto the PAC are presented in Figure 4.21. The initial concentration for all temperatures tested was 1±0,1 mg/L. Three temperature ranges are studied in this thesis, namely low temperature (15 ºC ± 2ºC), room temperature (25 ºC ± 2ºC), and high temperature (35 ºC ± 2ºC). The shaking speed was set to 160 rpm and the pH value was 7. The adsorbent dose was 25 mg/L of PAC.
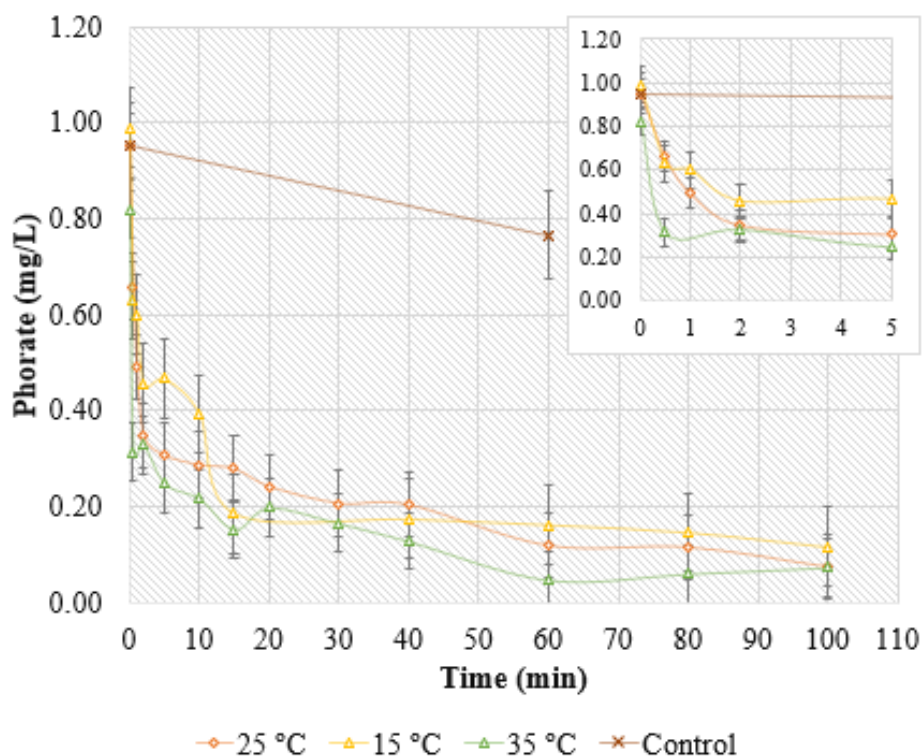
Figure 4.21 The effect of temperature on the adsorption kinetic of phorate on PAC (C_o=1 mg/L at 160 rpm, 25 mg PAC/L, pH 7)

The initial concentrations decreased by half in less than 30 sec for 35 ºC, 1 min for 25 ºC, and around 5 min for 15 ºC. Thus, it can be asserted the adsorption of phorate on PAC is a fast process at different temperature ranges as well. Moreover, all reactors reached the equilibrium at the same concentration which is around 0.1 mg/L at the end of the 60 min. Thus, it can be said that temperature does not have a significant impact on the equilibrium conditions when phorate is adsorbed onto PAC.

Kinetic Model:

In order to determine the kinetic model followed and the relevant rate constants at three temperatures, the experimental data provided in Figure 4.21, are subjected to the analysis for three different kinetic models, namely, PFO and PSO. The relevant analysis can be depicted in Figure 4.22.
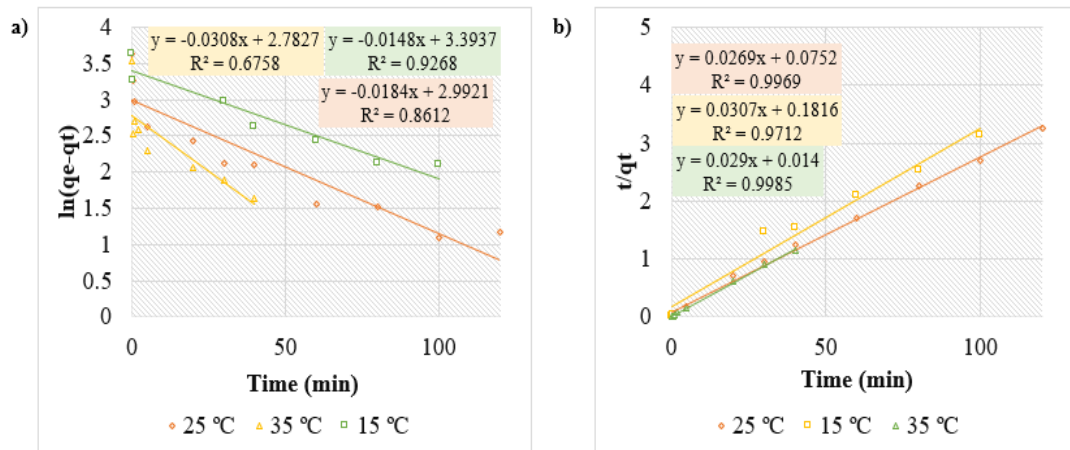
Figure 4.22 Kinetic models for different temperatures a) PFO, b) PSO

The results from the regression analysis, rate constant and equilibrium adsorption capacities with respect to kinetic models are presented in Table 4.11.

Table 4.11 The results of the adsorption kinetics model analysis for PAC at different temperatures

T (ºC)	Kinetic model	R^2	Rate constant	qe (mg/g)
15	PFO	0.927	0.015 min^{-1}	29.78
	PSO	0.971	0.005 g/mg.min	32.57
25	PFO	0.861	0.018 min^{-1}	19.93
	PSO	0.997	0.010 g/mg.min	37.18
35	PFO	0.676	0.009 min^{-1}	12.66
	PSO	0.999	0.010 g/mg.min	37.88

When the outcomes of the analysis are evaluated for all temperatures, it can be seen that the PSO model is the best-fitted model. It has R^2 values of 0.971 for 15 ºC, 0.997 for 25 ºC and 0.999 for 35 ºC . When the adsorption capacities at equilibrium conditions are compared, the temperature of 25 ºC and 35 ºC have very close values, which are 37 and 38 mg/g, respectively. A slightly lower adsorption capacity is

observed (33 mg/g) at 15 ºC. When the rate constants are observed, the rate of adsorption also increases with the increasing temperature until 25 ºC, then remains constant at 35 ºC. This can be interpreted as the adsorption of phorate onto PAC is an endothermic process. Nevertheless, the differences observed are very small. So, it could be stated that the adsorption of phorate onto PAC is not affected remarkably by the temperature variations within the studied range. Adsorption is known as an exothermic process (Benefield et al., 1982). However, there are some endothermic adsorption examples in the literature. For example, Mittal et al. (2007) studied the removal of tartrazine by using hen feather as an adsorbent and the results of their study showed that the process was endothermic since the rate increased with higher temperatures.

4.1.5.4   When CHA used as adsorbent

The results of the experiments conducted for examining the effect of temperature on the adsorption of phorate onto the CHA are presented in Figure 4.23. The initial concentration for all temperature values tested was 1±0.1 mg/L. Three temperature values were studied in this thesis, namely low temperature (15 ºC ± 2ºC), room temperature (25 ºC ± 2ºC) and high temperature (35 ºC ± 2ºC). A control reactor was prepared for every temperature, yet the profile drawn using the average of the data belonging to all three reactors is shown on the graph as the three controls yielded a similar trend. The shaking speed was set to 160 rpm and pH value was 7. The adsorbent dose was 25 mg/L.
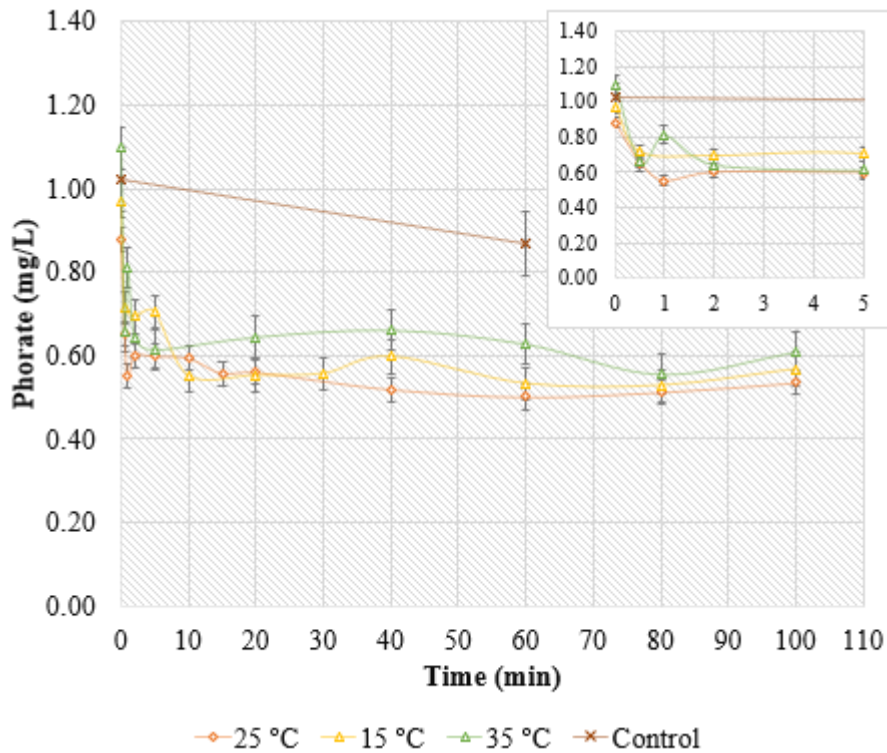
Figure 4.23 The effect of temperature on the adsorption kinetic of phorate on CHA (C_o=1 mg/L at 160 rpm, 25 mg CHA/L, pH 7)

Figure 4.23 shows that the adsorption of phorate onto CHA is a fast process as per the observations for the other operational conditions. The reactors at 15 ºC and 25 ºC have an equilibrium concentration of 0.5 mg/L attained at 60 min. Meanwhile, the reactor at 35 ºC establishes equilibrium at 20 min with a concentration of 0.6 mg/L. By looking at the equilibrium concentrations, it can be stated that there is not a considerable effect of temperature on the removal efficiency of phorate via adsorption onto CHA.

Kinetic Model:

In order to determine the kinetic model followed and the relevant rate constants at three temperatures, the experimental data provided in Figure 4.23 are subjected to the analysis for two different kinetic models, namely, PFO and PSO models. The relevant analysis can be depicted in Figure 4.24.
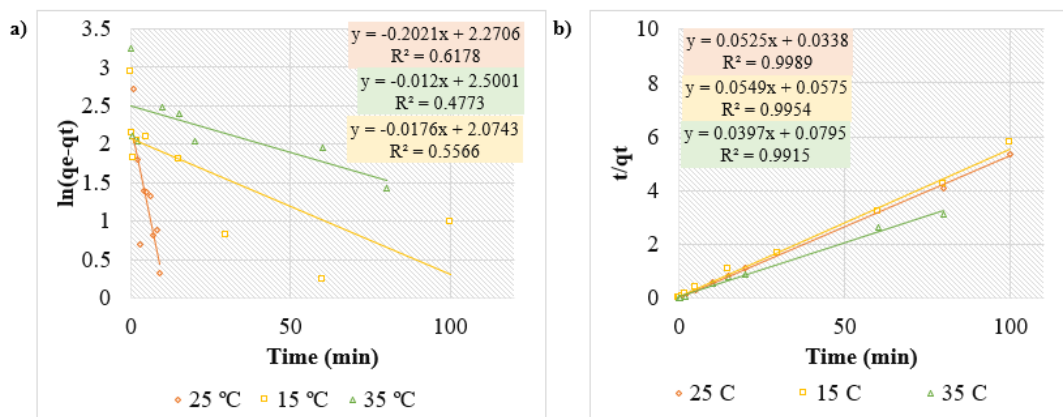
Figure 4.24 Kinetic models for different temperatures a) PFO, b) PSO

The results from the regression analysis, rate constant and equilibrium adsorption capacities with respect to kinetic models are presented in Table 4.12.

Table 4.12 The results of the adsorption kinetics model analysis for CHA at different temperatures

T (°C)	Kinetic model	R^2	Rate constant	q_e (mg/g)
15	PFO	0.557	0.012 min^{-1}	7.26
	PSO	0.995	0.060 g/mg.min	17.39
25	PFO	0.618	0.018 min^{-1}	5.44
	PSO	0.999	0.055 g/mg.min	19.88
35	PFO	0.477	0.012 min^{-1}	12.18
	PSO	0.992	0.020 g/mg.min	25.19

The results of the analysis indicate that for all temperatures, one can suggest the PSO model as the representative model for adsorption kinetics since it has high R^2 values. When the rate constants of the PSO model are examined it can be declared that the adsorption of phorate onto CHA is an exothermic process since, with the increasing temperature the rate constant decreases. The adsorption capacities are increased with increasing temperature (17 mg/g, 20 mg/g and 25 mg/g for 15, 25 and 35 °C,

respectively). Al-qodah et al. (2007) stated that there are three main factors of the temperature effect on adsorption. The first one is the increased solubility of pesticides in the water with increasing temperature. Secondly, due to the decrease in viscosity at high temperatures, the rate of diffusion of adsorbate molecules in the liquid film increases. Lastly, the diffusion of these molecules in the internal pores rises with increasing temperature owing to reduced viscosity of the solution. On the other hand, there is a rise in the equilibrium adsorption capacity with escalating temperature. This can be explained by the increasing water solubility of pesticides with increasing temperature and the exothermic nature of this process (Curren & King, 2001).

4.2   Adsorption equilibrium

In order to understand the interaction between phorate and the adsorbents, namely CHA and PAC, adsorption equilibrium experiments were conducted. The results obtained from these experiments are introduced and discussed in this section. The experimental conditions for the experiments were: temperature of 25 ± 2 ºC, pH of 7 and shaking speed of 160 rpm. For each adsorbent, initial phorate concentrations and adsorbent amounts applied during the adsorption equilibrium studies are provided in Table 4.13.

Table 4.13 The adsorption capacities attained during the isotherm experiments

	Adsorbent amount (mg/L)	Initial concentration (mg/L)	Equilibrium concentration (mg/L)	qe (mg/g)
PAC	25	7.6	2.96	19
	25	6.0	1.63	17
	25	3.0	0.75	9
	25	1.0	0.12	3
	25	0.8	0.12	3
	25	0.3	0.06	1
CHA	25	3.6	2.16	6

	Adsorbent amount (mg/L)	Initial concentration (mg/L)	Equilibrium concentration (mg/L)	qe (mg/g)
	12.5	1.9	0.85	9
	37.5	0.9	0.56	1
	25	5.8	2.6	13
	25	0.9	0.50	2
	25	0.6	0.40	1
	25	0.7	0.37	1
	12.5	0.3	0.04	2

Adsorption isotherms for PAC and CHA drawn are presented in Figure 4.25a and b, respectively.
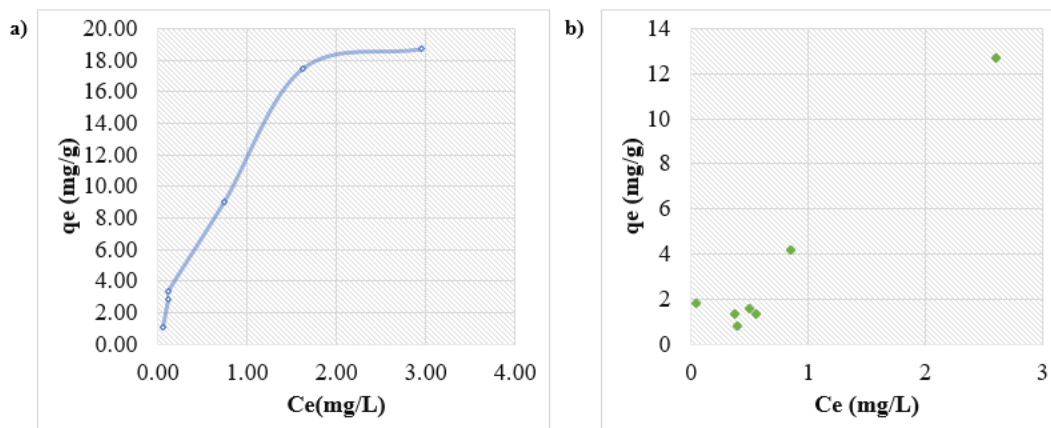
Figure 4.25 Adsorption isotherms for phorate on a) PAC, b) CHA

As seen from Figure 4.25a, qe values for PAC reached to a plateau level of 0.19 mg/mg when the equilibrium phorate concentration of 3 mg/L is reached. This indicates that the monolayer formation during the phorate adsorption onto PAC occurs, suggesting that the Langmuir Isotherm model is followed.

Regarding existing data, the difference between the adsorption capacities of PAC and CHA can be explained by the difference in the surface area of the two adsorbents. This

result indicates that PAC has a higher surface area than CHA. Indeed, the surface area of PAC varies between 400–1800 m^2/g (Krahnstöver & Wintgens, 2018), while the surface area of CHA is around 463 m^2/g (Ali, 2022). Also, the results suggest that pore size of PAC is higher than CHA which eases the diffusion into pores and yields higher adsorption capacities. Indeed, CHA has pore size of 3.8 °A (Ali, 2022) which is lower than the calculated kinetic diameter of phorate (7.9 °A) (Kowenje & Osewe, 2015).

Two isotherm models, namely, the Langmuir and Freundlich isotherm models, were applied to the equilibrium data. The relevant findings are provided and discussed in the subsequent sub-sections.

4.2.1   Langmuir isotherm model

The lineralized Langmuir isotherm plots are given in Figure 4.26 .
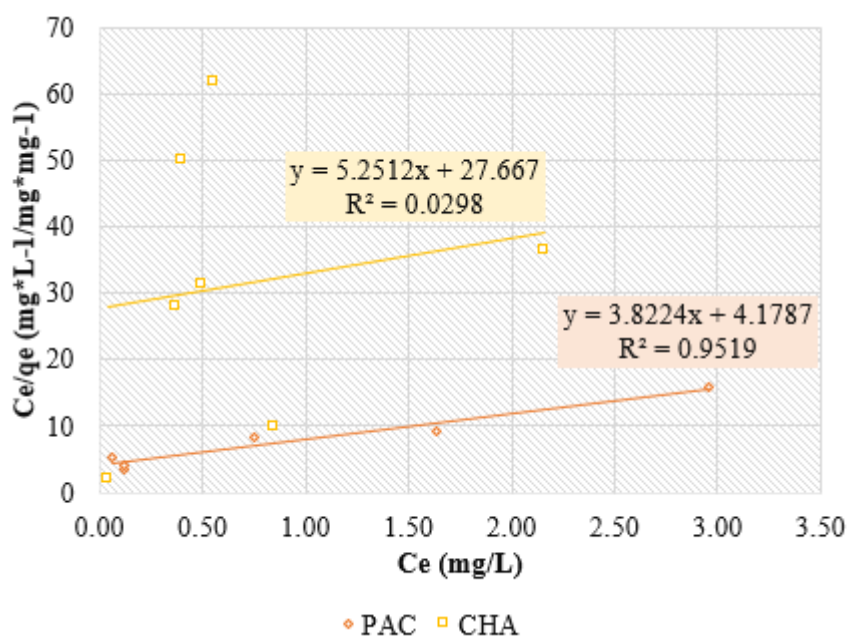
Figure 4.26 The linearized Langmuir adsorption isotherm of phorate onto CHA and PAC

As seen in Figure 4.26, the R^2 value for the adsorption onto PAC is 0.95, which is significantly higher than the value for CHA (about 0.03). These R^2 values indicate that

the Langmuir isotherm model is perfectly followed by the adsorption of phorate onto PAC, whereas the adsorption onto CHA can not be described by the Langmuir model as it was indeed apparent from the isotherm profile obtained (Figure 4.25b). As can be seen from Table 4.14, the maximum adsorption capacity for PAC was calculated as 26 mg/g. When the adsorption isotherm graph of PAC (Figure 4.25 a) is examined, the maximum adsorption capacity can read as 19 mg/g, which is different from q_{max} (26 mg/g) obtained from Langmuir isotherm. The reason behind this small difference can be explained by the implementation of the model. Since the correlation constant is not exactly equal to 1 even though it is close to 1, a small difference between the empirical and calculated may exist. The adsorption capacity determined by the PSO model was 37 mg/g (for the experimental conditions: pH of 7, at 25 ºC., shaking speed of 160 rpm, 25 mg/L of PAC and initial phorate concentration of 1 mg/L (Table 4.3). This value is also different from the empirical and calculated one by the Langmuir model. The Langmuir constant, b, for PAC was determined as 1.28 L/mg. This constant is related to the affinity of adsorbate toward the adsorbent (Nguyen et al., 2017). The parameters of the Langmuir isotherm model and separation factor for both of the adsorbents is presented in Table 4.14.

Table 4.14 The parameters of the Langmuir isotherm model for CHA and PAC

	q_{max} (mg/g)	b (L/mg)	R^2	R
PAC	26	1.28	0.95	0.44
CHA	19	0.01	0.03	0.99

When the affinity-related constant Langmuir constant, b, is evaluated, one can declare that phorate has a high affinity (1.28 L/mg) for PAC, which is aligned with the high adsorption capacity of PAC as well. On the other hand, it can be seen that the adsorption behavior of phorate on PAC is well-defined by the Langmuir model (R^2 value of 0.95). The separation factor is used for the determination of adsorption nature (Al-Ghouti & Da'ana, 2020). For PAC, R-value is between 0 and 1, which indicates that the adsorption of phorate on PAC was favorable. However, these comments and

deductions can not be made for CHA since it can not be defined (very low R^2 value) by the Langmuir isotherm model.

4.2.2 Freundlich isotherm model

The linearized Freundlich isotherm plots for PAC and CHA are given in Figure 4.27.
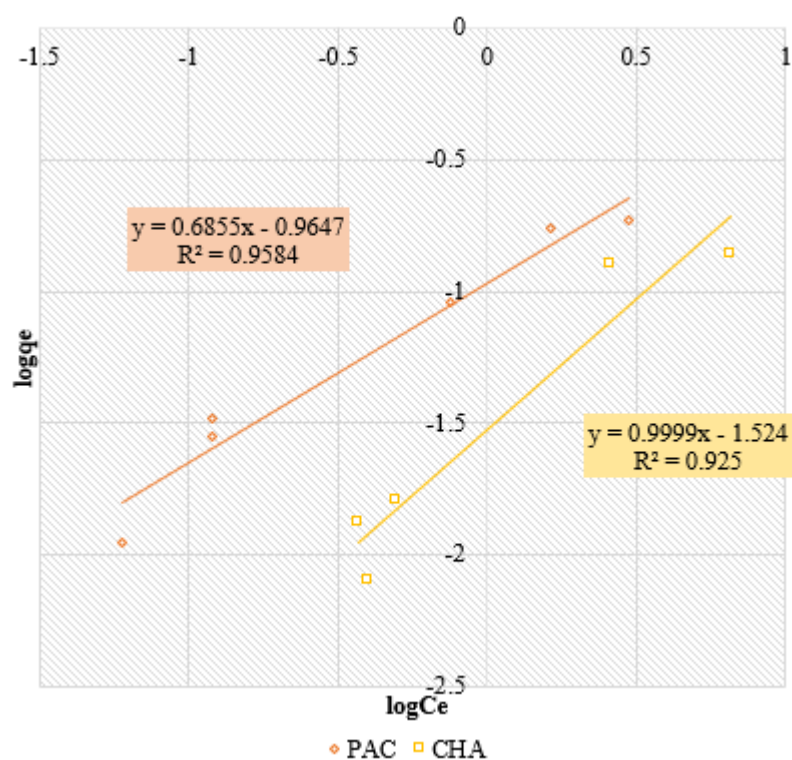
Figure 4.27 The Freundlich adsorption isotherm of phorate onto CHA and PAC

The results from the implementation of the Freundlich isotherm model yield correlation coefficient values of 0.93 and 0.96 for CHA and PAC, respectively. This suggests that for the modeling of adsorption of phorate onto PAC and CHA, Freundlich isotherm can be used. The Freundlich constant, Kf, for the adsorption of phorate is 0.38 L/mg for PAC. Meanwhile, n value is 1.46 for PAC. The model parameters for CHA are 0.22 L/mg for K_f and n value of 1. The aforementioned model constants is tabulated in Table 4.15.

Table 4.15 The parameters of the Freundlich isotherm model for PAC and CHA

	K_f (L/mg)	n	1/n	R^2
PAC	0.38	1.46	0.69	0.96
CHA	0.22	1.00	0.99	0.93

The adsorption potential, K_f, has a value of 0.38 for PAC and 0.22 L/mg for CHA. Since it is related to adsorption potential, when it is considered with the maximum adsorption capacity both calculated by the Langmuir model and obtained through experiments, it is safe to state that the adsorption potential of phorate onto PAC is higher. On the other hand, the value of constant, n, can be used to determine if the adsorption is favorable or not since 1/n values lower than 1 indicates favorable process while the values higher than 1 indicates unfavorable and if 1/n equals to 1 then adsorption process is irreversible (Al-Ghouti & Da'ana, 2020). 1/n value for PAC (0.69) and for CHA (0.99) are in the range of 0-1, which indicates that the adsorption of phorate is favorable.

Regarding the effect of kinetic diameter of the adsorbate on the extent of adsorption, the adsorption capacity of CHA for phorate is compared with those determined for malathion and carbendazim by Ali, 2022, is 2.50 and 4.56 mg/g, respectively. The adsorption capacity of CHA for phorate is 13 mg/g (Figure 4.25). The capacity for phorate may be expected to be between 2.50 and 4.56 mg/g since both the kinetic diameter and molecular weight of phorate (7.9 °A, 260.4 g/mol) is between the kinetic diameters and molecular weigths of carbendazim (7.4 °A, 191.2 g/mol) and malathion (8.6 °A, 330.4 g/mol). The reason of higher adsorption capacity than expected can be explained by the fact that the adsorption capacities of 2.5 and 4.56 mg/g belong to pre-treated CHA which is enchanced with iron while 13 mg/g belongs to raw CHA. Ali (2022) stated that the exchange of iron decreased the mesopore volume from 0.2 to 0.15 cm^3/g which may explain the lower adsorption capacities of iron-exchanged CHA.

4.3 The comparison of adsorption kinetic and equilibrium behavior of phorate onto PAC and CHA

In this section, the adsorption kinetic and equilibrium relationships between phorate and the two adsorbents, namely CHA and PAC, are discussed comparatively.

The effect of pH on the adsorption kinetics for PAC and CHA is presented in Table 4.16. The constant k_2 in this table represents the PSO rate constant since for all operational conditions, PSO is the best-fitted kinetic model for both PAC and CHA. Also, q_{emax} (calc.) represents the calculated value from PSO kinetic model while q_{emax} (exp.) represents calculated value by using the data presented in Table 4.13 and Eq.21 in .

Table 4.16 The effect of pH on the adsorption kinetics for PAC and CHA

		PAC	CHA
pH 3	C_e (mg/L)	0.1	0.2
	t_e (min)	60	20
	q_{emax} (calc.) (mg/g)	36	26
	q_{emax} (exp.) (mg/g)	35	25
	k_2 (g/mg.min)	0.035	0.243
pH 7	C_e (mg/L)	0.1	0.5
	t_e (min)	60	40
	q_{emax} (calc.) (mg/g)	37	20
	q_{emax} (exp.) (mg/g)	35	19
	k_2 (g/mg.min)	0.010	0.043
pH 9	C_e (mg/L)	0.1	0.5
	t_e (min)	60	40
	q_{emax} (calc.) (mg/g)	35	19
	q_{emax} (exp.) (mg/g)	36	19

(Table 4.16 continued)

		PAC	CHA
	k_2 (g/mg.min)	0.013	0.020

When the results presented in Table 4.16 are examined, it can be seen that pH has no effect on the equilibrium conditions (Ce and te) when the adsorbent is PAC; however, it has a remarkable effect on the equilibrium behavior of the adsorption onto CHA. For CHA, as the pH increases, both Ce and t_e increase. For all pH values tested, both qemax (calc.) and qemax(exp.) for PAC is greater than for CHA. However, the values of these parameters decreased from 26 and 25 mg/g to 19 and 19 mg/g, respectively, when pH increased from 3 to 9. Therefore, it could be inferred that CHA works better at lower pH conditions. On the other hand, when the rate constants are considered, it can be seen that the constants for CHA are higher than for PAC. This would be taken as an indication of faster adsorption of phorate onto CHA. Nevertheless, the Ce values attained are smaller in the case of PAC as compared to CHA. The difference between CHA and PAC can be explained by the different adsorbent properties such as surface area, surface chemistry, chemical structure, etc. To clarify, PAC has a larger surface area which could explain its larger adsorption capacity and maybe the smaller equilibrium concentration attained, whereas faster adsorption onto CHA could be attributed to the adsorption taking place dominantly onto the exterior surface rather than the pore (maybe due to the larger size of phorate than the pores of CHA), so that possibility of pore diffusion limitation is excluded.s. However, the latter attribution is just a speculation and remains to be proven. The effect of initial phorate concentration on the adsorption kinetics for PAC and CHA is presented in Table 4.17.

Table 4.17 The effect of initial phorate concentration (C_o) on the adsorption kinetics for PAC and CHA

C_o		PAC	CHA
1±0.1 mg/L	C_e (mg/L)	0.1	0.5
	t_e (min)	60	60
	q_{emax} (calc.) (mg/g)	37	20
	q_{emax} (exp.) (mg/g)	35	20
	k_2 (g/mg.min)	0.010	0.074
0.75 ±0.1 mg/L	C_e (mg/L)	0.1	0.5
	t_e (min)	60	60
	q_{emax} (calc.) (mg/g)	32	22
	q_{emax} (exp.) (mg/g)	30	22
	k_2 (g/mg.min)	0.012	0.036
0.5 ±0.1 mg/L	C_e (mg/L)	0.1	0.4
	t_e (min)	60	60
	q_{emax} (calc.) (mg/g)	14	27
	q_{emax} (exp.) (mg/g)	13	26
	k_2 (g/mg.min)	0.057	0.010

When the results presented in Table 4.17 are examined, it can be stated that C_o has no effect on the equilibrium conditions when the adsorbent is PAC; however, it has an effect, though slight, on the equilibrium behavior of the adsorption onto CHA. For example, for CHA, as the C_o decreases to 0.5 mg/L from 0.75 mg/L, Ce also slightly decreased to 0.4 from 0.5 mg/L. For both adsorbents, the equilibrium time is observed as 60 min for all the initial concentrations tested. For the lowest C_o value, both qe, cal. and qe, exp. for PAC is smaller than those for CHA. Thus, one can infer that at lower concentrations of phorate, CHA could be preferred. However, when the rate constants are considered, it can be seen that the constants for CHA are higher than PAC for higher initial concentrations. Therefore, one can assert that the adsorption rate of phorate on PAC is lower than the adsorption on CHA for larger Co values.

The effect of adsorbent amount on the adsorption kinetics for PAC and CHA is presented in Table 4.18.

Table 4.18 The effect of adsorbent amount on the adsorption kinetics for PAC and CHA

Adsorbent dose		PAC	CHA
12.5 mg/L	C_e (mg/L)	0.3	0.6
	t_e (min)	60	60
	q_{emax} (calc.) (mg/g)	31	15
	q_{emax} (exp.) (mg/g)	28	15
	k_2 (g/mg.min)	0.010	0.024
25 mg/L	C_e (mg/L)	0.1	0.5
	t_e (min)	60	60
	q_{emax} (calc.) (mg/g)	37	20
	q_{emax} (exp.) (mg/g)	36	20
	k_2 (g/mg.min)	0.010	0.042
37.5 mg/L	C_e (mg/L)	0.1	0.6
	t_e (min)	60	60
	q_{emax} (calc.) (mg/g)	37	19
	q_{emax} (exp.) (mg/g)	37	17
	k_2 (g/mg.min)	0.029	0.310

When the results presented in Table 4.18 are evaluated, it can be stated that the adsorbent amount does not have a considerable effect on the equilibrium conditions for both of the adsorbents. For all adsorbent doses, qe,cal and qe,exp for PAC are higher than CHA. However, when the rate constants are considered, one can state that the constants for CHA are higher than PAC for every adsorbent amount tested. Therefore, one can assert that the adsorption rate of phorate on CHA is higher than the

adsorption on PAC. The higher rates with increasing adsorbent amount are expected since the total available sites of the system increases; hence, the chance of finding a vacant site to bind for phorate is easier and faster when the adsorbent amount is high.

The effect of adsorbate to adsorbent ratio on the adsorption kinetics for PAC and CHA is presented in Table 4.19.

Table 4.19 The effect of adsorbate to adsorbent ratio on the adsorption kinetics for PAC and CHA

Adsorbate/Adsorbent		PAC	CHA
0.014 (for PAC) **0.024 (for CHA)**	C_e (mg/L)	0.1	0.4
	t_e (min)	60	60
	q_{emax} (calc.) (mg/g)	14	27
	q_{emax} (exp.) (mg/g)	13	26
	k_2 (g/mg.min)	0.057	0.010
0.027	C_e (mg/L)	0.1	0.6
	t_e (min)	60	60
	q_{emax} (calc.) (mg/g)	37	19
	q_{emax} (exp.) (mg/g)	37	17
	k_2 (g/mg.min)	0.029	0.310
0.034 (for PAC) **0.030 (for CHA)**	C_e (mg/L)	0.1	0.5
	t_e (min)	60	60
	q_{emax} (calc.) (mg/g)	32	22
	q_{emax} (exp.) (mg/g)	30	22
	k_2 (g/mg.min)	0.012	0.036
0.04	C_e (mg/L)	0.1	0.5
	t_e (min)	60	60

Adsorbate/Adsorbent			PAC	CHA
	q_{emax} (calc.) (mg/g)		37	20
	q_{emax} (exp.) (mg/g)		36	20
	k_2 (g/mg.min)		0.010	0.042
0.08	C_e (mg/L)		0.3	0.6
	t_e (min)		60	60
	q_{emax} (calc.) (mg/g)		31	15
	q_{emax} (exp.) (mg/g)		28	15
	k_2 (g/mg.min)		0.010	0.024

When the results presented in Table 4.19 are evaluated, it can be stated that the adsorbent amount does not have an effect on the equilibrium time for both of the adsorbents since they all reached the equilibrium at 60 min. For all adsorbate to adsorbent ratio, qe,cal and qe,exp for PAC are higher than CHA. However, when the rate constants are considered, one can state that the constants for CHA are higher than PAC for every ratio tested. Therefore, one can assert that the adsorption rate of phorate on CHA is higher than the adsorption on PAC. The rate constants decreases with increasing ratio for PAC; however, the rate constants do not show strong directly proportional relationship with adsorbate to adsorbent ratio when the adsorbent is CHA.

The effect of shaking speed on the adsorption kinetics for PAC and CHA is presented in Table 4.20.

Table 4.20 The effect of shaking speed on the adsorption kinetics for PAC and CHA

Shaking speed		PAC	CHA
120 rpm	C_e (mg/L)	0.2	0.4
	t_e (min)	60	20
	q_{emax} (calc.) (mg/g)	31	23
	q_{emax} (exp.) (mg/g)	31	15
	k_2 (g/mg.min)	0.060	0.024
160 rpm	C_e (mg/L)	0.1	0.5
	t_e (min)	60	60
	q_{emax} (calc.) (mg/g)	37	19
	q_{emax} (exp.) (mg/g)	36	20
	k_2 (g/mg.min)	0.010	0.042
200 rpm	C_e (mg/L)	0.1	0.2
	t_e (min)	60	30
	q_{emax} (calc.) (mg/g)	37	29
	q_{emax} (exp.) (mg/g)	38	28
	k_2 (g/mg.min)	0.060	0.310

When the results are evaluated, it can be stated that shaking speed has a considerable effect on the equilibrium conditions for both of the adsorbents. When shaking speed is 120 rpm, PAC has higher adsorption capacity and rate and lower Ce with higher te when compared to CHA. However, when the shaking speed increased to 160 rpm, te and rate for CHA increased to 60 min and 0.042 g/mg.min, respectively. Afterward, when the shaking speed increases further to 200 rpm, t_e decreases by half, and the rate increases drastically while Ce decreases. Hence, the performance of CHA is enhanced

with increasing shaking speed in terms of both speed and amount of adsorption, which may imply that the rate-limiting step for the adsorption onto CHA is film diffusion.

The effect of temperature on the adsorption kinetics for PAC and CHA is presented in Table 4.21.

Table 4.21 The effect of temperature on the adsorption kinetics for PAC and CHA

Temperature		PAC	CHA
15 ºC	C_e (mg/L)	0.1	0.5
	t_e (min)	60	60
	q_{emax} (calc.) (mg/g)	33	17
	q_{emax} (exp.) (mg/g)	34	15
	k_2 (g/mg.min)	0.005	0.060
25 ºC	C_e (mg/L)	0.1	0.5
	t_e (min)	60	60
	q_{emax} (calc.) (mg/g)	37	20
	q_{emax} (exp.) (mg/g)	36	20
	k_2 (g/mg.min)	0.010	0.055
35 ºC	C_e (mg/L)	0.1	0.6
	t_e (min)	60	20
	q_{emax} (calc.) (mg/g)	38	25
	q_{emax} (exp.) (mg/g)	36	28
	k_2 (g/mg.min)	0.010	0.020

When the results are evaluated, it can be stated that temperature has a considerable effect on the equilibrium conditions for both of the adsorbents. For all temperature values, PAC has higher qe and lower Ce with a lower rate constant; thus, it can be declared that the removal performance of PAC is better, yet the process occurs more

slowly when compared to CHA. The rate constants are increasing for PAC while they are decreasing for CHA with higher temperatures. Therefore, one can assert that the adsorption of phorate onto PAC is endothermic while it is exothermic for CHA.

In order to summarize the provided information for the isotherm study, Table 4.22 is presented below.

Table 4.22 The Langmuir and Freundlich isoterm model constants and parameters for PAC and CHA

Isotherm model	Parameter	PAC	CHA
Langmuir	qmax (mg/g)	26	19
	b (L/mg)	1.28	0.01
	R^2	0.95	0.03
	R	0.44	0.99
Freundlich	K_f	0.38	0.22
	1/n	0.69	0.99
	n	1.46	1.00
	R^2	0.96	0.93

From Table 4.22, one can state that the adsorption equilibrium behavior of PAC can be described by both Langmuir and Freundlich models since, for both of the models, it has R-square values close to 1. However, for CHA, equilibrium behavior can only be defined by the Freundlich isotherm model (R^2 value of 0.93). The adsorption of the phorate onto PAC could be defined as favorable by both of the isotherm models with respect to separation constant and 1/n values since both them is lower than one. The phorate adsorption can be considered favorable by the Freundlich model for CHA regarding 1/n value which is smaller than one. The maximum adsorption capacity revealed by the Langmuir model and adsorption potential by the Freundlich model indicates a higher adsorbed amount of phorate onto PAC.

A summary of the adsorption kinetics and equilibrium-related findings are presented in Table 4.23.

Table 4.23 Summary of adsorption kinetics and equilibrium findings for adsorbents

	pH					
	3		**7**		**9**	
	PAC	**CHA**	**PAC**	**CHA**	**PAC**	**CHA**
t_e (min)	60	10	60	20	60	20
C_e (mg/L)	0.1	0.2	0.1	0.5	0.1	0.5
q_e (exp.,mg/g)	35	25	35	25	36	19
q_e (calc.,mg/g)	36.4	26	37.2	19.7	34.6	18.7
Rate constant (g/mg.min)	0.035	0.243	0.01	0.043	0.013	0.02
	Initial concentration (mg/L)					
	1±0.1		**0.75±0.1**		**0.5±0.1**	
	PAC	**CHA**	**PAC**	**CHA**	**PAC**	**CHA**
t_e (min)	60	60	60	60	60	60
C_e (mg/L)	0.1	0.5	0.1	0.5	0.1	0.4
q_e (exp.,mg/g)	35	20	30	22	13	26
q_e (calc.,mg/g)	37.2	19.7	31.9	21.9	13.9	27.3
Rate constant (g/mg.min)	0.01	0.074	0.024	0.036	0.057	0.01
	Adsorbent Dose (mg/L)					
	12.5		**25**		**37.5**	
	PAC	**CHA**	**PAC**	**CHA**	**PAC**	**CHA**
t_e (min)	60	60	60	60	60	60
C_e (mg/L)	0.3	0.6	0.1	0.5	0.1	0.6
q_e (exp.,mg/g)	28	15	36	20	37	17
q_e (calc.,mg/g)	31	15.4	37.2	19.9	37.2	18.7
Rate constant (g/mg.min)	0.01	0.024	0.01	0.042	0.029	0.31
	Shaking speed (rpm)					
	120		**160**		**200**	
	PAC	**CHA**	**PAC**	**CHA**	**PAC**	**CHA**
t_e (min)	60	20	60	60	60	30
C_e (mg/L)	0.2	0.4	0.1	0.5	0.1	0.2

(Table 4.23 continued)

	Shaking speed (rpm)					
	120		160		200	
	PAC	CHA	PAC	PAC	CHA	PAC
q_e (exp.,mg/g)	31	15	37	19	38	28
q_e (calc.,mg/g)	30.7	23	37.2	19.2	36.9	28.9
Rate constant (g/mg.min)	0.06	0.149	0.01	0.157	0.031	0.035
	Temperature (ºC)					
	15		25		35	
	PAC	CHA	PAC	CHA	PAC	CHA
t_e (min)	60	60	60	60	60	20
C_e (mg/L)	0.1	0.5	0.1	0.5	0.1	0.6
q_e (exp.,mg/g)	34	15	36	20	36	28
q_e (calc.,mg/g)	32.6	17.4	37.2	19.9	37.9	25.2
Rate constant (g/mg.min)	0.005	0.06	0.01	0.012	0.01	0.02

CHAPTER 5

CONCLUSIONS

The main conclusions of this study can be listed as:

For the adsorption of phorate onto PAC;

- ➢ The effect of pH is insignificant on the equilibrium conditions. However, the adsorption rate is higher under acidic conditions.
- ➢ The initial concentration of phorate does not influence the equilibrium conditions; yet, the adsorption rate increases with decreasing initial concentration.
- ➢ The adsorbent dose does not affect the equilibration time; however, equilibrium concentration is the highest when the dose is the lowest.
- ➢ The rate constants of adsorption increases when the dose of PAC increases.
- ➢ Higher adsorbate to adsorbent ratios have higher capacity; yet, the rate constants decrease with increasing ratio
- ➢ Shaking speed affects the equilibrium concentration. The equilibrium concentration decreases with decreasing shaking speed, similar to the rate of adsorption.
- ➢ The change in temperature does not affect the equilibrium; however, the rate increases with higher temperatures implying that the nature of adsorption is endothermic.

For the adsorption of phorate on CHA;

- ➢ The effect of pH is significant on the equilibrium conditions. The equilibrium time and concentration decrease with low pH values.
- ➢ However, the adsorption rate is higher under acidic conditions.

- The initial concentration of phorate does not influence the equilibrium conditions; yet, the rate constant of adsorption increases with decreasing initial concentration.

- The adsorbent dose does not affect the equilibrium concentration; however, equilibrium time is the highest when the CHA amount is the lowest. Also, the rate drastically increased when CHA amount increased to the highest tested value.

- Shaking speed has an effect on the equilibrium concentration. The concentration decreases with an increase in high shaking speed. Similar to the equilibrium concentration, the adsorption rate decreases with a higher shaking speed; however, it increases again when the highest shaking speed is tested.

- The increase in temperature leads to a shorter equilibrium time and higher equilibrium concentration. The adsorption rate declined with higher temperatures which indicates that phorate adsorption on CHA is exothermic.

For all operational conditions studied, PSO is the best-fitted kinetic model for both PAC and CHA. The adsorption rate constants were determined to be within the ranges of 0.013-0.060 g/mg.min and 0.012- 0.243 g/mg.min, for PAC and CHA, respectively. The overall adsorption rates were possibly controlled by pore diffusion and surface film diffusion for PAC and CHA, respectively.

The equilibrium relationship between PAC and phorate is well-described by both Langmuir and Freundlich isotherm models. For CHA, the Freundlich isotherm model is the best-fitted model to describe the equilibrium relation with phorate.In general, PAC was found to be superior over CHA as an adsorbent to remove phorate. The maximum adsorption capacity of PAC was determined as 26 mg/g.

CHAPTER 6

RECOMMENDATIONS

For the future studies, the following recomendations can be suggested:

- The adsorbent properties such as morphology and surface chemistry of CHA and PAC should be analysed and the results should be re-evaluated with respect to the analysis results.
- Desorption studies can be performed to investigate the resuability of CHA and PAC.
- The adsorption of phorate can be studied when it is in a mixture of other pollutants.
- Column studies for each adsorbent can be conducted to observe the performance of CHA and PAC in adsorbing phorate in continuous process.

REFERENCES

Abdeen, Z., & Mohammad, S. G. (2022). *Study of the Adsorption Efficiency of an Eco-Friendly Carbohydrate Polymer for Contaminated Aqueous Solution by Organophosphorus Pesticide*. 1–16. https://doi.org/10.4236/ojopm.2014.41004

Ahmad, A. L., Tan, L. S., & Shukor, S. R. A. (2008). *Dimethoate and atrazine retention from aqueous solution by nanofiltration membranes*. *151*, 71–77. https://doi.org/10.1016/j.jhazmat.2007.05.047

Ahmad, T., Rafatullah, M., Ghazali, A., Hashim, R., Ahmad, A., Ahmad, T., Rafatullah, M., & Ghazali, A. (2010). *Environmental Carcinogenesis and Ecotoxicology Reviews Removal of Pesticides from Water and Wastewater by Different Adsorbents : A Review Removal of Pesticides from Water and Wastewater by Different Adsorbents : A Review*. *0501*. https://doi.org/10.1080/10590501.2010.525782

Ahn, J., Lee, S., Kim, S., You, J., Han, B., Weon, H., & Lee, S. (2018). International Biodeterioration & Biodegradation Biodegradation of organophosphorus insecticides with P e S bonds by two Sphingobium sp . strains. *International Biodeterioration and Biodegradation*, *132*(January), 59–65. https://doi.org/10.1016/j.ibiod.2018.05.006

Ahsan, N., Anwar, J., Qadir, A., Zameer, M., & Areas, A. (2014). *Removal of direct red 16 (textile dye) from industrial effluent by using feldspar Removal of Direct Red 16 (Textile Dye) from Industrial Effluent by using Feldspar*. *16*(April).

Aislabie, J. (1995). A Review of Bacterial Degradation of Pesticides. *Australian Journal of Soil Research*, *33*(6), 925.

Akashe, M., Pawade, U., & Nikam, A. (2018). CLASSIFICATION OF PESTICIDES: A REVIEW. *International Journal of Research in Ayurveda and Pharmacy*, *9*, 144–150. https://doi.org/10.7897/2277-4343.094131

Al-Ghouti, M. A., & Da'ana, D. A. (2020). Guidelines for the use and interpretation of adsorption isotherm models: A review. *Journal of Hazardous Materials*, *393*(January), 122383. https://doi.org/10.1016/j.jhazmat.2020.122383

Al-qodah, Z., Shawaqfeh, A. T., & Lafi, W. K. (2007). *Adsorption of pesticides from aqueous solutions using oil shale ash*. *208*, 294–305. https://doi.org/10.1016/j.desal.2006.06.019

Al-Zaben, M. I., & Mekhamer, W. K. (2017). Removal of 4-chloro-2-methyl phenoxy acetic acid pesticide using coffee wastes from aqueous solution. *Arabian Journal of Chemistry*, *10*, S1523–S1529. https://doi.org/https://doi.org/10.1016/j.arabjc.2013.05.003

Ali, M. (2022). *Development of a New Heterogeneous Catalyst for the Use in Fenton-like Process Toward the Removal of Pesticides From Water*. METU.

Aslan, Ş. (2005). Combined removal of pesticides and nitrates in drinking waters using biodenitrification and sand filter system. *Process Biochemistry*, *40*, 417–424. https://doi.org/10.1016/j.procbio.2004.01.030

Aysan, H., Edebali, S., Ozdemir, C., & Celi, M. (2016). *Microporous and Mesoporous Materials Use of chabazite , a naturally abundant zeolite , for the investigation of the adsorption kinetics and mechanism of methylene blue dye*. *235*, 78–86. https://doi.org/10.1016/j.micromeso.2016.08.007

Baser, B. (2021). *INTERFACIAL CHEMICAL BEHAVIORS AND SYNERGISTIC EFFECTS OF POTASSIUM HYDROXIDE AND UREA-MODIFIED SEWAGE SLUDGE BIOCHAR ON PHORATE REMOVAL FROM WATER*. METU.

Benefield, L., Judkins, J., & Weand, B. (1982). *Process Chemistry for Water and Wastewater Treatment*. Prentice-Hall.

Børgesen, C. D., Fomsgaard, I. S., Plauborg, F., Schelde, K., & Spliid, N. H. (2015). *Fate of Pesticides - in Agricultural Soils*.

Bouteh, E., Ahmadi, N., Abbasi, M., Torabian, A., Loosdrecht, M. C. M. Van, &

Ducoste, J. (2021). Biodegradation of organophosphorus pesticides in moving bed biofilm reactors : Analysis of microbial community and biodegradation pathways. *Journal of Hazardous Materials*, *408*(October 2020), 124950. https://doi.org/10.1016/j.jhazmat.2020.124950

Capel, P. D., Larson, S. J., & Winterstein, T. A. (2001). *The behaviour of 39 pesticides in surface waters as a function of scale*. *1269*(December 1999), 1251–1269. https://doi.org/10.1002/hyp.212

Cara, I. G., & Jităreanu, G. (2022). *Application of Low-Cost Adsorbents for Pesticide Removal*. *May*. https://doi.org/10.15835/buasvmcn-agr

Chen, J. P., Pehkonen, S. O., & Lau, C. (2004). *Phorate and Terbufos adsorption onto four tropical soils*. *240*(March), 55–61. https://doi.org/10.1016/j.colsurfa.2004.03.008

Cheremisinoff, N. (2002). *HANDBOOK OF WATER AND WASTEWATER TREATMENT TECHNOLOGIES*. Butterworth-Heinemann.

Close, M. E., Flintoft, M. J., & Flintoft, M. J. (2010). *National survey of pesticides in groundwater in New Zealand — 2002 National survey of pesticides in groundwater in New Zealand — 2002*. *8330*. https://doi.org/10.1080/00288330.2004.9517238

Curren, M. S. S., & King, J. W. (2001). *Solubility of Triazine Pesticides in Pure and Modified Subcritical Water*. *73*(4), 3808–3813.

Dahshan, H., Megahed, A. M., & Abd-elall, A. M. M. (2016). Monitoring of pesticides water pollution- The Egyptian River Nile. *Journal of Environmental Health Science and Engineering*, 1–9. https://doi.org/10.1186/s40201-016-0259-6

Dar, M. A., Baba, Z. A., & Kaushik, G. (2022). A review on phorate persistence , toxicity and remediation by bacterial communities. *Pedosphere: An International Journal*, *32*(1), 171–183. https://doi.org/10.1016/S1002-0160(21)60043-7

De Smedt, C., Ferrer, F., Leus, K., & Spanoghe, P. (2015). Removal of Pesticides from

Aqueous Solutions by Adsorption on Zeolites as Solid Adsorbents. *Adsorption Science & Technology*, *33*(5), 457–485. https://doi.org/10.1260/0263-6174.33.5.457

Demirhan, E., & Culhaloglu, E. (2018). Adsorption of 2,4-dichlorophenoxyacetic acid on peanut shells: effect of initial concentration. *Environmental Research & Technology*, *1*(1), 23–26.

Derbalah, A., Chidya, R., Jadoon, W., & Sakugawa, H. (2018). ScienceDirect Temporal trends in organophosphorus pesticides use and concentrations in river water in Japan , and risk assessment. *Journal of Environmental Sciences*, *79*, 135–152. https://doi.org/10.1016/j.jes.2018.11.019

Donia, A. M., Atia, A. A., Hussien, R. A., & Rashad, R. T. (2012). Comparative study on the adsorption of malathion pesticide by different adsorbents from aqueous solution. *Desalination and Water Treatment*, *47*(1–3), 300–309. https://doi.org/10.1080/19443994.2012.696419

E X T O X N E T. (1996). *Extension Toxicology Network Pesticide Information Profiles*.

Elodie, G., Oturan, N., & Oturan, M. (2003). Removal of organophosphorus pesticides from water by electrogenerated Fenton s reagent. *Environmental Chemistry Letters*, 165–168. https://doi.org/10.1007/s10311-003-0029-4

EPA. (1985). *Pesticide Fact Sheet*.

EPA. (2001). *Phorate IRED Facts*. https://archive.epa.gov/pesticides/reregistration/web/html/phorate_fs.html

EPA. (2022a). *Basic Information about Pesticide Ingredients*.

EPA. (2022b). *What are Biopesticides?*

Essiedu, J. A., Adepoju, F., & Ivantsova, M. (2020). Benefits and limitations in using biopesticides. In *AIP Conference Proceedings* (Vol. 2313).

https://doi.org/10.1063/5.0032223

Fishel, F. (2003). *Pesticides and the Environment*.

Foo, K. Y., & Hameed, B. H. (2010). *Insights into the modeling of adsorption isotherm systems. 156*, 2–10. https://doi.org/10.1016/j.cej.2009.09.013

Gandhi, K., Lari, S., Tripathi, D., & Kanade, G. (2016). Advanced oxidation processes for the treatment of chlorpyrifos , dimethoate and phorate in aqueous solution. *Journal of Water Reuse and Desalination*, *6*(1), 195–203. https://doi.org/10.2166/wrd.2015.062

Gassmann, M. (2021). *Modelling the Fate of Pesticide Transformation Products From Plot to Catchment Scale — State of Knowledge and Future Challenges. 9*(July), 1–12. https://doi.org/10.3389/fenvs.2021.717738

Gavrilescu, M. (2005). Fate of Pesticides in the Environment and its Bioremediation. *Engineering in Life Sciences*, *5*(6), 497–526. https://doi.org/10.1002/elsc.200520098

Guo, X., & Wang, J. (2019). Comparison of linearization methods for modeling the Langmuir adsorption isotherm. *Journal of Molecular Liquids*, *296*, 111850. https://doi.org/10.1016/j.molliq.2019.111850

Hamilton, D., & Crossley, J. (2004). *Wiley Series in Agrochemicals and Plant Protection* (D. HAMILTON & S. CROSSLEY (eds.)). John Wiley and Sons,Ltd.

Hamilton, D. J., Ambrus, Á., Dieterle, R. M., Felsot, A. S., & Harris, C. A. (2003). *COMMISSION ON AGROCHEMICALS AND THE ENVIRONMENT * REGULATORY LIMITS FOR PESTICIDE RESIDUES IN WATER (IUPAC Technical Report). 75*(8), 1123–1155.

Hodgson, E. (2012). Biotransformation of Individual Pesticides: Some Examples. *Pesticide Biotransformation and Disposition*, 195–208. https://doi.org/10.1016/B978-0-12-385481-0.00009-5

Hong, F., Pehkonen, S. O., & Brooks, E. (2000). *Pathways for the Hydrolysis of Phorate : Product Studies by NMR and GC-MS 31 P*. 3013–3017.

Husk, B., Sanchez, J. S., Leduc, R., Takser, L., Savary, O., & Cabana, H. (2019). *on the susceptibility to source contamination*. 88–103. https://doi.org/10.2166/wqrj.2019.038

Interações, A. E., Ambiente, C. O. M. O., Pereira, V. J., Paulo, J., & Rodrigues, A. (2016). *PHYSICAL-CHEMICAL PROPERTIES OF PESTICIDES : CONCEPTS , APPLICATIONS , AND INTERACTIONS WITH THE ENVIRONMENT PROPRIEDADES FÍSICO-QUÍMICAS DOS AGROTÓXICOS : 627–641.*

International Zeolite Association. (2022). *Chabazite Series*.

IPCS. (2002). *The WHO Recommended Classification of pesticides by hazard, Guidelines to Classification 2000–2002*.

Iwuozor, K. O., Emenike, E. C., Gbadamosi, F. A., Ighalo, J. O., Umenweke, G. C., Iwuchukwu, F. U., Nwakire, C. O., & Igwegbe, C. A. (2022). Adsorption of organophosphate pesticides from aqueous solution : a review of recent advances. In *International Journal of Environmental Science and Technology* (Issue 0123456789). Springer Berlin Heidelberg. https://doi.org/10.1007/s13762-022-04410-6

Jäger, J. E. (2019). Residues of pesticides. In F. J. M. Smulders, I. M. C. M. Rietjens, & M. Rose (Eds.), *Chemical hazards in foods of animal origin* (pp. 81–98). Wageningen Academic Publishers. https://doi.org/https://doi.org/10.3920/978-90-8686-877-3_03

Jayaraj, R., Megha, P., & Sreedev, P. (2016). *Organochlorine pesticides , their toxic effects on living organisms and their fate in the environment*. *9*, 90–100. https://doi.org/10.1515/intox-2016-0012

Kalavathy, M. H., Karthikeyan, T., Rajgopal, S., & Miranda, L. R. (2005). *Kinetic and isotherm studies of Cu (II) adsorption onto H 3 PO 4 -activated rubber wood*

sawdust. *292*, 354–362. https://doi.org/10.1016/j.jcis.2005.05.087

Knowell, L. (2018). *Pesticides in Groundwater*. https://www.usgs.gov/special-topics/water-science-school/science/pesticides-groundwater

Köck-schulmeyer, M., Ginebreda, A., Postigo, C., Garrido, T., Fraile, J., López, M., Alda, D., & Barceló, D. (2014). Science of the Total Environment Four-year advanced monitoring program of polar pesticides in groundwater of Catalonia (NE-Spain). *Science of the Total Environment, The*, *470–471*, 1087–1098. https://doi.org/10.1016/j.scitotenv.2013.10.079

Kowenje, C. O., & Osewe, E. T. (2015). Optimizing Zeolitic Catalysis for Environmental Remediation. *Advanced Catalytic Materials*, 411–438.

Krahnstöver, T., & Wintgens, T. (2018). Journal of Environmental Chemical Engineering Separating powdered activated carbon (PAC) from wastewater – Technical process options and assessment of removal efficiency. *Journal of Environmental Chemical Engineering*, *6*(5), 5744–5762. https://doi.org/10.1016/j.jece.2018.09.001

Krishna, S. S. S. K. P. K. (2015). *Adsorption of Organophosphorous Pesticide from Aqueous Solution Using Adsorption of Organophosphorous Pesticide from Aqueous Solution Using " Waste " Jute Fiber Carbon. May 2010.* https://doi.org/10.1155/2010/947070

Kumar, V., Singh, S., Singh, R., Upadhyay, N., Singh, J., Pant, P., Singh, R., Srivastava, B., Singh, A., & Subhose, V. (2018). Spectral , structural and energetic study of acephate , glyphosate , monocrotophos and phorate : an experimental and computational approach. *Journal of Taibah University for Science*, *12*(1), 69–78. https://doi.org/10.1080/16583655.2018.1451109

Kushwaha, S., Sreelatha, G., & Padmaja, P. (2011). Evaluation of Acid-Treated Palm Shell Powder for Its Effectiveness in the Adsorption of Organophosphorus Pesticides : Isotherm , Kinetics , and Thermodynamics. *Journal of Chemical & Engineering Data*, *56*, 2407–2415.

Lade, B. (2017). Nano Bio Pesticide to Constraint Plant Destructive Pests. *Journal of Nanomedicine Research*, *6*. https://doi.org/10.15406/jnmr.2017.06.00158

Lari, S. Z., Khan, N. A., Gandhi, K. N., Meshram, T. S., & Thacker, N. P. (2014). *ENVIRONMENTAL HEALTH Comparison of pesticide residues in surface water and ground water of agriculture intensive areas*. 1–7.

Li, W., Wu, R., Duan, J., Saint, C. P., & Leeuwen, J. Van. (2016). Impact of prechlorination on organophosphorus pesticides during drinking water treatment : Removal and transformation to toxic oxon byproducts. *Water Research*, *105*, 1–10. https://doi.org/10.1016/j.watres.2016.08.052

Marczewski, A. W., Seczkowska, M., Deryło-Marczewska, A., & Blachnio, M. (2016). Adsorption equilibrium and kinetics of selected phenoxyacid pesticides on activated carbon: effect of temperature. *Adsorption*, *22*(4), 777–790. https://doi.org/10.1007/s10450-016-9774-0

Marican, A., & Durán-lara, E. F. (2018). *A review on pesticide removal through different processes*. 2051–2064.

Marta, P., Carazo-rojas, E., Greivin, P., Chinchilla-soto, C., Chin-pampillo, J. S., Aguilar-mora, P., Alpízar-marín, M., Masís-mora, M., Rodríguez-rodríguez, C. E., & Vryzas, Z. (2018). *Pesticide monitoring and ecotoxicological risk assessment in surface water bodies and sediments of a tropical agro-ecosystem **. *241*, 800–809. https://doi.org/10.1016/j.envpol.2018.06.020

Martin, R. J. (1978). *ADSORPTION STUDIES USING GAS-LIQUID CHROMATOGRAPHY--III . EXPERIMENTAL FACTORS INFLUENCING ADSORPTION*. *12*(1967).

Mcknight, U. S., Rasmussen, J. J., Kronvang, B., Binning, P. J., & Bjerg, P. L. (2015). Sources , occurrence and predicted aquatic impact of legacy and contemporary pesticides in streams. *Environmental Pollution*, *200*, 64–76. https://doi.org/10.1016/j.envpol.2015.02.015

Mekonen, S., Argaw, R., Simanesew, A., Houbraken, M., Senaeve, D., Ambelu, A., & Spanoghe, P. (2016). Chemosphere Pesticide residues in drinking water and associated risk to consumers in Ethiopia. *Chemosphere*, *162*, 252–260. https://doi.org/10.1016/j.chemosphere.2016.07.096

Memon, G. Z., Bhanger, M. I., Akhtar, M., Talpur, F. N., & Memon, J. R. (2008). *Adsorption of methyl parathion pesticide from water using watermelon peels as a low cost adsorbent*. *138*, 616–621. https://doi.org/10.1016/j.cej.2007.09.027

Mendes, C. B., de Fátima Lima, G., Alves, V. N., Coelho, N. M. M., Dragunski, D. C., & Tarley, C. R. T. (2012). Evaluation of vermicompost as a raw natural adsorbent for adsorption of pesticide methylparathion. *Environmental Technology*, *33*(2), 167–172. https://doi.org/10.1080/09593330.2011.554890

Metwally, S. S., & Attallah, M. F. (2019). Impact of surface modi fi cation of chabazite on the sorption of iodine and molybdenum radioisotopes from liquid phase. *Journal of Molecular Liquids*, *290*, 111237. https://doi.org/10.1016/j.molliq.2019.111237

Mojiri, A., Zhou, J. L., Robinson, B., Ohashi, A., Ozaki, N., Kindaichi, T., Farraji, H., & Vakili, M. (2020). Chemosphere Pesticides in aquatic environments and their removal by adsorption methods. *Chemosphere*, *253*, 126646. https://doi.org/10.1016/j.chemosphere.2020.126646

Montana, A., Rapisarda, V., Esposito, M., Amico, F., Cocimano, G., Nunno, N. Di, Ledda, C., & Salerno, M. (2021). *Case Report A Rare Case of Suicide by Ingestion of Phorate : A Case Report and a Review of the Literature*.

Mostafa, M., Bin, M. N., Othman, S. I., Saleh, R., Salama, Y. F., & Allam, A. A. (2021). Environmental Technology & Innovation Effective removal of different species of organophosphorus pesticides (acephate , omthosate , and methyl parathion) using chitosan / Zeolite-A as multifunctional adsorbent. *Environmental Technology & Innovation*, *24*, 101875. https://doi.org/10.1016/j.eti.2021.101875

Moyer, R. (2018). *HHS Public Access*. 93–99. https://doi.org/10.1016/j.pestbp.2018.01.009.Kinetic

Münze, R., Hannemann, C., Orlinskiy, P., Gunold, R., Paschke, A., Foit, K., Becker, J., Kaske, O., Paulsson, E., Peterson, M., Jernstedt, H., Kreuger, J., Schüürmann, G., & Liess, M. (2017). Science of the Total Environment Pesticides from wastewater treatment plant ef fl uents affect invertebrate communities. *Science of the Total Environment*, *599–600*, 387–399. https://doi.org/10.1016/j.scitotenv.2017.03.008

National Center for Biotechnology Information. (2022). *PubChem Compound Summary for CID 4790, Phorate*.

Navarro-ortega, A., Pic, Y., Ccanccapa, A., Masi, A., & Val, U. De. (2016). *Pesticides in the Ebro River basin : Occurrence and risk assessment * Barcel o Dami a*. *211*, 414–424. https://doi.org/10.1016/j.envpol.2015.12.059

Nguyen, H., You, S., & Hosseini-bandegharaei, A. (2017). Mistakes and inconsistencies regarding adsorption of contaminants from aqueous solutions : A critical review. *Water Research*, *120*, 88–116. https://doi.org/10.1016/j.watres.2017.04.014

NPIC. (2021). *What happens to pesticides released in the environment?*

Ogunah, J. A., Kowenje, C. O., Osewe, E. T., Lalah, J. O., Jaoko, D. A., & Koigi, R. N. (2013). *Effects of zeolites X and Y on the degradation of malathion in water*. *1*(1), 7–13. https://doi.org/10.11648/j.sjc.20130101.12

Oliveira, B. R., Penetra, A., Cardoso, V. V, & Benoliel, M. J. (2015). *Biodegradation of pesticides using fungi species found in the aquatic environment*. 11781–11791. https://doi.org/10.1007/s11356-015-4472-0

Ormad, M. P., Miguel, N., Claver, A., Matesanz, J. M., & Ovelleiro, J. L. (2008). Pesticides removal in the process of drinking water production. *Chemosphere*, *71*, 97–106. https://doi.org/10.1016/j.chemosphere.2007.10.006

Özkara, A., Akyıl, D., & Konuk, M. (2016). Pesticides , Environmental Pollution , and Health. In Marcelo L. Larramendy and Sonia Soloneski (Ed.), *Environmental Health Risk* (pp. 3–28). Intech. https://doi.org/10.5772/61472

Papadakis, E., Tsaboula, A., Vryzas, Z., Kotopoulou, A., Kintzikoglou, K., & Papadopoulou-mourkidou, E. (2018). Science of the Total Environment Pesticides in the rivers and streams of two river basins in northern Greece. *Science of the Total Environment*, *624*, 732–743. https://doi.org/10.1016/j.scitotenv.2017.12.074

Pehkonen, S. O., & Zhang, Q. (2010). *Technology The Degradation of Organophosphorus Pesticides in Natural Waters : A Critical Review The Degradation of Organophosphorus Pesticides in Natural Waters : A Critical*. *3389*. https://doi.org/10.1080/10643380290813444

Piemonte, R., & Toscana, R. (2010). *Pesticides and their metabolites in selected Italian groundwater and surface water used for drinking*. *c*, 309–316. https://doi.org/10.4415/ANN

Pohanish, R. P. (2015). *Sittig's Handbook of Pesticides and Agricultural Chemicals* (2nd ed.). William Andrew Publishing. https://doi.org/10.1016/B978-1-4557-3148-0.00016-9

Pope, C. N. (2010). *Critical Reviews ORGANOPHOSPHORUS PESTICIDES : DO THEY ALL HAVE THE SAME MECHANISM OF TOXICITY ? ORGANOPHOSPHORUS PESTICIDES : DO THEY ALL HAVE THE SAME MECHANISM OF TOXICITY ? 7404*. https://doi.org/10.1080/109374099281205

Rani, L., Thapa, K., Kanojia, N., Sharma, N., Singh, S., Singh, A., Lal, A., & Kaushal, J. (2021). An extensive review on the consequences of chemical pesticides on human health and environment. *Journal of Cleaner Production*, *283*, 124657. https://doi.org/10.1016/j.jclepro.2020.124657

Rapo, E., & Tonk, S. (2021). Factors Affecting Synthetic Dye Adsorption ; Desorption Studies : A Review of Results from the Last Five Years. *Molecules*, *26*(17).

Reilly, T. J., Smalling, K. L., Orlando, J. L., & Kuivila, K. M. (2012). Chemosphere Occurrence of boscalid and other selected fungicides in surface water and groundwater in three targeted use areas in the United States. *Chemosphere*, *89*(3), 228–234. https://doi.org/10.1016/j.chemosphere.2012.04.023

Remucal, C. K. (2014). *Environmental Science The role of indirect photochemical degradation in the environmental fate of pesticides : a review †*. 628–653. https://doi.org/10.1039/c3em00549f

Sabarinathan, C., Karuppasamy, P., Vijayakumar, C. T., & Arumuganathan, T. (2019). Development of methylene blue removal methodology by adsorption using molecular polyoxometalate : Kinetics , Thermodynamics and Mechanistic Study. *Microchemical Journal*, *146*(October 2018), 315–326. https://doi.org/10.1016/j.microc.2019.01.015

Sabzevari, S., & Hofman, J. (2022). Science of the Total Environment A worldwide review of currently used pesticides ' monitoring in agricultural soils. *Science of the Total Environment*, *812*, 152344. https://doi.org/10.1016/j.scitotenv.2021.152344

Saleh, I. A., Zouari, N., & Al-ghouti, M. A. (2020). Environmental Technology & Innovation Removal of pesticides from water and wastewater : Chemical , physical and biological treatment approaches. *Environmental Technology & Innovation*, *19*, 101026. https://doi.org/10.1016/j.eti.2020.101026

Salman, J. M., Njoku, V. O., & Hameed, B. H. (2011). Adsorption of pesticides from aqueous solution onto banana stalk activated carbon. *Chemical Engineering Journal*, *174*(1), 41–48. https://doi.org/10.1016/j.cej.2011.08.026

Salvestrini, S., Sagliano, P., Iovino, P., Capasso, S., & Colella, C. (2010). Applied Clay Science Atrazine adsorption by acid-activated zeolite-rich tuffs. *Applied Clay Science*, *49*(3), 330–335. https://doi.org/10.1016/j.clay.2010.04.008

Sarkar, S., Gil, J., Keeley, J., Möhring, N., & Jansen, K. (2021). *Requested by the DEVE committee The use of pesticides in developing countries and their impact*

on health and the right to food (Issue January) [European Parliament's Committee on Development]. https://www.europarl.europa.eu/thinktank/en/document/EXPO_STU(2021)6536 22

Shawaqfeh, A. T. (2010). Removal of Pesticides from Water Using Anaerobic-Aerobic Biological Treatment. *Chinese Journal of Chemical Engineering*, *18*(4), 672–680. https://doi.org/10.1016/S1004-9541(10)60274-1

Skorodumova, N. V. (2018). *Environmental Science materials on the removal of organophosphorus*. 1482–1494. https://doi.org/10.1039/c8en00171e

Stehle, S., Schulz, R., Bline, A., Bub, S., Petschick, L. L., & Wolfram, J. (2019). Aquatic pesticide exposure in the U . S . as a result of non-agricultural uses. *Environment International*, *133*(July), 105234. https://doi.org/10.1016/j.envint.2019.105234

Sud, D., & Kaur, P. (2012). *Heterogeneous Photocatalytic Degradation of Selected Organophosphate Pesticides : A Review Heterogeneous Photocatalytic Degradation of Selected Organophosphate Pesticides : A Review*. *3389*. https://doi.org/10.1080/10643389.2011.574184

Syafrudin, M., Ayu, R., Yuniarto, A., Hadibarata, T., Rhee, J., Al-Onazi, W., Algarni, T., Almarri, A., & Al-Mohaimeed, A. (2021). Pesticides in Drinking Water—A Review. *International Journal of Environmental Research and Public Health*, *18*, 468. https://doi.org/10.3390/ijerph18020468

T3DB. (n.d.). *Phorate (T3D0225)*.

Tan, K. L., & Hameed, B. H. (2017). Journal of the Taiwan Institute of Chemical Engineers Insight into the adsorption kinetics models for the removal of contaminants from aqueous solutions. *Journal of the Taiwan Institute of Chemical Engineers*, *74*, 25–48. https://doi.org/10.1016/j.jtice.2017.01.024

Thommes, M., Kaneko, K., Neimark, A. V, Olivier, J. P., Rodriguez-reinoso, F.,

Rouquerol, J., & Sing, K. S. W. (2015). *Physisorption of gases , with special reference to the evaluation of surface area and pore size distribution (IUPAC Technical Report)*. https://doi.org/10.1515/pac-2014-1117

Tiryaki, O., & Temur Çinar, C. (2010). The fate of pesticide in the environment. *J Biol Environ Sci*, *4*, 29–38.

Torstensson, L. (2022). *Transport pathways of pesticides in the environment*. *May 2020*, 1–9.

UNEP/FAO. (2018). *Rotterdam Convention on the Prior Informed Consent Procedure for Certain Hazardous Chemicals and Pesticides in International Trade* (Issue December 2017).

University of Hertfordshire. (2022). *PPDB: Pesticide Properties DataBase*.

Vallero, D. A. (2021). *Climate Change* (T. M. Letche (ed.); Third, pp. 771–797). https://doi.org/10.1016/B978-0-12-821575-3.00034-7

Vela, N., Fenoll, J., Garrido, I., Pérez-lucas, G., Flores, P., Hellín, P., & Navarro, S. (2019). Science of the Total Environment Reclamation of agro-wastewater polluted with pesticide residues using sunlight activated persulfate for agricultural reuse. *Science of the Total Environment*, *660*, 923–930. https://doi.org/10.1016/j.scitotenv.2019.01.060

Vryzas, Z., Vassiliou, G., Alexoudis, C., & Papadopoulou-mourkidou, E. (2009). Spatial and temporal distribution of pesticide residues in surface waters in northeastern Greece. *Water Research*, *43*(1), 1–10. https://doi.org/10.1016/j.watres.2008.09.021

Wang, J., & Guo, X. (2020). Adsorption kinetic models : Physical meanings , applications , and solving methods. *Journal of Hazardous Materials*, *390*(November 2019), 122156. https://doi.org/10.1016/j.jhazmat.2020.122156

Wanjeri, V. W. O., Sheppard, C. J., Prinsloo, A. R. E., Ngila, J. C., & Ndungu, P. G. (2018). Journal of Environmental Chemical Engineering Isotherm and kinetic

investigations on the adsorption of organophosphorus pesticides on graphene oxide based silica coated magnetic nanoparticles functionalized with 2-phenylethylamine. *Journal of Environmental Chemical Engineering*, *6*(1), 1333–1346. https://doi.org/10.1016/j.jece.2018.01.064

Westlund, P., & Yargeau, V. (2017). Science of the Total Environment Investigation of the presence and endocrine activities of pesticides found in wastewater ef fl uent using yeast-based bioassays. *Science of the Total Environment*, *607–608*, 744–751. https://doi.org/10.1016/j.scitotenv.2017.07.032

World Health Organization. (2020). *The WHO Recommended Classification of Pesticides by Hazard and Guidelines to Classification 2019 edition*.

Wu, F., Tseng, R., Huang, S., & Juang, R. (2009). *Characteristics of pseudo-second-order kinetic model for liquid-phase adsorption : A mini-review*. *151*, 1–9. https://doi.org/10.1016/j.cej.2009.02.024

Wu, R., Chen, C., Lu, C., Hsu, P., & Chen, M. (2010). Phorate degradation by TiO 2 photocatalysis : Parameter and reaction pathway investigations. *DES*, *250*(3), 869–875. https://doi.org/10.1016/j.desal.2009.03.026

Yadav, I., & Devi, N. (2017). *Pesticides Classification and Its Impact on Human and Environment* (pp. 140–158).

Yang, Q., Wang, J., Zhang, W., Liu, F., Yue, X., Liu, Y., Yang, M., Li, Z., & Wang, J. (2017). Interface engineering of metal organic framework on graphene oxide with enhanced adsorption capacity for organophosphorus pesticide. *Chemical Engineering Journal*, *313*, 19–26. https://doi.org/10.1016/j.cej.2016.12.041

APPENDICES

A. Calibration Curves
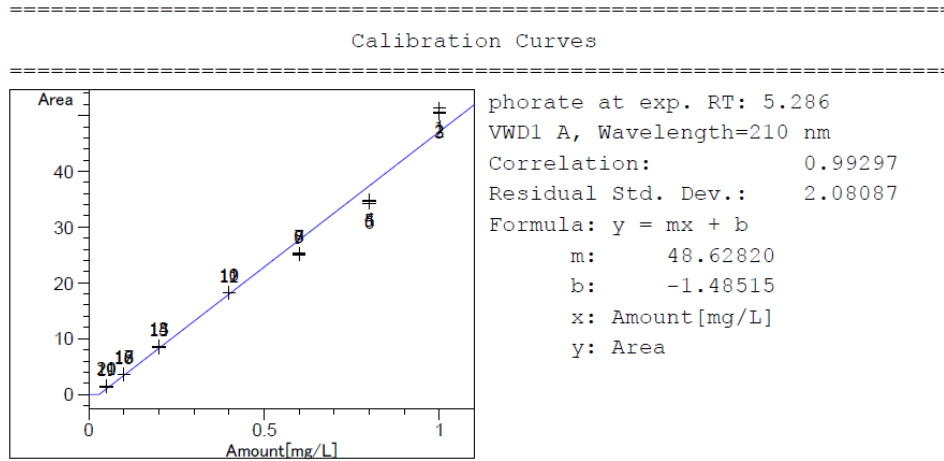
Figure A 1. The calibration curve obtained from HPLC at 15th of Jan 2021
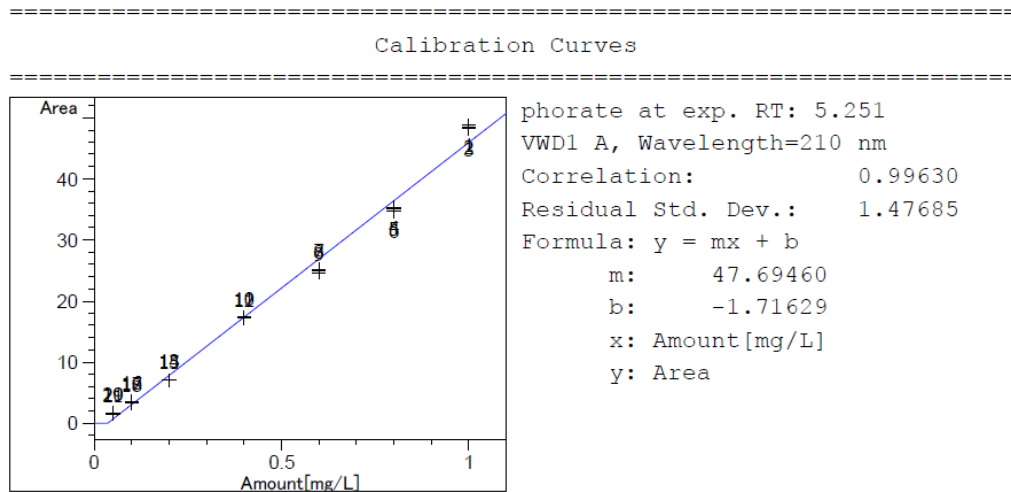
Figure A 2. The calibration curve obtained from HPLC at 19th of Jan 2021

```
========================================================================
                          Calibration Curves
========================================================================
```

phorate at exp. RT: 5.146
VWD1 A, Wavelength=210 nm
Correlation: 0.99967
Residual Std. Dev.:   0.56767
Formula: y = mx + b
        m: 61.17952
        b: 1.40586e-1
        x: Amount[mg/L]
        y: Area
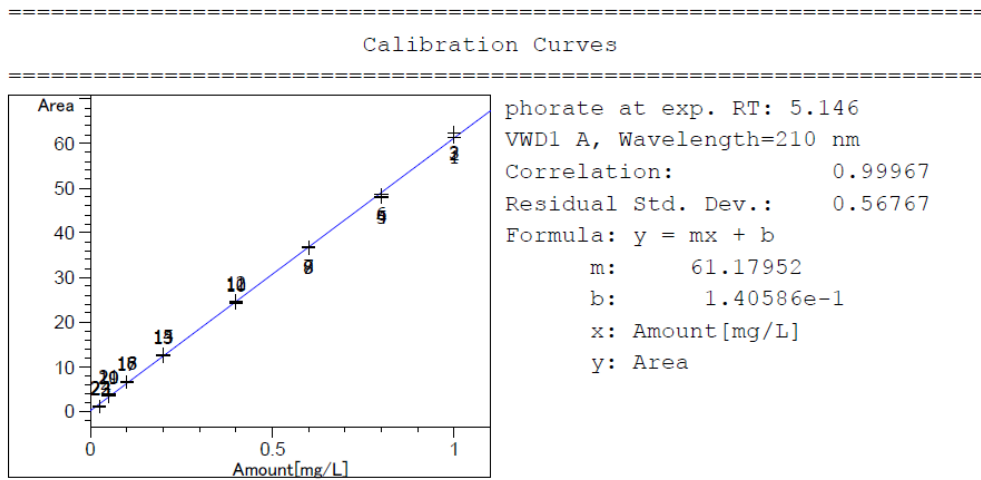
Figure A 3. The calibration curve obtained from HPLC at 5th of Jan 2022


```
========================================================================
                          Calibration Curves
========================================================================
```

phorate at exp. RT: 5.305
VWD1 A, Wavelength=210 nm
Correlation: 0.99920
Residual Std. Dev.:   0.96833
Formula: y = mx + b
        m: 68.28560
        b: 6.36317e-1
        x: Amount[mg/L]
        y: Area
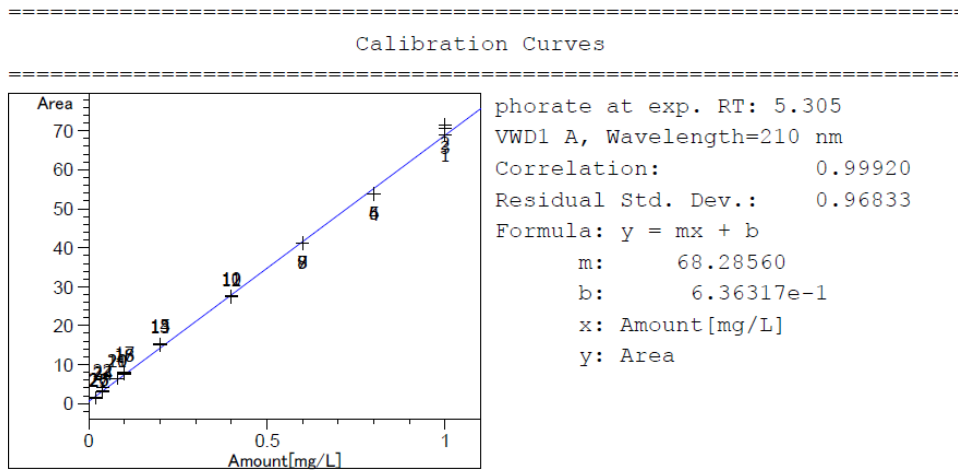
Figure A 4. The calibration curve obtained from HPLC at 26th of Feb 2022

150

```
========================================================================
                        Calibration Curves
========================================================================

Area                                  phorate at exp. RT: 5.317
 60                                +  VWD1 A, Wavelength=210 nm
                                   1  Correlation:        0.99973
 50                                   Residual Std. Dev.:  0.48462
                            +
 40                         5         Formula: y = mx + b
                       +                   m:      57.26758
 30                    9                   b:      2.87427e-1
               10                          x:  Amount[mg/L]
 20            +                           y:  Area
          15
 10      16  +
        20 +
  0     +
        0         0.5         1
            Amount[mg/L]
```
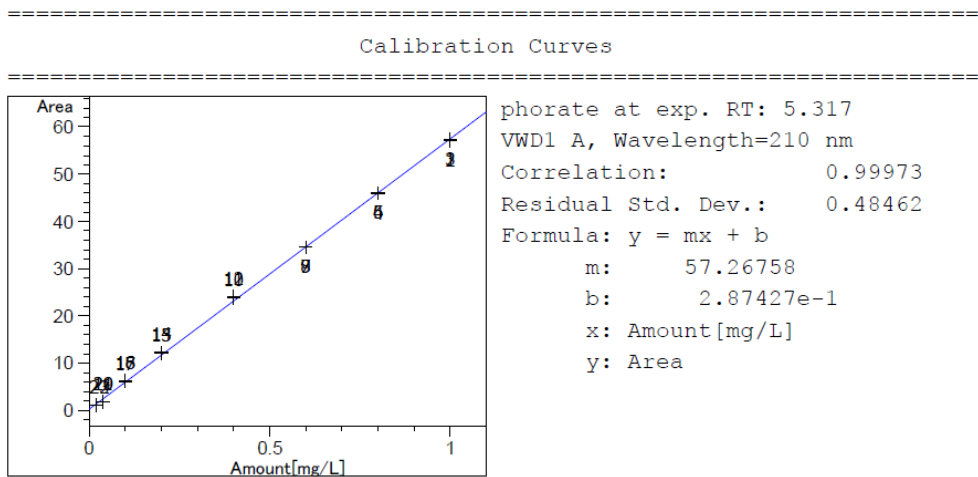
Figure A 5. The calibration curve obtained from HPLC at 8^(th) of Mar 2022

```
========================================================================
                        Calibration Curves
========================================================================

Area                                  Phorate at exp. RT: 5.450
                            +         VWD1 A, Wavelength=210 nm
120                         1         Correlation:        0.99960
                                      Residual Std. Dev.:  1.04696
100
                                      Formula: y = mx + b
 80                                        m:      25.82248
           5                               b:      1.63985
 60        +                               x:  Amount[mg/L]
                                           y:  Area
 40        8
        10 +
 20   2016+
      +
  0   +
      0       2         4
          Amount[mg/L]
```
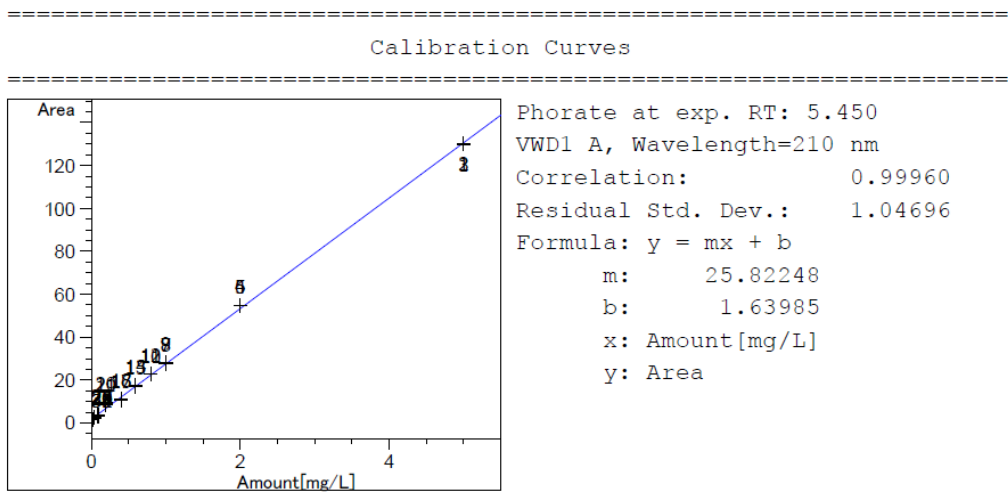
Figure A 6. The calibration curve obtained from HPLC at 26^(th) of Mar 2022